Advances in Anatomy
Embryology and Cell Biology
180

D. N. Angelov · O. Guntinas-Lichius
K. Wewetzer · W. F. Neiss · M. Streppel

Axonal Branching and Recovery of Coordinated Muscle Activity after Transection of the Facial Nerve in Adult Rats

Springer

180
Advances in Anatomy Embryology and Cell Biology

D. N. Angelov · O. Guntinas-Lichius ·
K. Wewetzer · W. F. Neiss · M. Streppel

Axonal Branching and Recovery of Coordinated Muscle Activity after Transection of the Facial Nerve in Adult Rats

With 21 Figures and 19 Tables

Springer

Prof. Dr. Doychin N. Angelov
Prof. Dr. Wolfram F. Neiss
Institut I für Anatomie
Universität zu Köln
Joseph-Stelzmann-Str. 9
50931 Köln
Germany
e-mail: angelov.anatomie@uni-koeln.de

Dr. Konstantin Wewetzer
Hannover Veterinary School
Department of Pathology
30559 Hannover
Germany

Dr. Orlando Guntinas-Lichius
Prof. Dr. Michael Streppel
Klinik für Hals-, Nasen- und Ohrenheilkunde
Universität zu Köln
50931 Köln
Germany

Library of Congress Catalog Number 2005924371

ISSN 0301-5556
ISBN-10 3-540-25654-7 Springer Berlin Heidelberg New York
ISBN-13 978-3-540-25654-0 Springer Berlin Heidelberg New York

Springer is a part of Springer Science+Business Media
springeronline.com

Printed in Germany

Editor: Simon Rallison, Heidelberg
Desk editor: Anne Clauss, Heidelberg
Production editor: Nadja Kroke, Leipzig
Cover design: design & production GmbH, Heidelberg
Typesetting: LE-TEX Jelonek, Schmidt & Vöckler GbR, Leipzig
Printed on acid-free paper SPIN 11330813 27/3150/YL – 5 4 3 2 1 0

List of Contents

Acknowledgements

This work has been supported by the DFG (D.N.A.) and the Jean Uhrmacher-Foundation (M.S. and O.G.-L.), the Imhoff-Foundation (D.N.A) and the Köln Fortune Programm (D.N.A). The authors are grateful to Christine Radtke for the isolation and purification of bone marrow stroma cells. The skillful technical assistance of D. Felder, I. Rohrmann, M. Strauss, C. Zyntek, the fine photographical work of I. Koch, and the precise drawings of J. Ribbers are highly appreciated.

1
Outline of the General Neurobiological Problem

Peripheral nerve injury is always followed by attempted regeneration of the injured axons (Wilson and Perry 1990). In the everyday clinical practice, however, functional recovery after peripheral nerve injury is the exception rather than the rule (Hall 1989; Lisney 1989; Thomas 1989). Due to misdirection of regenerating axons there occur supernumerary sprouts (Ito and Kudo 1994) that are misrouted through the endoneural tubes of wrong fascicles toward improper targets (Trachtenberg and Thompson 1996).

Successful regeneration of a peripheral nerve requires the involvement of at least three beneficial responses (Bisby 1995):

1. A "*central response*", meaning that the perikarya respond to injury with metabolic changes supporting axonal regrowth
2. A "*space-providing response*", meaning that the micro-environment around the injured nerve permits the regrowth of sufficient amount of axons and axonal branches
3. A "*growth-promoting response*", meaning that the endoneural space contains or provides guidance cues necessary for the specific reinnervation of their original targets

The experimental work described here is based on the hypothesis that during regeneration of a transected peripheral nerve, e.g., the facial nerve, all three responses are unnecessarily strong. The conclusion is that these responses impair rather than support the recovery of coordinated function of the facial musculature.

1.1
The Perikarya Supporting Axonal Regrowth Are Hyperexcitable

The regeneration program of the axotomized motoneurons (see Moran and Graeber 2004 for a recent review) includes a wide spectrum of reactions generally characterized by (1) an immediate switch to an intense biosynthetic activity, necessary to replace the sectioned axon and (2) an abrupt stop of neurotransmission (Lieberman 1971). This sudden interruption of the neurotransmission renders the motoneurons hyperexcitable.

1.1.1
Increase in Biosynthetic Activity

After axotomy, the motoneurons increase the uptake of glucose (Kreutzberg and Emmert 1980; Singer and Mehler 1986), activate the pentose phosphate shunt (Kreutzberg 1963; Härkönen and Kauffman 1974), and increase the production of ribose and NADPH. Ribose is necessary for the increased synthesis of RNA (enhanced protein synthesis). NADPH furnishes proton equivalents for the synthesis of lipids necessary for membrane restoration during axonal regrowth and

branching (Tetzlaff and Kreutzberg 1985b). The amount of RNA and the uptake of amino acids in motoneurons increase (Lieberman 1971). The activity of ornithine decarboxylase, a key enzyme in the polyamine biosynthesis, reaches 300% over control (Tetzlaff and Kreutzberg 1985a). The resulting production of the polyamines spermine, spermidine, and putrescine (Paschen 1992) and the activity of the transglutaminase, the enzyme through which the polyamines presumably exert their effects, are also enhanced (Tetzlaff et al. 1988). In consequence of this intensive regeneration program, the synthesis of the cytoskeletal proteins is increased (Bisby and Tetzlaff 1992). Whereas the transport of the neurofilament protein is slowed down (Hoffman and Lasek 1980), that of tubulin and actin is increased (Hoffman et al. 1987).

Axotomy of facial and hypoglossal motoneurons in Wistar rats causes the migration of the cytosolic enzyme neuron-specific enolase (NSE) into the nuclei of the axotomized neurons (Angelov et al. 1994). This intranuclear migration of NSE may represent an important step in a neuronal-survival program: Pyruvate has been shown to promote a potent protection of the whole intracellular machinery against peroxide-induced damage (Perez-Polo et al. 1990). This theory is strongly supported by the finding that NSE directly promotes the survival of embryonic rat neurons in primary culture (Takei et al. 1991).

1.1.2
Hyperexcitability of the Axotomized Perikarya

In response to transection of the facial nerve, the resident microglia show a dramatic increase in mitotic activity, rapidly migrate toward the neuronal cell surface (Rotter et al. 1979), and displace the afferent synaptic terminals (Blinzinger and Kreutzberg 1968; Neiss et al. 1992). This "synaptic stripping" leads to a deafferentation mainly of proximal, but not of peripheral dendrites (Bratzlavsky and vander Eecken 1977; Titmus and Faber 1990; Nacimiento et al. 1992; Graeber et al. 1993). The axotomized motoneurons "respond" to their deafferentation with a decrease in the synthesis of transmitter-related compounds, e.g., muscarinic and glycine receptors (Rotter et al. 1979; Senba et al. 1990) and a decrease in activity of enzymes involved in the biosynthesis of transmitters, e.g., dopamine-β-hydroxylase, tyrosine-hydroxylase, cholineacetyltransferase, cytochrome oxidase and acetylcholinesterase (Engel and Kreutzberg 1986; Engel et al. 1988). These changes correspond to the electrophysiological status of regenerating neurons: increased excitability (Eccles et al. 1958; Kuno and Llinas 1970) with preserved integrity of the dendritic input (Lux and Schubert 1975; Kreutzberg et al. 1975; Borgens 1988; Titmus and Faber 1990).

1.2
Axonal Regrowth Is Compromised by Ephaptic Cross-Talk Between the Branches

1.2.1
The Endoneural Micro-Environment Permits a Rapid and Extensive Axonal Growth

After injury, each parent axon may give rise to 25 daughter axons (Shawe 1954; Jenq et al. 1988). As regeneration proceeds, some of these supernumerary branches are pruned off over a period of up to 12 months (Mackinnon et al. 1991; Brushart et al. 1998). Those that are lost presumably fail to make a connection with a peripheral target. There are, however, persistently higher numbers of myelinated and unmyelinated axons in regenerated segments of peripheral nerves than in the corresponding parent nerves (Horch and Lisney 1981; Murphy et al. 1990).

1.2.2
Excessive Firing by the Transected Axons

Excessive firing by the transected axons is a consequence of trans-axonal exchange of abnormally intensive nerve impulses (ephaptic cross-talk) between axons from adjacent fascicles (Sadjadpour 1975). This usually occurs when axonal forward growth is blocked and the branches are stunted forming a tangled terminal mass (a "neuroma"). The growth process and the steering of the cones is further complicated by the presence of branches from the distal nerve stump (Shaw and Bray 1977) and by collateral branches of nearby intact nerve fibers (Diamond et al. 1987). The initially formed growth cones transform into swollen "end-bulbs" and form disseminated "microneuromas" scattered along the distal nerve trunk, its branches, and its target tissue. After about one week these neuromas begin to discharge action potentials spontaneously, perhaps as the result of the concentration of large numbers of sodium channels (Devor et al. 1989). In the peripheral nervous system (PNS), tissue injury and inflammation trigger excess firing by the transected axons. This includes both an increase in the sensitivity of the surviving endings ("peripheral sensitization") and the generation of ectopic impulses in the damaged nerve fibers ("ectopia"). The resulting abnormal firing is processed by a network in the central nervous system (CNS) that itself is abnormally excitable. This "central sensitization" is thought to be triggered by the acute nociceptive volley generated at the time of the injury and by the sustained abnormal activity in the injured axons (Schwarz et al. 1983; Spielmann et al. 1983; Bowe et al. 1985).

1.3
Biological Significance of Axonal Branching

Injury to the peripheral nerve initiates a complex series of changes distal to the lesion, collectively known as Wallerian degeneration. Within 24 h after injury, the axonal content begins to necrotize and axonal debris is phagocytosed by blood-borne macrophages and proliferated Schwann cells (Perry and Brown 1992;

Hirata and Kawabuchi 2002; McPhail et al. 2004). When resorption is complete, the Schwann cells form long chains of cells (bands of Büngner) that bridge the interfragmentary gap and form guiding channels for the regenerating branches on their way to the target(s). The architectural pattern of the Büngner's bands of the peripheral stump remains unchanged for 3 months, after which progressive distortion by proliferating connective tissue occurs. The process of Wallerian degeneration creates an environment highly supportive for axonal growth. The preference for axonal growth into a degenerating nerve ensures that the vast majority of axons will regrow into the distal stump if it remains in continuity with the proximal stump (Bisby 1995).

In spite of that, the regenerating axons do not merely elongate toward the distal stump, but respond with axonal branching (sprouting) by lateral budding mainly at the nodes of Ranvier, up to 6 mm proximal to the injury site. As regeneration proceeds, some of these supernumerary branches are pruned off over a period of up to 12 months (Bray and Aguayo 1974). There are, however, persistently higher numbers of myelinated and unmyelinated axons in regenerated segments of peripheral nerves than in intact nerves.

What is the general biological significance of branching? To answer this question one needs more information about the structural and biochemical events that accompany the process of axonal sprouting. Most of the recent reports suggest that axonal branching is part of the neuronal response to injury within a complex program of regeneration. This attempt is associated with substantial cytoskeletal reorganization (King et al. 2001), resulting in the elaboration of fine protrusions (sprouts) into and across lesion sites (McHale et al. 1995).

Observations in vitro show that axonal branching begins from the end-bulb within 3 h after injury (Sjoberg and Kanje 1990). The regenerating branches initially lie on the surface of the Schwann cells. Later, these branches increase in diameter and become surrounded by Schwann cell processes. The guidance of these immature axons to their final destination can be considered as a series of short-range projections to intermediate targets under the influence of local guidance cues. Neurons respond to these cues by means of motile sensory apparatus at the tip of the advancing axon termed the "*growth cone*", which very often does not emerge from the axon at the precise site of injury, but proximal to it (Borgens 1988; Ziv and Spira 1997). The initial formation of growth cones occurs before the necessary newly synthesized proteins have time to arrive at the site of axon injury, i.e., too rapidly to be dependent on metabolic changes in the cell body (Smith and Skene 1997).

The growth cone borne by neurites (axons) is shaped like a webbed foot (Fawcett and Keynes 1990). Flattened processes called *lamellipodia* and numerous stiff, fine processes called *filopodia* extend from a swollen central core. Current studies have identified three major intracellular cytoskeletal components responsible for the cytomechanical forces in the leading edge of elongating axons: actin microfilaments, myosin, and microtubules (Challacombe et al. 1996). The growth cone formation begins with a restructuring of the neurofilaments and microtubules to form an altered cytoskeletal region proximal to the tip of the transected axon in which

vesicles accumulate. This rearrangement of the cytoskeleton forms a transient cellular compartment that traps the transported vesicles and serves as a locus for microtubule polymerization. Microtubuli, in turn, facilitate the fusion of vesicles with the plasma membrane, promoting the extension of growth cone lamellipodia (Spira et al. 2003).

Navigation of the growth cone involves detection and integration of extracellular signals, followed by a response that can include forward migration, retraction, branching, and turning. Detection of guidance cues is facilitated by protrusion and retraction of filopodia and lamellipodia from the peripheral region (P-domain) of the growth cone, which contains bundles and networks of actin filaments (Letourneau and Ressler 1984). Being very sensitive to extrinsic guidance cues, such as chemotropic factors, cell adhesion glycoproteins, and extracellular matrix molecules, growth cones turn when confronted with a sharp border between permissive and non-permissive substrates (Taylor et al. 1993). Despite their localization in the proximal region of the growth cone, microtubules do not passively follow growth cone turning, but actively reorganize by redistribution of their distal terminations. In this way, microtubules may stabilize the turns of growth cones and thus also direct the movement of organelles to the appropriate regions of growth cones (Williamson et al. 1996).

The recognition of specific guiding cues is performed by the actin-rich filopodia which have a guidance and/or sensory role, sniffing out gradients of trophic or adhesive factors (Lin and Forscher 1993). Isolated filopodia can respond to alterations in their environment by changes in internal calcium concentrations, and filopodia on different parts of the growth cone respond independently (Bixby and Harris 1991; Letourneau and Cypher 1991; Gordon-Weeks 1997).

1.4
Role of the Cytoskeleton Reorganization During Axonal Regrowth

1.4.1
The Role of Cytoskeletal Proteins in Axonal Elongation

In response to axotomy, the synthesis of cytoskeletal proteins in the perikarya is increased (Hoffman and Lasek 1980; Tetzlaff and Bisby 1989). A post-axotomy increase in overall tubulin synthesis has been documented (Oblinger and Lasek 1988), and it is thought that upregulated levels of tubulin in the perikarya and increased delivery of mictotubules to regrowing axon tips are essential for effective regeneration after injury (Tetzlaff et al. 1988, 1991, 1996).

The structural unit of microtubules, tubulin, is synthesized in the soma and delivered to the growing axon by active slow transport. There has been considerable debate over possible mechanisms underlying the formation of the axonal microtubule network. Two main models exist for its construction. In one model, all microtubules are nucleated by the microtubule organizing center (MTOC) in the cell body, and after a short period of growth are released and transported into

the axon at a rate of 1–2 mm/day with their "plus" ends toward the growth cone (Baas and Ahmad 1993; Joshi and Baas 1993; Ahmad and Baas 1995). This concept is supported by the observations of anterograde movement of microtubules as revealed by photoactivation (Okabe and Hirokawa 1992) and photobleaching (Okabe and Hirokawa 1993) techniques.

Conversely, since these techniques fail to detect translocating microtubules, it has been suggested that the majority of axonal tubulin is in the form of non-translocating but dynamic microtubules (Bamburg et al. 1986; Okabe and Hirokawa 1990; Sabry et al. 1995; Funakoshi et a. 1996). The critical intrinsic aspects of axonal microtubule dynamics may be directly controlled by the mechanical tension produced by both the growth cones and some exogenous factors such as attachment to the substrate (Chang et al. 1998).

The rate of elongation of an axon is determined by the rate at which the growth cone can advance over the substrate. In rat sciatic nerve, both large and small diameter sensory axons elongate at nearly the same rate as do somatic motor axons (about 4 mm/day; Fawcett and Keynes 1990). In the regeneration of a crushed facial nerve of a rat, the rate of axonal elongation is 4.3 mm/day, as measured by the transport of radiolabeled protein (Tetzlaff and Bisby 1989).

Axonal elongation depends on the advance of microtubules that provide structural support and serve as tracks for axonal transport of membranous organelles. Stable microtubule bundles project from the axon into the central region (C-domain) of the growth cone, whereas the ends of dynamic microtubules expand and stretch into the actin-rich P-domain (Gordon-Weeks 1991). Goldberg and Burmeister (1986) and Aletta and Greene (1988) have described three phases of axonal elongation. First, lamellipodia and filopodia extend from the tip of the axon (*protrusion*). Second, microtubules enter the recently protruded regions of the growth cone (*engorgement*). Third, the portions of the growth cones lateral to the engorged regions become quiescent and coalesce to form a new portion of the axon (*consolidation*).

Protrusion

Elimination of growth cone filopodia and lamellipodia greatly reduces the rate of axon elongation (Marsh and Letourneau 1984; Letourneau et al. 1987). Similarly, growth cones devoid of filopodia are unable to detect and respond to guidance cues (Bentley and Torojan-Raymond 1986; Challacombe et al. 1996). The filopodia and lamellipodia of growth cones are long distance antennae that detect guidance cues in the environment. For example, the contact of a single filopodium with a guidance cue is sufficient to redirect axonal elongation either toward or away from the point of contact (reviewed by Gallo and Letourneau 1999, 2004).

The net protrusion of lamellae and filopodia is largely determined by the rates of F-actin polymerization and retrograde flow (Lin et al. 1994). If actin polymerization is blocked, leading edge protrusion does not occur and F-actin is removed from the P-domain by retrograde transport. On the other hand, if F-actin retrograde flow is inhibited, then the rate of protrusion of the leading edge will be determined

primarily by the polymerization of F-actin. Rho-family GTPases (Rho, Rac, Cdc42) have been found to mediate the formation of filopodia and lamellipodia, i.e., to be involved in axon guidance (see Gallo and Letourneau 1998 for review) and also in growth cone responses to collapsing guidance cues (Jin and Strittmatter 1997).

Microtubules and F-actin are often closely associated in the P-domain of growth cones (Letourneau 1979, 1983). Rochlin et al. (1999) describe the formation of foci of F-actin polymerization in growth cones (termed "intrapodia") that are often associated with microtubule ends. On the basis of these associations and findings that pharmacological disruption of microtubules decreases the rate of intrapodia formation, Rochlin et al. (1999) suggest that microtubules are involved in regulating F-actin dynamics in growth cones. Consistent with these findings, pharmacological inhibition of microtubule dynamics in growth cones decreases the extent of lamellipodial protrusion (Gallo 1998). Interestingly, depolymerization of microtubules can result in a transient hyperextension of lamellipodia and filopodia (Gallo 1998) suggesting that microtubules may also be part of a mechanism that limits protrusive activity to the ends of the axons (Bray et al. 1978).

Engorgement

Following protrusion of the growth cone leading edge, microtubules and the associated organelle cargo invade the P-domain. Time-lapse observations of fluorescently labeled microtubules have shown that the tips of microtubules continuously probe the P-domain (Tanaka and Kirschner 1995). These microtubule tips invade the P-domain in a manner mostly dependent on microtubule dynamic instability, i.e., any inhibition of dynamic instability reduces the rate of axon elongation (Rochlin et al. 1996; Challacombe et al. 1997; Gallo 1998; Gallo and Letourneau 1999). In confirmation, it has been shown that inhibition of microtubule dynamic instability prevents the movement of organelles from the C- to the P-domain (Gallo 1998) and the insertion of membrane into the growth cone plasmalemma (Zakharenko and Popov 1998).

Results from some additional experiments have suggested that axonal growth requires microtubules (both, addition of tubulin to polymer, as well as transport of pre-established polymer) at the growth cone (Yu and Baas 1995; Baas 1997, 1999). Tanaka and Kirschner (1991, 1995) report that microtubules in growth cones appear to be transported by "pushing" toward the leading edge of the P-domain. Consistent with this interpretation, Challacombe et al. (1997) report that looped microtubules in growth cones stain with a marker for stable microtubule polymer (i.e., detyrosinated α-tubulin). Therefore, both microtubule polymerization and transport contribute to axonal elongation by advancing microtubules into the P-domain of the growth cones.

Consolidation

Two alterations occur during consolidation: (1) microtubules become bundled, and (2) the generation of new F-actin protrusions largely stops in the regions of the plasma membrane lateral to the bundled microtubules (Tanaka et al. 1995).

Summary Tubulin directly participates in the mechanism of axonal elongation as microtubules are assembled, transported to, and inserted into the elongating axonal branches. Both α- and β-subunits of this dimer are delivered by the slow component of axonal transport.

1.4.2 Role of Cytoskeletal Proteins in Axonal Branching at the Growth Cone

As already indicated, the complicated interactions between actin filaments (F) and microtubules play a fundamental role in axonal regrowth, elongation, branching, and pathfinding (Tanaka and Sabry 1995). Still, the exact nature of F-actin-microtubule interactions in the axon growth cone is not well understood.

Growth cones at the tips of rapidly extending axons are small and highly active. However, in preparation for branching, they may pause for many hours, greatly enlarge, and maintain motility without a forward advance. Subsequently, a new growth cone develops from the tip of the large, pausing growth cone and forms a new leading axon. Remnants of the larger growth cone remain behind on the axon shaft as filopodial and lamellar expansions that subsequently give rise to axon collaterals (Halloran and Kalil 1994; Szebenyi et al. 1998).

Microtubules in the central region of advancing growth cones get stretched out. In slowly growing axons microtubules become bundled, and in pausing growth cones they form prominent loops (Tanaka and Kirschner 1991). Transition to new axonal growth and branch formation is accompanied by splaying of looped microtubules and formation of short microtubule fragments that invade the lamellipodium (Dent et al. 1999). Thus growth cone pausing is closely related to the mechanism of branching (Dent and Kalil 2001).

1.4.3 Role of Cytoskeletal Proteins in Collateral Axonal Branching at the Axon Shaft

Within the axon, the microtubule array is continuous from the cell body into the terminal growth cone, but individual microtubules vary in length, stopping and starting at various points within the array (Bray and Bunge 1981; Yu and Baas 1994). All microtubules have a consistent 13-protofilament lattice (Tilney et al. 1973; Burton et al. 1975) and are uniformly oriented with regard to their intrinsic polarity, with plus end directed away from the cell body (Heidemann et al. 1981; Baas et al. 1988).

Axons branch principally by the formation of collaterals rather than by bifurcation of the terminal growth cone (O'Leary and Terashima 1988). The generation of axon collateral branches involves a re-initiation of cell surface motility from regions of the axon that have been quiescent (Bastmeyer and O'Leary 1996). The first step of axon collateral branch formation involves the protrusion of filopodia from the axon shaft (Yu et al. 1994). Most of these filopodia have a short life, but a subset becomes stabilized by the entry of stable, though few, microtubules and

continues to grow, developing into collateral branches that can reach a significant length (Dent et al. 1999).

Results of Yu et al. (1994) show that the region of the parent axon, from which a collateral branch forms, contains about 20% less polymer compared to regions of parent axon not forming a branch. Moreover, there are ten times as many free microtubule ends and the microtubules on average are about ten times shorter. (That is to say, even in the reduced amount of polymer, ten times more free ends belong to unconsolidated microtubules.) The microtubules within the newly formed collateral branches are on average the same as within the parent axon, indicating that these microtubules were assembled in the parent axon and then transported into the branch. These observations provide strong support for the view that there is a local fragmentation of the microtubules during collateral branch formation.

1.5 The Individual Guidance Cues Promoting Reinnervation of Original Targets Are Still Unknown

As already mentioned in the section "Biological Significance of Axonal Branching", the process of Wallerian degeneration creates an environment that is highly supportive of axonal elongation. Two major groups of substances have been reported to be of decisive importance: (1) extracellular matrix (ECM) glycoproteins and (2) neurotrophic factors.

1.5.1 ECM Glycoproteins, Axonal Regrowth, and Pathfinding

Each myelinated axon and its ensheathing Schwann cell are enclosed in a basal laminar tube, made up of type IV collagen, laminin, heparin sulfate, and fibronectin (Tohyama and Ide 1984). All transection and laceration injuries disrupt the continuity of these tubes. Regenerating axons grow in furrows on the surface of Schwann cells within the basal lamina tube. Thus, intimate contact with Schwann cells and basal lamina seems to be an absolute prerequisite for good regeneration (Hall 1989). The Schwann cells increase the synthesis of the following adhesion molecules: N-cadherin and neural cell adhesion molecule (N-CAM) are integral membrane glycoproteins that are, respectively, the most abundant Ca^{2+}-dependent and Ca^{2+}-independent adhesion molecules present on vertebrate neuroectodermal cells. Both molecules promote cell adhesion via a homophylic mechanism, i.e., cell binding is mediated by the interaction of the same molecular species on apposing surfaces of interacting cells. The axons of differentiated neurons also express high levels of N-cadherin and N-CAM, and antibodies to these glycoproteins reduce the outgrowth of central and peripheral axons. These two molecules may therefore permit neurons to extend axons. The relatively uniform expression of *N*-cadherin and N-CAM in most parts of the nervous system suggests, however, that they do not play primary roles as directional guidance cues (Martini and Schachner 1988).

Laminin is a major component of substrate pathways over which developing axons project and has been shown to promote axon extension from both central and peripheral neurons. Laminin is not as widely expressed as N-CAM or N-cadherin and may therefore play a more specific role in promoting directional outgrowth in vivo. Laminin promotes axon extension by interacting with axonal glycoproteins that are members of the integrin family of receptors. The integrins are surface proteins consisting typically of noncovalently linked α and β subunits that mediate cell adhesion to other surface and ECM glycoproteins. Distinct ligand binding specificities result from the particular subunit combinations expressed by individual cells. Antibodies against integrins inhibit the extension of central and peripheral axons on laminin or ECM substrates.

Since laminin is not expressed in all regions of the nervous system, other cell surface or ECM molecules may also play important roles in axon extension: Ng-CAM/L1 (Daniloff et al. 1986), collagens (Siironen et al. 1992), fibronectin (Lefcort et al. 1992), and tenascin (Martini 1994; Martini et al. 1990) have been identified in the vicinity of outgrowing central and peripheral axons. However, these molecules are less effective than laminin in promoting axon growth in vitro, and their pattern of expression correlates less directly with axonal trajectories (Liuzzi and Tedeschi 1991).

1.5.2 Increased Production of Trophic Factors

The best characterized soluble neurotrophic agents are distributed into five different families:

1. The neurotrophins with the nerve growth factor (NGF), the brain-derived neurotrophic factor (BDNF), and the neurotrophins NT-3, NT-4, and NT-5
2. The neuropoietin family with the neurocytokine ciliary neurotrophic factor (CNTF)
3. The TGF-β superfamily with the glial-cell-line-derived neurotrophic factor (GDNF), neuturin (NTN), and parsephin
4. The fibroblast growth factor family with the basic fibroblast growth factor (bFGF, FGF-2), the acidic fibroblast growth factor (aFGF), and FGF-5
5. The somatomedin family with the insulin-like growth factor I (IGF-I) and IGF-II

In the nerve cells, the efficacy and the specificity of neurotrophic factors depend on the presence and amount of the respective receptors. The receptors for NGF, FGF-2, BDNF, GDNF, and IGF-I are synthesized by neurons and are up-regulated following axotomy (Meyer et al. 1992; Raivich and Kreutzberg 1993; McMahon and Priestley 1995). In theory, uptake of trophic factors produced by the distal nerve stumps could substitute for the target-derived amounts of trophic factors and keep the regenerating axons trophically satisfied until the axons regain their target-derived source (Toma et al. 1992; Unsicker et al. 1992).

CNTF is produced by the myelinating Schwann cells of the peripheral nerves (Henderson et al. 1994; Sendtner et al. 1994), but all the other factors are at

least in part target-derived, i.e., they are produced by the target tissue, taken up at synaptic terminals, and reach the neuronal somata via retrograde axonal transport (Taniuchi et al. 1988; Thoenen 1991). Accordingly, it has been shown that the intact facial nucleus of rats does not contain immunocytochemically detectable amounts of BDNF, CNTF, GDNF, or NGF (Stöckli et al. 1991; Baumgartner and Shine 1997). Furthermore, tissue from intact rat facial nucleus does not contain mRNA for BDNF, CNTF, and GDNF (Stöckli et al. 1991; Baumgartner and Shine 1997).

Neurotrophins

The facial motoneurons express a functional TrkB receptor for NT4/5 (Koliatsos et al. 1994; Yan et al. 1997) and in retrograde fashion readily transport NGF, NT-3, NT-4, and NT-5, all of which act to prevent injury-induced death of facial motor neurons in neonatal rats (Hughes et al. 1993; Koliatsos et al. 1993; Yan et al. 1993; Arenas and Persson 1994). Overexpression of NT-3 by facial motoneurons prevents their degeneration (Gravel et al. 1997).

BDNF is synthesized in skeletal muscle and, after peripheral nerve injury, in Schwann cells (Sendtner et al. 1994). It is retrogradely transported by the facial motoneurons (Yan et al. 1993). Neonatal and adult facial motoneurons have been shown to respond to the action of BDNF (Sendtner et al. 1992a; Hughes et al. 1993; Koliatsos et al. 1993; Clatterbuck et al. 1994; Fawcett et al. 1998; Gimenez y Robota et al. 1997; Veisada et al. 1994; Yan et al. 1994). Using in situ hybridization (ISH) and reverse transcription polymerase chain reaction (RT-PCR), Kobayashi et al. (1996) showed that after axotomy rat facial motoneurons increase the expression of BDNF and its receptor TrkB. The BDNF mRNA expression in the perikarya increased two- to fourfold. Since it is well known that BDNF may also be anterogradely transported to fibers and terminals (Fawcett et al. 1998), BDNF is considered to provide a mechanism for modulating cellular circuitry in the developing or injured nervous system.

The Neurocytokine CNTF

CNTF is neurotrophic for motoneurons during ontogenetic neuron death (Wewetzer et al. 1990; Oppenheim et al.1991) and rescues facial motoneurons after neonatal axotomy (Sagot et al. 1995; Sendtner et al. 1990, 1992b; Tan et al. 1996; Ulenkate et al. 1996; Gravel et al. 1997), an effect associated with increased expression of CNTF α-receptor (Duberly and Johnson 1996).

The TGF-β Superfamily

Recent studies have shown that GDNF is retrogradely transported to facial motoneurons (Yan et al. 1995), mRNA for the synthesis of the GDNF receptor has been detected in facial motoneurons (Glazner et al. 1998), and facial motoneurons have been shown to respond to the action of GDNF (Henderson et al. 1994; Zurn et al. 1994; Gimenez y Robota et al. 1997; Matheson et al. 1997; Sagot et al. 1996).

The Members of the Fibroblast Growth Family

Members of the FGF family (FGF-2, FGF-5) have been shown to exert neurotrophic activity for motoneurons in vitro (Hughes et al. 1993, 1993a; for review see Grothe

and Wewetzer 1996). Initially it was found that FGF-2 and FGF-5 did not rescue facial motoneurons after neonatal axotomy (Hughes et al. 1993). However, in a more recent work, Cuevas et al. (1995) demonstrated that treatment with FGF-1 increased the survival of axotomized neonatal rat facial motoneurons from 18% to 80% (i.e., 62% increase).

IGF-I

This member of the somatomedin family is able to rescue facial motoneurons following neonatal axotomy (Sendtner et al. 1990; Hughes et al. 1993). Muscle-derived IGF-I has been shown to promote survival and differentiation of facial motoneurons (Eustache et al. 1994).

Meanwhile, neurotrophic factors are among the most commonly proposed therapeutic agents in neurological diseases because of their role in promoting motoneuron cell survival during embryonic and early postnatal development. Still, even if all trophic factors are found to have a protective effect against specific causes of motoneuron injury, three major concerns must be raised with respect to their role in treatment. *First,* there has been no clear demonstration that any of the neurotrophic factors, which can enhance motoneuron repair and pathfinding, are deficient after the lesion. The *second* concern is the limited half-life of injected neurotrophic factors. *Third*, accumulating evidence shows that despite the abundance of local short-ranged guiding cues, the growth cones can actively choose their own way by releasing proteases that modify the immediate environment. Consequently, only a perfect synchronization between the degenerative changes in the distal nerve stump (usually containing most of the guiding cues) and the branching from the proximal nerve stump allows recovery of the original reinnervation (Brown and Hopkins 1981; Fu and Gordon 1995a, b; Dodd and Jessell 1988).

1.6 Conclusion

Peripheral nerve regeneration along the distal nerve stump is a pointless process unless the regenerating axons grow back to reinnervate their original muscle targets. There is no clinical evidence for any specificity in mammalian nerve regeneration; ECM proteins and/or neurotrophic factors that confer specificity on the regrowth of axons are unknown. Thus, if mechanisms exist in adult mammals to promote specific motor axon regeneration, they are clearly not strong enough to prevent the mismatching between motor neurons and muscles caused by the excessive axonal branching. Still, some results indicate that restoration of functionally correct connections after regeneration may occur. Classical experiments showing segmental selectivity in the post-transectional reconnection of autonomic preganglionic axons with postganglionic nerve cells (Langley, 1895) have been confirmed (Purves et al.1981). A degree of positional selectivity has also been shown in the reinnervation of the adult rat diaphragm and serratus anterior muscle (Laskowski and Sanes 1988) and in neonatal rats (Aldskogius and Thomander 1986).

1.7 Outline of the Clinical Problem

The facial nerve is the most frequently damaged nerve in head and neck traumata. Apart from traffic-accident injuries (temporal bone fractures, or lacerations of the face), most facial nerve lesions are postoperative (removal of cerebellopontine-angle tumors, parotid resections because of malignancy). Despite the use of fine microsurgical techniques for repair of interrupted nerves in man, the recovery of voluntary movements of all 42 facial muscles, and emotional expression of the face remains poor (Vaughan and Richardson 1993; Ferreira et al. 1994; Anonsen et al. 1986; Goodmurphy and Ovalle 1999).

The "post-paralytic syndrome", including mass movements (synkinesia) and altered blink reflexes (Kimura et al. 1975; Bento and Miniti 1993; Baker et al. 1994), has been attributed to (1) "misdirected" reinnervation (Montserrat and Benito 1988; Sumner 1990), (2) trans-axonal exchange of abnormally intensive nerve impulses between axons from adjacent fascicles (Sadjadpour 1975), and (3) alterations in synaptic input to facial motoneurons (Bratzlavsky and van der Eecken 1977; Graeber et al. 1993; Moran and Neely 1996).

The misdirected or "aberrant" reinnervation has been recognized as the major reason for the post-paralytic syndrome. At the site of injury it has two components: (1) perhaps due to an insufficient and/or malfunctioning axonal guidance, a muscle receives reinnervation by "alien" axons, which have been misrouted along the "wrong" nerve fascicle (Aldskogius and Thomander 1986); (2) due to the presence of competing supernumerary branches from all transected axons (Dyck and Hopkins 1972), one muscle fiber can be reinnervated by several motoneuronal axons (polyinnervation; Gorio et al. 1983; Fu and Gordon 1997).

Aberrant axonal sprouting has been also described during regeneration of the CNS and implicated in the development of post-traumatic epilepsy following brain trauma in man (McKinney et al. 1997) and in the pathogenesis of Alzheimer's disease (Masliah et al. 1991). Whereas numerous aspects of post-traumatic aberrant reinnervation of muscles have been extensively studied, no experimental approaches have been thus far identified that are able to interfere with this peripheral phenomenon. Attempts to counteract with aberrant reinnervation and thus achieve a "topographic" specificity have been made using fascicular surgical repair in rats (Mackinnon et al. 1986; Evans et al. 1991). These attempts, however, had little success. So far it is technically impossible to properly steer the growth cones of several thousands axons growing out from the proximal stump of a transected nerve. Likewise, efforts to reduce the degree of axonal branching in rats using an artificial conduit as a guiding scaffold have been unsuccessful: the process of axonal branching follows a rather constant pattern irrespective of local alterations of the extracellular matrix.

1.8
Question Still Open

The present synopsis of our results should provide answers to three direct questions:

1. Trying to act at the level of the axotomized perikarya, can qualitative alterations of their afferents (from the trigeminal nuclei and/or from the cerebral cortex) lead to reduction of collateral axonal branching?
2. Trying to act at the level of the lesion, can local application of agents, which are known to foster neurite elongation, suppress axonal branching?
3. Does reduced collateral axonal branching improve the specificity of reinnervation?

1.9
Methodological Approach

The answers to these questions have been sought by an extensive and combined methodological approach consisting of:

1. Simultaneous multiple fluorescent neuronal labeling to quantitatively estimate the degree of axonal branching (Angelov et al. 1999; Dohm et al. 2000; Guntinas-Lichius et al. 2001; Streppel et al. 2002)
2. Successive pre- and postoperative retrograde fluorescent neuronal labeling to study the accuracy of target reinnervation (Popratiloff et al. 2001; Guntinas-Lichius et al. 2002; Skouras et al. 2002; Tomov et al. 2002)
3. Investigation into the biometrics of whisking behavior, which provides a very sensitive tool for study of facial nerve regeneration (Guntinas-Lichius et al. 2001; Tomov 2002)

2
Materials and Methods: Experimental Sets

In this synopsis we summarize and discuss several experiments, which can be divided into two sets. In the first we report on our efforts to reduce post-transectional axonal branching, trying to "calm down" the axotomized and hence hyperexcitable *facial perikarya* by altering both their trigeminal and cortical input.

In the second set we describe several experiments in which we tried to reduce collateral axonal branching at the *site of lesion*.

Before and after experiments, all rats used for this report were kept on standard laboratory food (Altromin, 32791, Lage, Germany) and tap water ad libitum with an artificial light–dark cycle of 12 h on, 12 off. All experiments were conducted in accordance with the German Law for Animals Protection and were approved by the local animal care committee (Bezirksregierung Köln).

1.8
Question Still Open

The present synopsis of our results should provide answers to three direct questions:

1. Trying to act at the level of the axotomized perikarya, can qualitative alterations of their afferents (from the trigeminal nuclei and/or from the cerebral cortex) lead to reduction of collateral axonal branching?
2. Trying to act at the level of the lesion, can local application of agents, which are known to foster neurite elongation, suppress axonal branching?
3. Does reduced collateral axonal branching improve the specificity of reinnervation?

1.9
Methodological Approach

The answers to these questions have been sought by an extensive and combined methodological approach consisting of:

1. Simultaneous multiple fluorescent neuronal labeling to quantitatively estimate the degree of axonal branching (Angelov et al. 1999; Dohm et al. 2000; Guntinas-Lichius et al. 2001; Streppel et al. 2002)
2. Successive pre- and postoperative retrograde fluorescent neuronal labeling to study the accuracy of target reinnervation (Popratiloff et al. 2001; Guntinas-Lichius et al. 2002; Skouras et al. 2002; Tomov et al. 2002)
3. Investigation into the biometrics of whisking behavior, which provides a very sensitive tool for study of facial nerve regeneration (Guntinas-Lichius et al. 2001; Tomov 2002)

2
Materials and Methods: Experimental Sets

In this synopsis we summarize and discuss several experiments, which can be divided into two sets. In the first we report on our efforts to reduce post-transectional axonal branching, trying to "calm down" the axotomized and hence hyperexcitable *facial perikarya* by altering both their trigeminal and cortical input.

In the second set we describe several experiments in which we tried to reduce collateral axonal branching at the *site of lesion*.

Before and after experiments, all rats used for this report were kept on standard laboratory food (Altromin, 32791, Lage, Germany) and tap water ad libitum with an artificial light–dark cycle of 12 h on, 12 off. All experiments were conducted in accordance with the German Law for Animals Protection and were approved by the local animal care committee (Bezirksregierung Köln).

2.1 First Set of Experiments: Attempts to Reduce Collateral Axonal Branching by Alterations of the Trigeminal Input to the Facial Perikarya

The rationale for this experimental set was the fact that the abnormal activity pattern of the axotomized facial motoneurons is a key issue in the pathogenesis of axonal branching. On one side, the increase in resting potential and the presence of still-functioning axo–dendritic synapses (Sumner and Watson 1971; Lux and Schubert 1975) render them hyperexcitable upon intracellular current injections (Eccles et al. 1958; Ferguson 1978). On the other side, the decreased synthesis of transmitter-related compounds (Lieberman 1971) and reduced axo-somatic synaptic input (Blinzinger and Kreutzberg 1968), make the axotomized facial motoneurons less excitable upon afferent stimulation and unable to discharge (Titmus and Faber 1990).

At the initial stage of our work we hypothesized that the abnormal activity, i.e., the axotomy-caused "silence" of the facial motoneurons, could be improved by alterations in the input from the trigeminal sensory nucleus. Support to this hypothesis is found in anatomical, electrophysiological, and clinical evidence for involvement of the trigeminal system in the generation of facial muscle responses and blink reflexes (Moller and Jannetta 1986; Valls-Sole and Tolosa 1989). To test our hypothesis we compared behavioral, physiological and morphological parameters after reconstructive surgery on the facial nerve and its branches (e.g., the buccal branch) with those obtained after identical surgery but combined with lesions of the ipsilateral or contralateral trigeminal ganglion cells.

One hundred and seventy-three adult female Wistar rats (175–200 g; strain HsdCpb:WU; Harlan Winkelmann, Borchen, Germany) were used in five different sets of experiments and the rats were accordingly distributed in five major experimental groups (A, B, C, D, E). We tried to elucidate the:

- Effect of altered trigeminal input to axotomized facial perikarya on *axonal branching* (rats were distributed in groups A_1–A_{17})
- Effect of altered trigeminal input to axotomized facial perikarya on the *rate of axonal elongation* (groups B_1–B_4)
- Effect of altered trigeminal input on the *accuracy of reinnervation* estimated by sequential intramuscular injection of neuronal tracers (groups C_1–C_4)
- Effect of altered trigeminal input to axotomized facial perikarya on the *compound muscle action potential (CMAP)* of the vibrissal muscles as established by electrophysiological measurements (groups D_1–D_4)
- Effect of altered trigeminal input to axotomized facial perikarya on the recovery of coordinated facial muscles' activity estimated by video-based motion analysis of the vibrissae movements (groups E_1–E_{16})

In a subsequent part of our work we studied the effect of putatively enlarged cortical representation of the vibrissae on the quality of target reinnervation and compared morphological and physiological parameters of post-transectional fa-

cial nerve recovery between visually normal and blind rats. For this separate experiment we used 48 Sprague-Dawley rats, divided in groups F_1 and F_2.

2.1.1 Effect of Altered Trigeminal Input to Facial Perikarya on Axonal Branching as Estimated by Application of Crystalline Tracers to Transected Superior and Inferior Buccolabial Nerves

Animals

Group A consisted of 64 rats divided into seven subgroups (A_1–A_7). The rats of subgroup A_1 (10 animals) served as normal unoperated control. The animals of subgroups A_2, A_3, and A_4 (each of 12 rats) were used for comparative assessment of axonal regrowth and branching by means of retrograde neuronal labeling with tracer crystals. All rats were subjected to identical transection and suture of the right buccal branch of the facial nerve (buccal–buccal anastomosis, BBA). The rats of subgroup A_2 were subjected to BBA only. The animals of subgroup A_3 underwent BBA plus excision of the ipsilateral (right) infraorbital nerve (ION) and those of subgroup A_4 BBA plus excision of the contralateral (left) ION. Retrograde labeling was performed 28 days after surgery and 4–5 days after retrograde labeling the animals were sacrificed. The survival time was selected according to behavioral observations showing initial restoration of rhythmic vibrissae whisking after this period.

The animals of subgroups A_5, A_6, and A_7 (each of 6 rats) served to estimate the retraction of axonal branches (pruning or elimination of branches) after BBA. The rats of subgroup A_5 underwent BBA only, those of A_6, BBA plus excision of the ipsilateral (right) ION and those of group A_7, BBA plus excision of the contralateral (left) ION. The survival time was 112 days post surgery and 116–117 days post retrograde labeling.

Buccal–Buccal Anastomosis

All operations were carried out under an operating microscope by trained microsurgeons (OGL and MS). After intraperitoneal injection of Ketamin plus Xylazin [100 mg Ketanest (Parke-Davis, Berlin) plus 5 mg Rompun (Bayer, Leverkusen, Germany) per kg body weight], the buccal branch of the facial nerve was exposed, transected, and immediately sutured with one epineural atraumatic 11–0 suture (Ethicon, Braunschweig, Germany). Since one experimental set of the present study (group C) focused on the accuracy of post-transectional reinnervation by the buccal branch of the facial nerve, we had to eliminate any additional innervation to the whisker pad muscles by the marginal mandibular branch (Semba and Egger 1986). This is the reason why BBA was always accompanied by transection and proximal ligature (to prevent regeneration) of the marginal mandibular branch of the facial nerve (Fig. 1).

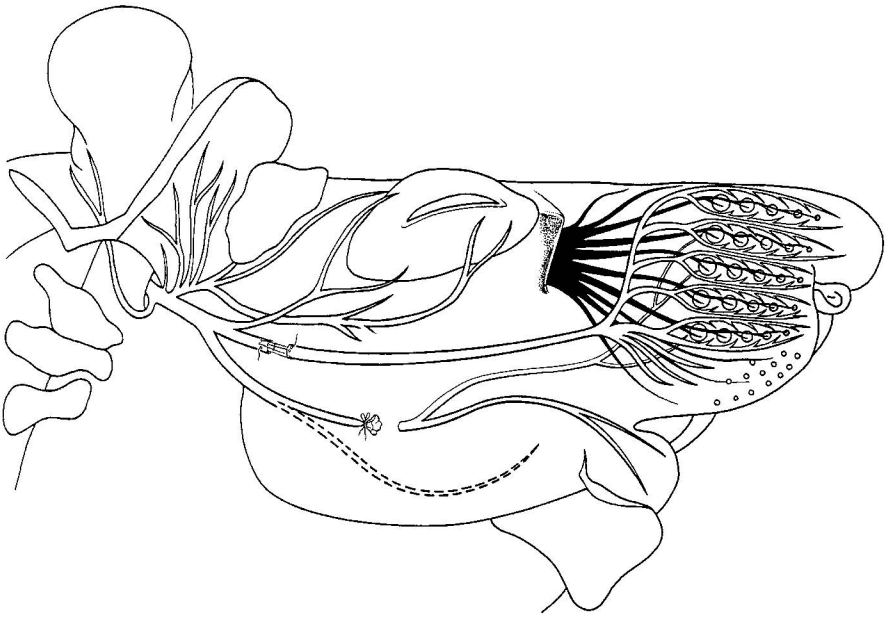

Fig. 1 Schematic drawing illustrating the close relationship between the peripheral fascicles of the facial nerve and those of the infraorbital nerve (*in black*) and the sites of transection and suture in the buccal branch and of the transection and ligature of the marginal mandibular branch of the facial nerve. The cervical branch of the facial nerve is indicated by a *dotted line*. (Adapted from Dörfl 1985 and Semba and Egger 1986; reprinted from Skouras et al. 2002, with permission from IOS Press)

Excisions of ION

Were performed only in combination with BBA. Under Ketamin/Xylazin anesthesia, the infraorbital nerve ipsi- or contralateral to the side of BBA was transected at its exit from the infraorbital foramen and all its peripheral fascicles were removed (resection paradigm). The aim of this combined facial and trigeminal surgical treatment was to prove whether alterations in the trigeminal input to the axotomized facial motoneurons would reduce the number of branches emerging from the transected facial axons. The rationale takes the existence of direct ipsilateral and "crossed" connections between the trigeminal and facial nucleus into consideration (Kimura and Lyon 1972; Erzurumlu and Killackey 1979; Travers and Norgren 1983; Isokawa-Akesson and Komisaruk 1987).

In subgroups A_2–A_7 we performed combined surgery on the buccal facial nerve branch and the infraorbital nerve but studied axonal regrowth only into the distal stump of the buccal nerve and its bifurcation. Our aim was to estimate both regrowth and collateral branching of transected axons (Brown and Hopkins 1981; Jenq and Coggeshall 1984; Duncan and Baker 1987; Brushart 1993). To this end, we counted neurons labeled by the fluorescent retrograde tracers FG and DiI applied to the superior and inferior buccolabial nerves (Fig. 2).

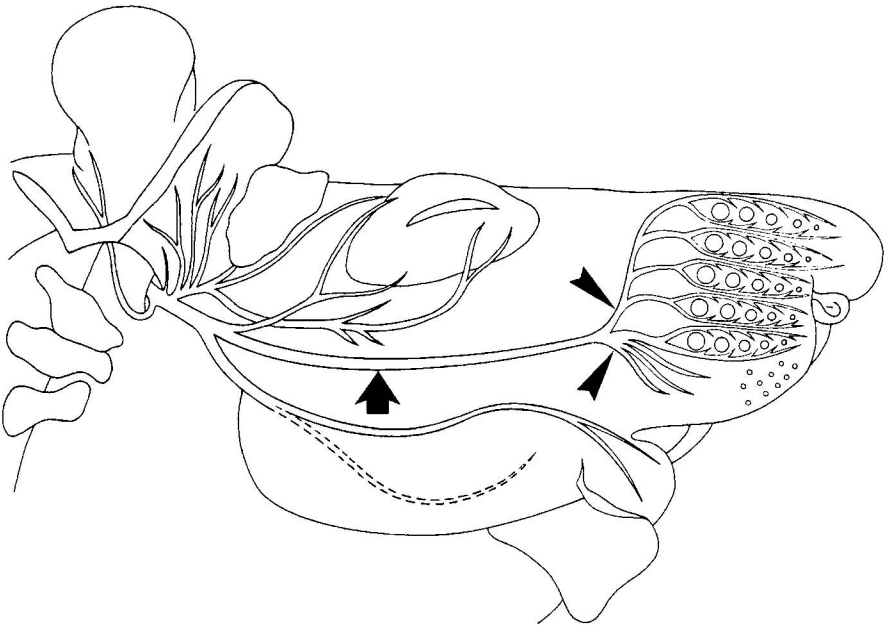

Fig. 2 Schematic drawing of all fascicles of the infratemporal portion of the rat facial nerve. *Large arrow* indicates the transection and suture site in the buccal branch of the facial nerve. Transection and tracer application sites in the superior and inferior buccolabial nerves are indicated by *arrowheads*. (Reprinted from Angelov et al. 1999)

Retrograde Neuronal Labeling with Two Crystalline Tracers

In four anesthetized animals of subgroup A_1 (unoperated control animals), the right superior and inferior buccolabial nerves were transected and labeled with crystals of 1,1'-dioctadecyl-3,3,3',3'-tetramethylindo-carbocyanine perchlorate (DiI; Molecular Probes, Leiden, Netherlands) or Fluoro-Gold (FG; Fluorochrome Inc., Denver) respectively. In the other four animals of this subgroup, the tracers were interchanged, i.e., crystals of DiI were applied to the transected inferior and crystals of FG to the transected superior buccolabial nerve. Identical bilateral labeling was done 28 days or 112 days after surgery in all other subgroups.

Fixation and Tissue Processing

Five days after the bilateral double labeling, rats were transcardially perfused with 0.9% NaCl in distilled water for 60 s followed by a fixation with 4% paraformaldehyde in 0.1 M phosphate buffer pH 7.4 for 20 min under deep ether anesthesia. After removal of the whole brain, the brainstem was cut into 50-µm-thick coronal sections on a vibratome (FTB-vibracut; Plano, Marburg, Germany).

Microscopy

Vibratome sections were observed through Filter Set 01 (Excitation BP 365/12, Emission LP 397; Cark Zeiss AG, Göttinger, Germany), which allows recognition

of FG-labeled motoneurons (appearing white). Observations through Filter Set 15 of Carl Zeiss (Excitation BP 546/12, Emission LP 590) revealed all motoneurons retrogradely labeled by DiI (appearing red). There was no fluorescence "cross-talk" between the two tracers used, i.e. no DiI-labeled cells were visible through Filter Set 01 and no FG-labeled motoneurons could be observed using Filter Set 15. Employing a CCD Video Camera System (Optronics Engineering Model DEI-470, Goleta, CA, USA) combined with the image analyzing software Optimas 6.1 (Optimas Corporation, Bothell, Washington, USA), the image observed with Filter Set 01 was superimposed on the image taken with Filter Set 15. The FG/DiI combined pictures of all unlesioned and lesioned facial nuclei in each of 30–33 vibratome sections per animal were saved in a color-coded TIFF file format. For manual counting of retrogradely labeled motoneurons, the necessary TIFF file was simply loaded.

Quantitative Determination

Single postoperative retrograde labeling of facial motoneurons with HRP injected into the whisker pad has shown that the reinnervation of the whisker pad muscles after transection and suture of the main trunk of the facial nerve causes qualitative and quantitative changes (Thomander 1984; Aldskogius and Thomander 1986; Angelov et al. 1993, 1996). The qualitative changes are represented by the complete lack of myotopic organization: HRP-labeled motoneurons are scattered throughout the whole facial nucleus. This loss of myotopic organization in the facial nucleus following transection of the peripheral nerve is a direct morphological proof for the occurrence of "misdirected reinnervation" (termed also "misdirected resprouting", "excessive reinnervation", "aberrant reinnervation", "aberrant regeneration", or "misdirected regrowth of axons"). The quantitative changes of misdirected reinnervation we called hyper-innervation, since our counts of HRP-labeled cells showed that, following facial-nerve surgery there were up to 60% more motoneurons projecting into the whisker pad muscles than under normal conditions (Angelov et al. 1996; Streppel et al. 1998). Therefore, we also evaluated the reinnervation in quantitative manner in the present report.

Counting

Employing the fractionator principle (Gundersen 1986; Guntinas-Lichius and Neiss 1996), all retrogradely labeled motoneurons with a clearly discernible nucleus in the 50-µm-thick sections were counted in every third section through the facial nucleus on both the operated and unoperated side (Neiss et al 1992; Guntinas-Lichius et al. 1993; Valero-Cabre et al. 2004).

Statistical Evaluation

All values are given as means±SD or as percentages of the total number of labeled motoneurons. To determine whether the difference in number of the labeled neurons between the control and the experimental subgroups was statistically significant, a one-way ANOVA followed by a post hoc Bonferroni-Holm correction

(Holm 1979) were applied. A *P* value of less than 0.05 was considered to indicate statistically significant differences.

2.1.2
Effect of Altered Trigeminal Input on the Rate of Axonal Elongation

Animals
Group B consisted of 24 rats which were divided into four subgroups (B_1–B_4, 6 rats per subgroup). Animals of subgroup B_1 served as intact control animals. The remaining 18 rats underwent surgery identical to that of subgroups A_2–A_4. These animals served to provide anatomical evidence for differences in the rate of axonal elongation among the three different types of surgery. Intramuscular injection of the retrograde neuronal label Fast Blue (FB; EMS-Chemie GmbH, D-64818 Groß-Umstadt, Germany) was performed on the 3rd day after surgery. Animals were fixed by perfusion fixation 24 h later and tissue was processed and analyzed as described above.

To assess the rate of axon elongation we chose to select a single postoperative time point and to count the number of motoneurons projecting into a selected target after intramuscular injection of a retrograde label. Based on our behavioral observations (see Results) we decided to apply the label on the 3rd day after surgery. Ideally, this postoperative survival period would result in retrograde labeling only in the group with unilateral BBA plus excision of the contralateral infraorbital nerve.

Surgery
These surgical procedures were identical to those described in the previous section.

Retrograde Labeling by Intramuscular Application of a Tracer
The fluorescent retrograde label FB was injected bilaterally, i.e., both on the operated side and on the contralateral side. As we wanted to compare the number of retrogradely labeled motoneurons in different animals, particular care was taken to ensure identical injection conditions in each animal. Under deep ether anesthesia, 1 mg FB (dissolved in 100 µl distilled water containing 2% dimethyl sulfoxide) was injected under the skin always at the identical site, exactly in the mid-point between the two dorsal vibrissal rows A and B (Arvidsson 1982, Angelov et al. 1993 1996; Streppel et al. 1998; Fig. 3).

Fixation and tissue processing were identical to those described in Sect. 2.1.1.

Microscopy
Vibratome sections were observed through Filter Set 01 of Carl Zeiss (Excitation BP 365/12, Emission LP 397), which allows recognition of FB-labeled motoneurons (appearing blue). The pictures of all unlesioned and lesioned facial nuclei in each of 30–33 vibratome sections per animal were saved in a TIFF file format.

Counting and statistical evaluation were performed as described in Sect. 2.1.1.

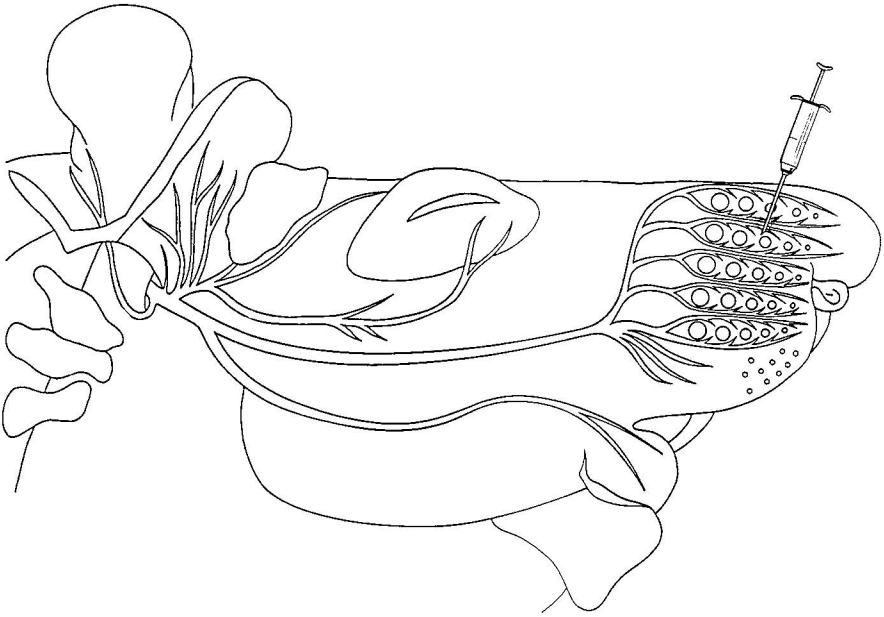

Fig. 3 Schematic drawing of the extratemporal rat facial nerve indicating the site of intramuscular injection of Fluoro-Gold and Fast Blue. (Adapted from Dörfl 1985, Semba and Egger 1986; reprinted from Popratiloff et al. 2001)

2.1.3 Effect of Altered Trigeminal Input to Axotomized Facial Perikarya on the Accuracy of Reinnervation

Animals

Group C consisted of 41 rats distributed in four subgroups (C_1–C_4). These rats were used for counts after retrograde labeling of facial motoneurons by intramuscular application of tracers. The animals of subgroup C_1 (14 rats) were unoperated controls. Four of them were injected with 1% FG into the right whisker pad and with 1% FB into the left whisker pad. Another 4 rats were injected with FB into the right whisker pad and with FG into the left whisker pad. These experiments established whether both tracers had similar efficiency in retrograde neuron labeling. Six other rats of the same subgroup were injected with 1% FG into the right whisker pad and with 1% FB injected at the same site 28 days later. These experiments tested whether the sequential injection of FG and FB in identical muscles can provide a reliable distinction between the FG-, FB-, and FG+FB-labeled neurons.

All nine animals of subgroup C_2 received a bilateral intramuscular injection of FG. After 10 days they underwent unilateral BBA only. After further 28 days, a bilateral postoperative labeling with FB was performed at the site of the earlier

FG injection. The aim of this postoperative labeling was not only to depict the motoneurons projecting into the selected muscles after surgery, but also to compare their location and number with those of the original innervation pool that were permanently labeled by the non-degradable tracer FG.

The rats of subgroup C_3 (nine animals) underwent identical preoperative labeling with FG. The postoperative labeling with FB was done 28 days after BBA and excision of the ipsilateral ION.

All nine rats of subgroup C_4 underwent preoperative labeling with FG and postoperative labeling with FB 28 days after BBA and excision of the contralateral ION.

Surgical procedures, retrograde labeling with intramuscular application of a tracer, fixation, and tissue processing were performed as described in Sect. 2.1.1.

Microscopy

Using standard procedures, FG and FB were simultaneously visualized with the same UV epi-fluorescence excitation filter (Zeiss, Filter set 01). However, previous experiments had shown that the blue emission of FB obscured the white emission of FG resulting in the demonstration of far too low numbers of FG-labeled neurons. Thus, the quantitative analysis of FG+FB double labeling required selective custom-made filter sets that exclude most fluorescence crosstalk between FG and FB, but also reduce sensitivity (Popratiloff et al. 2001a).

To demonstrate FG a HQ-Schmalband-filter set (no. F36–050; excitation D 369/40; beamsplitter 400DCLP; Barrierfilter HQ 635/30 supplied by AHF Analysentechnik Tübingen, Germany) was used. To demonstrate FB a bandpass-filter set (no. F31–000; excitation D 436/10; beamsplitter 450 DCLP; Barrierfilter D470/40, AHF Analysentechnik) was used. Employing these selective special filter sets and a CCD Video Camera System (Optronics Engineering) combined with the image-analyzing software Optimas 6.5., separate images of the FG and FB retrogradely labeled facial motoneurons were created. The generated masks of FG-labeled cells were superimposed over the FB image for the unlesioned as well as for the lesioned facial nucleus. With this approach, all cells stained by FG, FB, and double-labeled by FG+FB could be readily identified and counted.

Counting and statistical evaluation were performed as described in Sect. 2.1.1.

2.1.4
Effect of Altered Trigeminal Input to Axotomized Facial Perikarya on the Compound Muscle Action Potential (CMAP) of the Vibrissal Muscles

Animals

Group D consisted of 20 animals that served for electrophysiological evaluations. Rats were divided into four subgroups each consisting of five animals: D_1, intact rats (control group); D_2, rats with unilateral BBA_{only}; D_3, rats with BBA plus excision of the ipsilateral ION; and D_4, rats with BBA plus excision of the contralateral ION. Recordings were performed 28 days after surgery.

Ideally, the electrophysiological tests should be performed on the same rats as were injected with the retrotracers. This would, of course, provide the most accurate correlation between the two methods. Recently, however, Naumann et al. (2000) provided evidence for possible neurotoxic effects of FG in the medial septal nucleus/diagonal band complex about 6 weeks after retrograde labeling. Although this study focused on a different system and utilized a prolonged "post-labeling" period, we decided to avoid a potential risk of neurotoxicity by conducting the electrophysiological tests on rats that had not been injected with FG.

Stimulation and Recording

Animals were deeply anesthetized with Nembutal (40 mg/kg body weight) and the body temperature was controlled during the entire recording session. Stimulation and recording were performed with a Neuropack 2 (Nihon Kohden Co., 1–31–4 Nishlochial, Shinjuku-ku, Tokyo) employing hooked subcutaneous silicone-coated silver wire electrodes (AG-10T; Science Products GmBH, Hofheim, Germany). The silicone coating at the electrode tip was removed to allow adequate conduction.

Each electrode was inserted into a 20 G needle and hooked over its end. After insertion, the needle was gently retracted, leaving the electrode under the skin. In some animals, this procedure caused bleeding associated with a decline of the recorded signal. In these animals, all further experiments were cancelled. The monitor was set to display 20 ms triggered by each stimulus. Recorded signals below 100 Hz and above 10 KHz were cut off. Stimulation was applied in the "current mode" of Neuropack 2.

Two stimulation electrodes were placed subcutaneously just in front of the anterior edge of the parotid gland, one above and one below the buccal branch of the facial nerve. The distance between the two electrodes was approximately 5 mm. For recordings, a monopolar electrode was placed between the middle vibrissal rows C and D (Arvidsson 1982). Recordings were made with a negative-active electrode. On all traces, depolarization of the muscles was indicated by a negative deflection.

To avoid interference from the excitation of other facial muscles, the reference (indifferent) recording electrode was placed at a site as close as possible to the recorded ipsilateral vibrissal muscles. However, this procedure could not always be performed perfectly. The innervation domain of the buccal branch, i.e., the piloerector muscles and the levator labii superioris muscle, often receive a thin communicating branch from the marginal mandibular branch of the facial nerve (Semba and Egger 1986). In these cases, we had to attach the indifferent recording electrode proximal to the adjoining point of the communicating branch, which was distal from the whisker pad musculature. Animals were grounded with the aid of a subcutaneous stainless steel needle.

Providing valuable information about the extent of reinnervation and the speed of motor axon conduction, these experiments were designed to evaluate the compound muscle action potential (CMAP) generated by the whisker pad muscles after supramaximal stimulation of the buccal branch of the facial nerve. Once a maxi-

mal stimulus had been identified, the stimulation current was increased by 10%. Usually 7–10 CMAPs were recorded.

Quantitative Analysis of the Electrophysiological Measurements

Two parameters were taken into account: (1) the duration and (2) the amplitude of CMAP. The amplitude was expressed as difference between the maximum peak of CMAP and the base line (in mV). The duration of CMAP was calculated by the distance between the points where the baseline was crossed by the rising and declining curves of the CMAP. For quantitative and qualitative purposes the mean duration and amplitude of each experimental subgroup (D_2–D_4) were compared with values obtained in unoperated control animals. The Kolmogorov–Smirnov one-sample test was used to test the normal distribution within the groups. All values are given as means±SD (standard deviation). Statistical comparisons of the CMAP measurements among the four groups were performed with ANOVA and followed by a Dunett T3 post hoc test. A *P* value of less than 0.01 was considered to indicate statistical significance. Unpaired *t*-test was used to prove whether the mean values for duration and amplitude of CMAPs were significantly different between each experimental group and the control group.

2.1.5 Effect of Altered Trigeminal Input on the Recovery of Vibrissae Motor Performance Estimated by Video-Based Motion Analysis

Animals

Group E consisted of 24 rats that were divided into four subgroups each consisting of six animals: E_1, intact rats (control group); E_2, rats with unilateral facial–facial anastomosis (FFA_{only}); E_3, rats with FFA plus excision of the ipsilateral ION; and E_4, rats with FFA plus excision of the contralateral ION. To analyze the recovery progress in motor performance rats were videotaped 2, 4, 6, and 12 months after surgery.

Surgery

Transection and immediate end-to-end suture of the right facial nerve (facial–facial anastomosis, FFA) was performed in 18 animals (6 from subgroup E_2, 6 from subgroup E_3, and 6 from subgroup E_4). Following an intraperitoneal injection of Ketamin/Xylazin, the main trunk of the facial nerve was exposed and transected close to its emergence from the foramen stylomastoideum but distal to the posterior auricular branch. The proximal stump was then microsurgically reconnected to the distal stump with two 11–0 atraumatic sutures (Ethicon EH 7438G, 22851 Norderstedt, Germany; Fig. 4). Finally the wound was closed by three 4–0 skin sutures (Ethicon). The rats of subgroups E_3 and E_4 were subjected to excision of the ipsi- or contralateral ION respectively (see Sect. 2.1.1).

The degree of post-transectional recovery of vibrissal motor performance was estimated at four post-operative survival periods, i.e., 2, 4, 6, and 12 months after

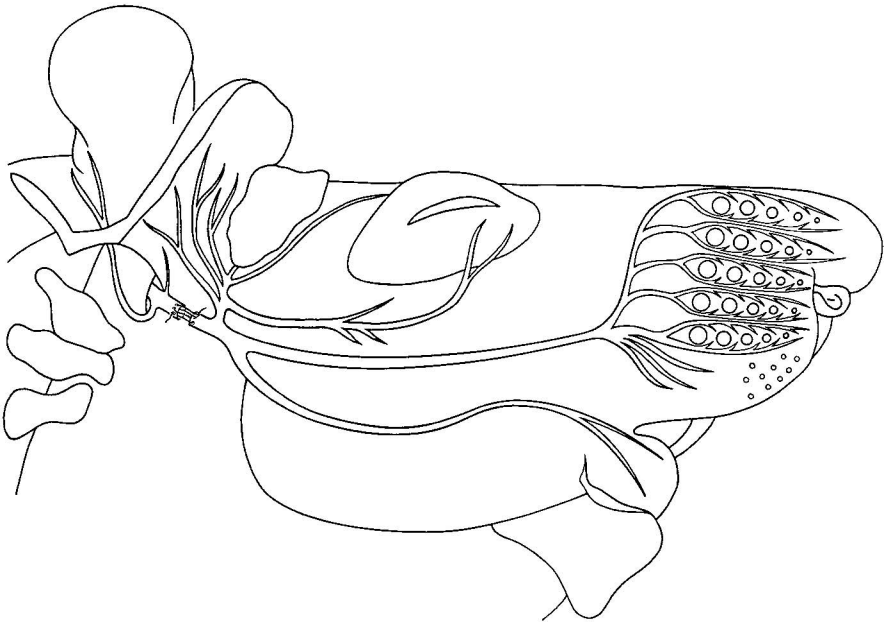

Fig. 4 Schematic drawing of the infratemporal portion of the rat facial nerve indicating the site of transection and end-to-end suture of the facial nerve trunk, i.e., facial–facial anastomosis (FFA). (Reprinted from Popratiloff et al. 2001)

any kind of surgery. Under normal physiological conditions, the mystacial vibrissae of the rat simultaneously sweep, performing thus an explorative "whisking" or "sniffing." The key movements of this motor activity are the protraction (Fig. 5A) and retraction (Fig. 5B) of the vibrissal hairs by the piloerector muscles. All muscles are innervated by the buccal branch of the facial nerve (Dörfl 1985).

Videotaping

Only two large vibrissae of the caudal "C-row" on each side of the face were used for biometric analysis. Under light ether anesthesia, all other vibrissae were clipped with small fine scissors. Thereafter the animals were inserted into a rodent restrainer (Hugo Sachs Electronik–Harvard Apparatus GmbH, March-Hugstetten, Germany) and left in peace for approximately 30 min to calm down. Video-taping of the whisking (retraction and protraction) of the C-row vibrissae followed. Employing a digital camcorder (Panasonic NV DX-110 EG) animals were video-taped for 3–5 min during active exploration. After calibration, video images of whisking behavior were sampled at 50 Hz (50 fields per second), the video-camera shutter opened for 4 ms. Images were recorded on professional Panasonic AY-DVM60XK digital video cassettes (Matushita, Osaka). Captured video sequences were reviewed and 1.5 s sequence fragments from each animal selected for analysis of whisking biometrics. Thereby, the stable position of the animal's head, the fre-

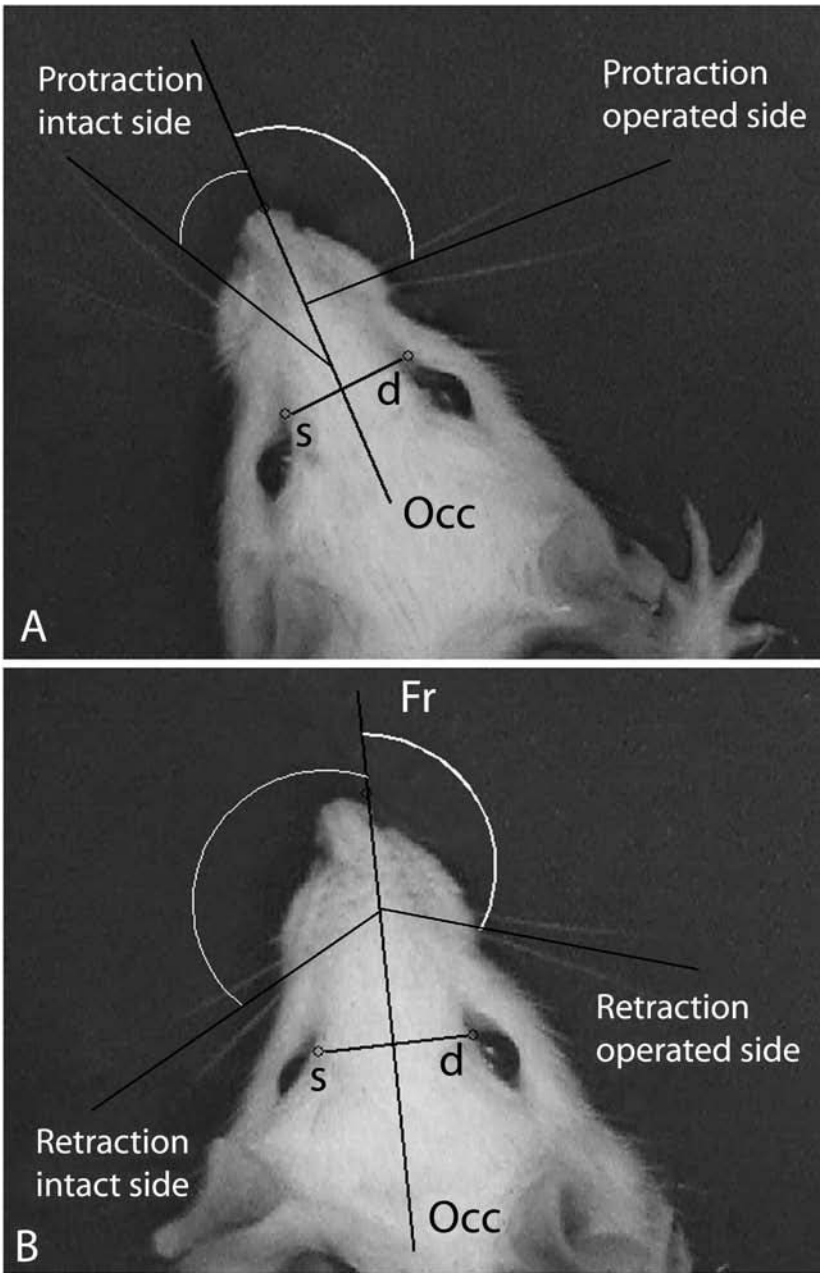

Fig. 5 Analysis of the vibrissae motor performance with precise measurement of angles, angular velocity, and angular acceleration of the intact (*s*) and operated side (*d*) during protraction (**A**) and retraction (**B**) of the vibrissae. Note the significant change in angle between the *sagittal line Fr-Occ* during protraction and retraction on the intact side. The vibrissae on the operated side remain stiff. (Reprinted from Tomov et al. 2002)

quency of whisking, and the degree of vibrissae protraction were considered as selection criteria (Tomov et al., manuscript in preparation).

Data Acquisition and Analysis

Selected sequences were captured by a 2D/Manual Advanced Video System (PEAK Motus 2000, PEAK Performance Technologies, Inc., Englewood, CO, USA). The spatial model consisted of three reference points (Fig. 5):

1. A point in the medial sagittal line Fr-Occ (perpendicular to a line connecting both orbits) close to the end of the nose. We selected this reference point because the permanent sniffing movements of the nose tip would jeopardize the measurements.
2. A point corresponding to the medial angle of the left (s) orbit.
3. A point corresponding to the medial angle of the right (r) orbit.

Parameters

Each vibrissa was represented in the spatial model by two points—its base and a point on the shaft 0.5 cm distal to the base. Using this model we were able to collect and evaluate data on:

- Protraction (forward movement of the vibrissae) as measured by the rostrally open angle (in degrees) between the mid-sagittal plane and the hair shaft, maximal protractions represented by minimal angles (Fig. 5A)
- Whisking frequency in cycles of protraction and retraction (passive backward movement, Fig. 5B) per second
- Amplitude (the difference between maximal retraction and maximal protraction in degrees)
- Angular velocity during protraction (in degrees per second)
- Angular acceleration during protraction (in degrees per second^2)

2.1.6 Effect of Putatively Enlarged Cortical Representation of the Vibrissae in Blind Rats on the Quality of Target Reinnervation

Animals

Group F consisted of 48 rats. Subgroup F_1 consisted of 24 adult female Sprague-Dawley rats with normal visual perception (purchased from Charles River, Sulzfeld, Germany). Subgroup F_2 consisted of 24 blind adult female Sprague-Dawley (SD) rats (substrain Royal College of Surgeons, RCS). The RCS rats lose their photoreceptor cells 2 weeks after birth due to a genetic defect of the retinal pigment epithelium (Sheedlo et al. 1991; D'Cruz et al. 2000;). Thus, the mystacial vibrissae are the only available means for these animals to receive and resolve spatial information (Brecht et al. 1997).

These animals were used in three experimental sets. In the first set we compared the accuracy of postoperative target reinnervation between six visually normal SD rats and six blind SD/RCS rats using pre- and post-transectional labeling of motoneurons after intramuscular injections of the retrograde tracers FG and FB (cf. Sect. 2.1.2.).

In a second experimental set, the degree of post-transectional axonal branching between six visually normal SD rats and six blind SD/RCS rats was compared using retrograde labeling with three different fluorescent dyes applied simultaneously to three different branches of the facial nerve.

In a third experimental set, the degree of post-transectional recovery of vibrissal motor performance between six visually normal SD rats and six blind SD/RCS rats was compared using video based motion analysis. Two months after end-to-end suture of the right facial nerve (facial–facial anastomosis, FFA) they were videotaped and thereafter operated for triple retrograde labeling. Six animals from subgroups F_1 and F_2 were used as intact controls to establish the normal extent of labeling after intra-muscular injections of retrograde tracers. Another six animals taken from subgroups F_1 and F_2 were used as intact controls to demonstrate the normal extent of triple retrograde labeling.

Surgery, sequential retrograde labeling, fixation, tissue processing, microscopy, counting, and statistical evaluations were performed as described in Sect. 2.1.1.

Retrograde Labeling with Three Tracers

All operations were carried out under microscope by trained microsurgeons (MS and OGL). After intraperitoneal injection of Ketamin plus Xylazin (100 mg Ketanest plus 5 mg Rompun per kg body weight), the zygomatic, buccal, and marginal mandibular branches of the facial nerve in all rats were transected and crystals of DiI, FG, and FB applied to them (Fig. 6). Ten days later, the animals were fixed by perfusion. Sections were observed with a Zeiss Axioskop 50 epifluorescence microscope through a custom-made Bandpass filter set for Fast Blue, which only allows recognition of FB-labeled motoneurons. Observations through a custom-made HQ-Schmalband filter set for Fluoro-Gold (2.1.3.) visualized all motoneurons containing FG. Observations through a filter set 15 of Carl Zeiss (Excitation BP 546/12, Emission LP 590) revealed the red fluorescence of those motoneurons retrogradely labeled by DiI. The fluorescence "cross-talk" between the tracers was restricted to a minimum with this filter combination: (1) no DiI-labeled cells were visible through the Bandpass and HQ-Schmalband filter sets, (2) no FG-labeled cells could be observed through filter set 15 or the Bandpass filter sets, and (3) no FB-labeled motoneurons could be observed using filter set 15 (Popratiloff et al. 2001). Unfortunately, some FB-labeled motoneurons could be seen through the HQ-Schmalband filter set. This raised serious difficulties in distinguishing between single- (FG or FB) or double- (FG+FB) labeled motoneurons. Therefore we counted as double-labeled neurons only those containing DiI+FG or DiI+FB, but did not evaluate those labeled by FG+FB.

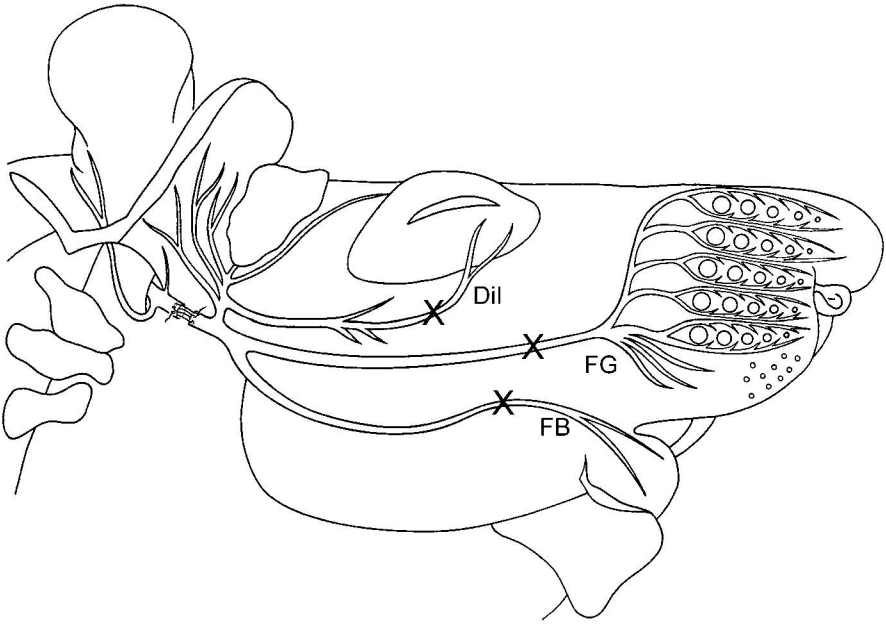

Fig. 6A, B Schematic drawing of the infratemporal portion of the rat facial nerve. The tracer application sites in the zygomatic, buccal and mandibular nerves are indicated by ×. (Adapted from Dörfl 1985; reprinted from Dohm et al. 2000)

Image Analysis

Separate color (24 bit RGB) images of retrogradely labeled facial motoneurons were created using a CCD video camera system combined with the image-analyzing software Optimas 6.5 (see Sect. 2.1.1.). All images of DiI-labeled motoneurons were used to create "DiI-masks" by the Optimas: frames were binarized, dilated, and the outlines of each DiI-labeled cell depicted. Using "arithmetic options" from the image menu, the generated masks were superimposed over the FB or FG picture. In this way, all cells stained by DiI_{only}, FG_{only}, FB_{only}, as well as all those double stained by DiI+FG or DiI+FB could be readily identified and were manually counted on the computer screen (Dohm et al. 2000). All retrogradely labeled motoneurons with a visible cell nucleus were counted in every third 50-µm section through the facial nucleus of the operated and unoperated sides. The analysis of post-transectional recovery of vibrissal motor performance was performed as described in Sect. 2.1.5.

2.2 Second Set of Experiments: Attempts to Reduce Collateral Axonal Branching at the Lesion Site

Five different experiments were performed to elucidate the:

- Effect of extracellular matrix proteins added into a tube at the lesion site (animals distributed in subgroups G_1–G_7)
- Time course of the expression of trophic factors after lesion (subgroups H_1–H_{17})
- Effect of neutralization of trophic factors at the site of lesion (subgroups I_1–I_{20})
- Effect of cells transplanted into a silicone tube inserted between the fragments of the transected facial nerve (subgroups J_1–J_6)
- Effect of autologous olfactory mucosa transplanted to the transected and sutured facial nerve (subgroups K_1–K_3)

2.2.1 Effect of Extracellular Matrix Proteins Known to Foster Neurite Elongation on Axonal Branching

Animals

Group G consisted of 42 adult female Wistar rats (175–200 g; strain HsdCpb:WU; Harlan Winkelmann, Borchen, Germany), which were divided into seven subgroups (G_1–G_7), each consisting of six animals.

Subgroup G_1 served to determine the number of motoneurons projecting through ramus zygomaticus, ramus buccalis, and ramus marginalis mandibulae of the facial nerve in unoperated control rats.

Subgroup G_2 served to determine the portion of axons that divided and projected, via daughter branches, simultaneously through the zygomatic and buccal ramus, or through the zygomatic and marginal mandibular ramus after transection and end-to-end suture of the facial nerve trunk (facial–facial anastomosis, FFA).

Subgroups G_3–G_7 were subjected to identical transection and entubulation of the facial nerve trunk into a silicone tube filled with either phosphate-buffered saline, collagen type I, laminin, fibronectin, or tenascin-R. The survival time was 56 days post surgery and 10 days post triple retrograde labeling for all rats.

Facial–facial anastomosis (FFA) was performed as described in Sect. 2.1.5.

Entubulation of the Facial Nerve Trunk

Under anesthesia, the main trunk of the facial nerve was transected and the two stumps inserted into a silicone precision tube with an inner diameter of 1.47 mm and outer diameter of 1.96 mm (Aromando Medizintechnik, Cat. Nr. 602–235, 40213 Düsseldorf, Germany; Fig. 7). To prevent tension, both ends were attached to the tube through epineural sutures with an interstump distance of 5 mm. Literature data have shown that rat axons are able to bridge gaps of up to 10 mm (Lundborg et al. 1982; Labrador et al. 1988; Evans et al. 1991).

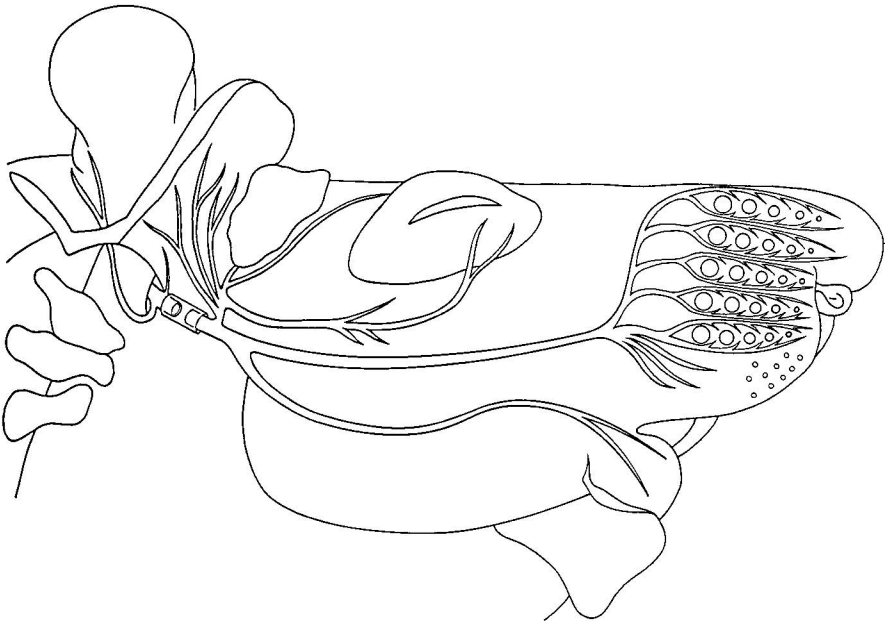

Fig. 7 Schematic drawing showing the entubulation site of the facial nerve trunk after transection. (Adapted from Dörfl 1985 and Seckel 1990; reprinted from Dohm et al. 2000)

Application of ECM Proteins

The transected nerve was inserted into a silicone tube, which served as a regeneration chamber. The empty space between the proximal and distal nerve stumps was filled with a solution of approximately 8 mm^3 [5 mm×(1,47/2^2 mm)×π] consisting of:

- Phosphate-buffered saline pH 7.4 (PBS; control chamber)
- PBS containing 100 μg/ml collagen type I (Serva, Cat. No. 47254)
- PBS containing 20 μg/ml laminin (Boehringer Mannheim, Cat. No. 1243217)
- PBS containing 20 μg/ml fibronectin (Sigma, Cat. No. F2006)
- PBS containing 20 μg/ml tenascin-R purified from adult rat brain by immunoaffinity chromatography using a tn-R2 monoclonal antibody column (Angelov et al. 1998; Pesheva et al. 1989)

Because perfusion fixation of the brain was necessary for the microscopic analysis, the ECM protein concentrations in the regeneration chamber could not be determined at the end of the postoperative survival period.

Retrograde labeling with three tracers, tissue preparation, microscopy, and statistical evaluations were performed as described in Sect. 2.1.1.

2.2.2
Time Course of Trophic Factor Expression at the Lesion Site

Animals
Group H (68 animals) was divided into subgroups H_1–H_{17} (each of 4 rats) and served to establish the time course of the expression of nerve growth factor (NGF), brain-derived neurotrophic factor (BDNF), basic fibroblast growth factor (bFGF, FGF-2), ciliary neurotrophic factor (CNTF), insulin-like growth factor I (IGF-I), and glial-cell-line derived neurotrophic factor (GDNF) in the proximal and distal fragments of a transected facial nerve as well as in its target (vibrissal) musculature.

Surgery
All procedures were carried out under an operating microscope (OGL and MS). After an intraperitoneal injection of Ketamin/Xylazin (100 mg Ketanest plus 5 mg Rompun per kg body weight), the buccal and marginal mandibular branches of the facial nerve were exposed. Thereafter the buccal facial branch (BFB) was transected and a 1 mm piece removed. The marginal mandibular branch was also transected and its regeneration prevented by a proximal ligature (Fig. 1). The latter procedure was necessary to eliminate the additional nerve supply to the whisker pad musculature by the marginal mandibular branch (Semba and Egger 1986). The postoperative survival time was 6, 12, 18, 24, 48, 72, and, 96 h, 5, 6, 7, 8, 10, 14, 18, 22, 26, and 30 days. Four animals were studied at each of these 17 time points.

Tissue Processing
Rats were transcardially perfused with 0.9% NaCl in distilled water for 60 s followed by a fixation with 4% paraformaldehyde in 0.1 M phosphate buffer pH 7.4 under deep ether anesthesia. To gain information about the expression of neurotrophic factors at the lesion site, we employed the "nerve-muscle-plate" approach. The masseter muscle with the transected nerves on it (ramus buccalis and ramus marginalis mandibulae) and the levator labii superioris muscle (together with the whisker pad) were dissected, postfixed, cryoprotected (in 30% sucrose in 0.1 M phosphate buffer, pH 7.4) and cut tangentially into 20-µm-thick sections, which were mounted on poly-L-lysine-coated slides.

Immunocytochemistry
Incubation with (1) 5.0% (w/v) bovine serum albumin (BSA; Sigma-Aldrich Chemie GmbH, Deisenhofen, Germany) in Tris-buffered saline (TBS) pH 7.4 for 60 min; (2) the primary antibody in TBS plus 0.8% (w/v) BSA overnight at room temperature; (3) 5.0% (v/v) normal goat serum (NGS, Alexis Deutschland GmbH, Grünberg, Germany) plus 0.8% BSA in TBS for 15 min; (4) 1:400 biotinylated secondary antibody in TBS plus 0.8% NGS for 1 h; (5) FluoroLink-Cy3-conjugated streptavidin (1:100; Amersham Pharmacia Biotech Europe GmbH, Freiburg, Germany). Steps (2), and (5) were followed by a 4-min wash, and step (4) by two 10 min washes in TBS. Finally, sections were dehydrated with ethanol and

Histoclear (National Diagnostics, Atlanta) and coverslipped with Fluoromount (BDH Laboratory Supplies, Poole, England).

The following primary antibodies were used:

1. Mouse monoclonal anti-NGF (1:50; Roche, Mannheim)
2. Mouse monoclonal anti-BDNF (1:1,000; R&D Systems, Wiesbaden)
3. Mouse monoclonal anti-FGF-2 (1:50; UBI/Biomol, Hamburg)
4. Polyclonal goat anti-rat CNTF (1:100; R&D Systems)
5. Mouse monoclonal anti-IGF-I (1:50; UBI/Biomol)
6. Mouse monoclonal anti-GDNF (1:500; R&D Systems)
7. Rabbit polyclonal anti-S-100 protein (1:1,000; DAKO Diagnostika, Hamburg)

The following secondary antibodies (all diluted 1:400) were used:

1. Biotinylated goat anti-mouse IgG (Fab-specific; Sigma, Deisenhofen, Germany)
2. Biotinylated goat anti-mouse IgG (Fc specific, Sigma)
3. Biotinylated rabbit anti-goat IgG (DAKO Diagnostika)
4. Biotinylated goat anti-rabbit IgG (DAKO Diagnostika, No. E0432)

Specificity Controls

Omission of the primary or secondary antibody yielded blank sections. Incubation of sections with non-relevant biotinylated secondary antibodies (e.g., goat anti-rabbit IgG for recognition of mouse primary antibodies) also yielded blank sections.

Fluorescence Microscopy

The immunopositive (CY3-positive) structures were observed through Zeiss filter set 15 (excitation BP546/12, beamsplitter FT580, emission LP590). Both localization of reaction product and intensity of fluorescent immunostaining were estimated separately and independently by two observers (Natalie Azzolin and D.N. Angelov). A scale with a minimum of 0 and maximum of 40 was used for graphical representation of the results. According to this scale sections with "no fluorescence" received zero points and those with "very strong fluorescence" 40 points. The levels between these extremes were evaluated between 5–10 points for "very faint fluorescence", 15–20 points for "faint fluorescence", and 25–30 points for "fluorescence."

2.2.3 Effect of Neutralization of Trophic Factors at the Site of Lesion on Axonal Branching

Animals

Group I consisted of 141 animals, which served to establish the portion of motoneurons whose axons branched after entubulation of the facial nerve into a silicone tube filled with neutralizing antibodies to neurotrophic factors.

Surgery

After an intraperitoneal injection of Ketamin/Xylazin, the zygomatic, buccal, and marginal mandibular rami of the facial nerve in intact rats were transected and the proximal stumps instilled with crystals of DiI, FG; and FB (Fig. 6). Ten days later, these animals (subgroup I_1) were fixed by perfusion, their brains cut in 50-μm thick vibratome sections, and all retrogradely labeled motoneurons in the brainstem were counted.

Both main surgical procedures, FFA (subgroup I_2) and entubulation of the transected facial nerve into a silicone tube (subgroup I_3), were identical to those described in Sects. 2.1.5. and 2.2.1.

In experimental subgroups I_4–I_{20}, the space between the proximal and distal nerve stumps was filled with a solution of approximately 8 μl (5 mm × 0.735 mm × 0.735 mm × π^2) containing collagen type I or collagen gel containing antibodies to trophic factors. The neutralizing concentrations, taken from the data sheet of each product as supplied by the manufacturers, were:

- 40 μg/ml anti-NGF (Bedi et al. 1992; Diamond et al. 1992; Ro et al. 1996)
- 160 μg/ml anti-BDNF (Tonra et al. 1998)
- 100 μg/ml anti-FGF-2 (Tuttle et al. 1994; Murai et al. 1996)
- 30 μg/ml anti-IGF-I (Zheng et al. 1997)
- 3 μg/ml anti-GDNF (Vega et al. 1996)
- 100 μg/ml anti-CNTF (Ding et al. 1994; Tokiwa et al. 1994)

The facial nerves of animals from subgroups I_{12}–I_{17} were transected and inserted into tubes with antibodies in concentrations fivefold higher than the neutralizing ones. In subgroups I_{18}–I_{20} the silicone tube contained combinations of the same antibodies to NGF, BDNF, and FGF-2 in neutralizing concentrations.

The entubulation of the facial nerve in a gel with 160 μg/ml mouse non-immune IgG (Sigma) served as control (subgroup I_5) for the effect(s) of the antibodies that, with the exception of anti-CNTF, were generated in mice.

The collagen gel was prepared from a collagen stock solution (Serva, Heidelberg) which was mixed with ×10 concentrated PBS and 0.1 M NaOH until the pH reached 7.4. For polymerization the collagen/antibody mixture was left at 37°C for 2 h (Guidry and Grinnel 1987; Mauch et al. 1988).

Retrograde labeling with three tracers, tissue preparation, microscopy, and statistical evaluations were performed as described in Sect. 2.1.1.

2.2.4 Effect of Cell Transplantation on Axonal Branching

Animals

Group J consisted of 36 adult female Sprague-Dawley rats (175–200 g) purchased from Charles River. The rats were distributed in six subgroups (J_1-J_6) each consisting of six animals.

The observation that the focal application of neutralizing antibodies to soluble neurotrophic factors reduced collateral axonal sprouting suggested that the amount of trophic factor at the lesion site is critical to determine the sprouting response. In order to further test this hypothesis, we transplanted dissociated glial cells and examined whether implantation of a trophic source at the lesion site might affect axonal collateral sprouting.

Schwann cells (SCs) and olfactory ensheathing cells (OECs) were used since they are closely-related glial cells types that commonly express a number of neurotrophic molecules (Wewetzer et al. 2002), e.g., the brain-derived neurotrophic factor (BDNF) and the ciliary neurotrophic factor (CNTF). These molecules have been shown to affect neurite outgrowth and sprouting (Kwon and Gurney 1994; Siegel et al. 2000). Bone marrow contains undifferentiated cells able to differentiate into a glial phenotype (Azisi et al. 1998; Kopen et al. 1999). Bone marrow stroma cells (BMSCs) applied either directly into the demyelinated area or indirectly via the blood stream have recently been shown to remyelinate the spinal cord (Akiyama et al. 2002a, b).

Entubulation of the facial nerve trunk was performed as described in Sect. 2.2.1 (Fig. 7). These experiments were not performed in Wistar rats (strain HsdCpb:WU; Harlan Winkelmann), but in Sprague-Dawley rats; therefore two controls were repeated: the intact control subgroup (J_1) and the subgroup of animals which underwent FFA (J_2). In the other four subgroups of rats, the space between the proximal and distal nerve stump was filled with:

- A gel consisting of collagen type I purchased from Serva, Cat. No. 47254 ($J_{3)}$)
- A gel containing of 66 µl collagen type I plus 33 µl of suspension containing 2,000,000 OECs (J_4)
- A gel containing of 66 µl collagen type I plus 33 µl of suspension containing 2,000,000 SCs (J_5)
- A gel containing of 66 µl collagen type I plus 33 µl of suspension containing 2,000,000 BMSC (J_6)

A total of 100 µl gel (collagen plus OECs or SC or BMSCs) was divided into 10 tubes, each to contain 10 µl, i.e., each animal received ca. 200,000 cells.

Cell Preparation

Olfactory ensheathing cells (OECs) were prepared from neonatal rats as described (Wewetzer et al. 2001; Guntinas-Lichius et al. 2001). Tissue dissociation into single cells was done by gentle trituration using a flame-constricted Pasteur pipette. Cells were then seeded onto poly-L-lysine-coated (0.5 mg/ml) culture flasks and treated with cytosine arabinoside (Sigma, 10^{-5}M) for 4 days to remove contaminating fibroblasts. Cells were then expanded by use of forskolin 2 µM (Calbiochem,Bad Soden, Germany) and Dulbecco's Modified Eagle Medium (DMEM, Life Technologies, Paisley, UK) supplemented with 10% fetal calf serum (FCS) under standard conditions. The purity of the cultures was over 95% as determined by immunostaining of vital OECs with antibodies for the low-affinity nerve growth factor

receptor p75 (generously provided by E. Shooter). Prior to transplantation, the FCS was successively eliminated from the medium. The cells were transferred to 5% FCS (5 h) and cultured overnight in 1% FCS before the medium was finally changed to a serum-free condition (5 h).

Schwann cells (SCs) were prepared from dorsal root ganglia (Sprague Dawley rat, newborn) as previously described (Wewetzer et al. 1996, 1997). In brief, ganglia were treated with trypsin/collagenase and mechanically triturated in the presence of DNase I (0.05%) using a flame-constricted Pasteur pipette. After percoll (35%) centrifugation (1,200 rpm, 20 min, 4°C), cells were plated onto uncoated plastic dishes and cultured for 4 days in DMEM supplemented with 10% FCS and cytosin arabinoside to kill dividing fibroblasts. After detachment (0.25% trypsin, 1 mM EDTA), cells were plated onto poly-L-lysine-coated plastic dishes and expanded in the presence of forskolin (Calbiochem, 2 μM) in DMEM containing 10% FCS. Immunostaining with anti-$p75^{NTR}$-antibodies confirmed that more than 95% of the cells were Schwann cells (data not shown).

Bone-marrow-derived stromal cells (BMSCs) were prepared as previously described with modifications (Akiyama et al. 2002a, b). Cells were prepared from bone marrow (10 μl), which was isolated from femur and tibia of adult rats using a heparinized 24G needle. The samples were diluted in 5 ml culture medium (DMEM/10% FCS) using a Pasteur pipette. The cells were collected from the mononuclear cell layer following centrifugation at room temperature (2,000 rpm, 25 min) and resuspended in culture medium supplemented with epidermal growth factor (EGF, 10 ng/ml, Peprotech/TEBU GmbH, Frankfurt/Main) and basic fibroblast growth factor-2 (FGF-2, 10 ng/ml, Peprotech/TEBU GmbH). The cells were then plated on untreated plastic culture dishes and incubated for 3 days. Non-adherent cells were removed by replacing the medium. Cultures were maintained at 37°C in a humidified atmosphere (5% CO_2). After reaching confluency, the cells were detached from the dish using trypsin/EDTA for 5 min and re-plated to new culture dishes at a density of 7,000 cells/cm^2. Cells were used for transplantation after 7 days of cultivation. Immunostaining of the cells with anti-fibronectin antibodies (Sigma, Taufkirchen, Germany, Cat. Nr. F3648 and F7387) demonstrated that the purity of the BMSC preparations was more than 85% (data not shown).

Retrograde labeling with three tracers, tissue preparation, microscopy, statistical evaluations, and estimation of functional recovery of whisking were performed as described in Sect. 2.1.1.

2.2.5
Effect of Transplanted Autologous Olfactory Mucosa on Axonal Branching

Animals

Group K consisted of 40 female and 6 male inbred Lewis rats. Transection and immediate end-to-end suture of the right facial nerve (facial–facial anastomosis, FFA, Fig. 4) was performed in the female rats only.

Surgery

Olfactory mucosa (OM), freshly prepared from deeply anesthetized syngeneic male rats, was cut in small pieces, briefly rinsed in Hank's balanced salt solution (HBSS; Life Technologies Overseas GmbH, Eggenstein-Leopoldshafen, Germany, Cat. Nr. 24020083) and then gently laid over the sutured epineurium in half of the female rats. Male rats were chosen as donors in order to facilitate the identification of the transplant in the female hosts. Finally, the wound was closed by three 4–0 skin sutures (Ethicon).

In four other female rats, buccal mucous membrane (BMM) obtained from the cheeks of deeply anesthetized syngeneic male animals was laid over the sutured epineurium. These control rats were used to prove that the improved regeneration was due to OM, and not to nonspecific mechanical effect(s) of any transplanted tissue.

Determination of postoperative axonal branching, estimation the accuracy of reinnervation, and analysis of vibrissae motor performance were performed as described in Sect. 2.1.5.

3 Results

3.1 Influence of the Altered Input to Axotomized Facial Perikarya on the Quality of Reinnervation

3.1.1 Altered Trigeminal Input to Axotomized Facial Perikarya Reduces Axonal Branching

3.1.1.1 Behavioral Observations

The "facial nerve-lesion model" described here provides a unique opportunity to observe postoperative vibrissae paralysis and the gradual recovery of rhythmical whisking; it allowed us to record the rapidly improving motor performance of the mystacial vibrissae after a combined facial-trigeminal (contralateral) lesion.

Following *buccal–buccal anastomosis* (BBA_{only}), i.e., after transection and suture of the buccal ramus of the facial nerve, the vibrissae were paralyzed, i.e., they drooped and acquired a inferior orientation. At 10–14 days post operation (DPO), the vibrissae "rose" again to the level of the mouth and acquired a posterior orientation. Initial signs of restoration of rhythmical whisking occurred at 21–28 DPO.

Following *BBA plus excision of the ipsilateral infraorbital nerve* the vibrissae "rose" to the level of the mouth and acquired a posterior orientation also at 10–14 DPO. However, all operated rats showed no sign of recovery of rhythmical whisking until 28 DPO, the end of the observation period.

Surgery

Olfactory mucosa (OM), freshly prepared from deeply anesthetized syngeneic male rats, was cut in small pieces, briefly rinsed in Hank's balanced salt solution (HBSS; Life Technologies Overseas GmbH, Eggenstein-Leopoldshafen, Germany, Cat. Nr. 24020083) and then gently laid over the sutured epineurium in half of the female rats. Male rats were chosen as donors in order to facilitate the identification of the transplant in the female hosts. Finally, the wound was closed by three 4–0 skin sutures (Ethicon).

In four other female rats, buccal mucous membrane (BMM) obtained from the cheeks of deeply anesthetized syngeneic male animals was laid over the sutured epineurium. These control rats were used to prove that the improved regeneration was due to OM, and not to nonspecific mechanical effect(s) of any transplanted tissue.

Determination of postoperative axonal branching, estimation the accuracy of reinnervation, and analysis of vibrissae motor performance were performed as described in Sect. 2.1.5.

3 Results

3.1 Influence of the Altered Input to Axotomized Facial Perikarya on the Quality of Reinnervation

3.1.1 Altered Trigeminal Input to Axotomized Facial Perikarya Reduces Axonal Branching

3.1.1.1 Behavioral Observations

The "facial nerve-lesion model" described here provides a unique opportunity to observe postoperative vibrissae paralysis and the gradual recovery of rhythmical whisking; it allowed us to record the rapidly improving motor performance of the mystacial vibrissae after a combined facial-trigeminal (contralateral) lesion.

Following *buccal–buccal anastomosis* (BBA_{only}), i.e., after transection and suture of the buccal ramus of the facial nerve, the vibrissae were paralyzed, i.e., they drooped and acquired a inferior orientation. At 10–14 days post operation (DPO), the vibrissae "rose" again to the level of the mouth and acquired a posterior orientation. Initial signs of restoration of rhythmical whisking occurred at 21–28 DPO.

Following *BBA plus excision of the ipsilateral infraorbital nerve* the vibrissae "rose" to the level of the mouth and acquired a posterior orientation also at 10–14 DPO. However, all operated rats showed no sign of recovery of rhythmical whisking until 28 DPO, the end of the observation period.

Following *BBA plus excision of the contralateral infraorbital* nerve the vibrissae "rose" to the level of the mouth and initiated movements at 3 DPO; an almost full restoration of rhythmical whisking occurred at 7–10 DPO.

The observation that the excision of the contralateral infraorbital nerve provided not only the most rapid, but also the best functional recovery (rhythmical whisking of the vibrissae) from facial nerve transection was so unexpected and exciting that we analyzed the morphological and electrophysiological bases of this phenomenon.

3.1.1.2 Lesion to the Contralateral Trigeminal Ganglion Cells Reduced the Branching of Transected Facial Axons

Intact Rats

Application of Fluoro-Gold crystals to the superior and DiI crystals to the inferior buccolabial ramus of the facial nerve yielded 1,724±375 FG- and 134±125 DiI-labeled motoneurons, respectively (mean±SD, n=4). All retrogradely labeled cells (total of 1,858±424) were exclusively localized in the lateral facial subnucleus. The FG-labeled cells were found in its ventrolateral portion and the DiI-labeled cells in its dorsomedial portion. No double-labeled motoneurons were observed.

Application of DiI to the superior and FG to the inferior buccolabial ramus yielded 1,937±156 DiI- and 94±30 FG-labeled motoneurons (mean±SD, n=4). All DiI-labeled cells were located in the ventro-lateral portion and all FG-labeled cells were observed in the dorso-medial portion of the lateral facial subnucleus, which contained a total number of 2,031±178 retrogradely labeled motoneurons. No double-labeled motoneurons were observed. The statistical evaluation showed that the numbers determined in the two experiments are practically identical (t-test for unpaired data) and that the labeling efficiencies of FG and DiI are similar. Pooling of these data revealed a total number of 1,920±288 labeled motoneurons in the lateral facial subnucleus. About 91% of these motoneurons (1,747±375) projected into the superior, and 9% (174±92) into the inferior buccolabial ramus (Table 1). No motoneurons were found to project through both buccolabial rami of the facial nerve.

Buccal–Buccal Anastomosis

Neuron labeling at 28 days after BBA showed that all retrogradely labeled neurons were localized in the lateral facial subnucleus. Quantitative analyses revealed no neuronal loss (Table 1). However, a myotopic organization of this subnucleus into a ventrolateral portion (for the superior buccolabial ramus) and a dorsomedial portion (for the inferior buccolabial ramus) was no longer evident (Fig. 8B).

Accordingly, the number of motoneurons whose axons or axonal branches projected into the superior buccolabial ramus was lower than that in intact rats: only about 56% of all neurons in the lateral facial subnucleus projected into the superior buccolabial nerve. On the contrary, due to the misguided growth of axons

Table 1 Effect of altered trigeminal input to facial perikarya on axonal branching as estimated by application of crystalline tracers to transected superior and inferior buccolabial nerves

Animals	Superior buccolabial nerve	Inferior buccolabial nerve	Superior + Inferior buccolabial nerves	Buccal facial nerve
Intact rats	1746±375	174±91	0	1920±288
(subgroup A_1); n=10	(91%)	(9%)		(100%)
28 days after buccal-buccal anastomosis (BBA)	838±499^{A1}	312±142^{A1}	342±352^{A1}	1491±604
(subgroup A_2); n=12	(56%)	(21%)	(23%)	(100%)
28 days after BBA + excision of ipsilateral infraorbital nerve (ION) group A_3	860±439^{A1}	678±426$^{A1–A3}$	237±249	1776±476
(subgroup A_3); n=12	(48%)	(39%)	(13%)	(100%)
28 days after BBA + excision of contralateral ION	1271±352	418±247	164±115	1855±581
(subgroup A_4); n=12	(69%)	(23%)	(8%)	(100%)
112 days after BBA only	1,004±393	416±288	172±84	1,591±484
(subgroup A_5); n=6	(63%)	(26%)	(11%)	(100%)
112 days after BBA + excision of the ipsilateral ION	1,064±422	511±204	198±70	1,772±375
(subgroup A_6); n=6	(60%)	(29%)	(11%)	(100%)
112 days after BBA + excision of contralateral ION	1,266±263	312±238	89±54	1,667±243
subgroup A_7); n=6	(76%)	(19%)	(5%)	(100%)

Mean numbers and standard deviations of retrogradely labeled motoneurons, the axons of which project within the superior, inferior, or both buccolabial nerves in group A. Indices on the right side above some values indicate the subgroup with significantly different values according to a nonparametric analysis for unpaired (Mann-Whitney test) and paired values (Wilcoxon test). The values in parentheses indicate the portion of the motoneurons that project through the superior, inferior, or both buccolabial branches of the buccal branch of the facial nerve

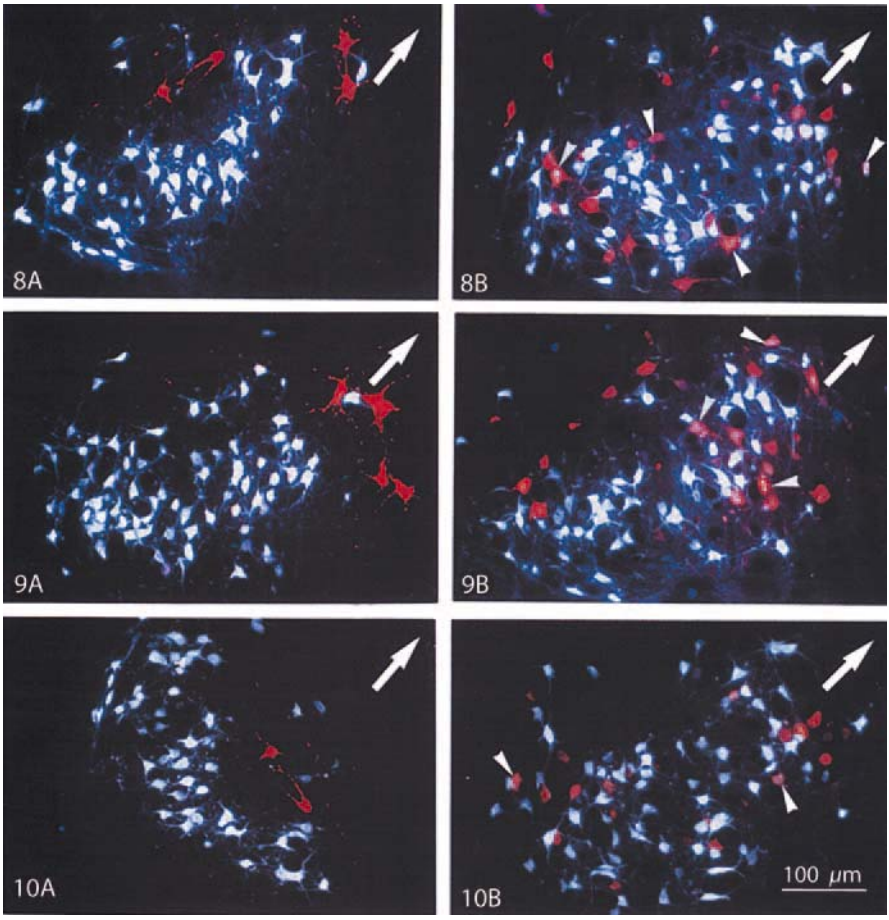

Fig. 8–10 A, B **8** Rat brainstem 28 days after BBA. Photographs produced by double exposure. The dorsomedial portion of the facial nucleus is indicated by an *arrow*. **A** Contralateral unlesioned lateral facial subnucleus with preserved myotopic organization of the motoneurons whose axons project into the superior buccolabial nerve (retrogradely labeled in *white* by Fluoro-Gold) and into the inferior buccolabial nerve (labeled in *red* by DiI). Whereas most FG-labeled motoneurons are localized in the ventrolateral portion, those labeled with DiI are in the dorsomedial part of the subnucleus. **B** Lesioned lateral facial subnucleus after BBA and application of FG to the superior and DiI to the inferior buccolabial nerve. Note the complete lack of myotopic organization: the FG-labeled *(white),* DiI-labeled *(red),* and DiI+FG-labeled *(arrowheads)* motoneurons are scattered throughout the whole lateral facial subnucleus. **9** Rat brainstem 28 days after BBA plus excision of the ipsilateral infraorbital nerve. **A** Contralateral unlesioned lateral facial subnucleus with myotopic organization. **B** Lesioned facial subnucleus 28 days after BBA plus excision of the ipsilateral infraorbital nerve. **10** Rat brainstem 28 days after BBA plus excision of the contralateral infraorbital nerve. **A** Contralateral unlesioned lateral facial subnucleus with myotopic distribution of the motoneurons. **B** Lateral facial subnucleus 28 days after BBA plus excision of the contralateral infraorbital nerve; 50-µm vibratome sections. (Reprinted from Angelov et al. 1999)

into wrong fascicles, the number of motoneurons whose axons projected into the inferior buccolabial ramus was increased in comparison with that in intact rats: the motoneurons whose axons had regrown into the inferior buccolabial ramus comprised about 21% of all neurons in the lateral facial subnucleus (Table 1). Compared to the values in intact rats, there was a statistically significant decrease in the number of motoneurons projecting through the superior buccolabial nerve.

Another major difference from unoperated animals was the presence of motoneurons containing both tracers in the lesioned facial nucleus. The only explanation for this phenomenon is that these double-labeled cells (23% of all motoneurons in the lateral facial subnucleus) regrew several sprouts not a single sprout, from any transected axon, which postoperatively projected into the superior and inferior buccolabial nerves (Shawe 1954; Esslen 1960; Brushart and Mesulam 1980; Ito and Kudo 1994; Choi and Raisman 2002).

This suggestion was confirmed by the neuron counts performed at 112 days after BBA: The portion of double-labeled motoneurons in group A_5 was reduced to 11% (Table 1) and confirmed earlier results that most of the supernumerary sprouts were pruned (Mackinnon et al. 1991; Brushart 1993).

BBA Plus Excision of the Ipsilateral Infraorbital Nerve

Four weeks after BBA plus excision of the ipsilateral infraorbital nerve all retrogradely labeled neurons (1,776±476) were localized in the lateral facial subnucleus, but with no myotopical organization (Fig. 9B).

The motoneurons whose axons projected into the superior buccolabial ramus comprised about 48% of all neurons in the lateral facial subnucleus. Additionally, the portion of neurons whose axons projected postoperatively into the inferior buccolabial ramus rose to about 39% (Table 1). Double-labeled neurons, projecting into both fascicles of the buccal nerve, comprised about 13% of all motoneurons in the lateral facial subnucleus.

Compared to the values in intact rats, there was a statistically significant decrease in the number of motoneurons projecting into the superior ramus and a significant increase in the number of those projecting into the inferior ramus.

Compared to values in rats subjected to BBA alone, there was no statistically significant change in the number of motoneurons projecting into the superior ramus. There was, however, a significant increase in the number of neurons projecting into the inferior ramus and a statistically significant decrease in the number of motoneurons projecting into both fascicles.

The neuron counts performed at 112 days after surgery showed no significant differences from the values obtained at 4 weeks after surgery (Table 1).

BBA Plus Excision of the Contralateral Infraorbital Nerve

Neither obvious neuronal loss, nor involvement of other facial subnuclei occurred after BBA plus blockade of the contralateral trigeminal input: all retrogradely labeled neurons (1,855±581) were localized in the lateral facial subnucleus, no myotopical organization was apparent (Fig. 10B).

The number of motoneurons whose axons or axonal branches projected into the superior buccolabial ramus comprised 69% of all neurons in the lateral facial subnucleus. The mean number of neurons, whose axons projected into the inferior buccolabial ramus, decreased to 23% (Table 1), and the mean number of double-labeled neurons to about 8% of all motoneurons in the lateral facial subnucleus (Table 1).

Compared to the values in intact rats, there were no statistically significant changes in the number of motoneurons projecting into the superior and inferior ramus. Compared to animals treated with BBA alone, there was a statistically significant increase in the number of motoneurons projecting into the superior ramus, no significant change in the number of cells projecting into the inferior ramus, and no statistically significant decrease in the number of motoneurons projecting into both nerves. Compared to rats treated with BBA plus excision of the ipsilateral ION, there was a statistically significant increase in the number of motoneurons projecting into the superior ramus, a statistically significant decrease in the number of neurons projecting into the inferior ramus, and a statistically significant decrease in the number of motoneurons projecting into both nerves.

The neuron counts performed at 112 days after surgery showed significant reduction only in the number of double-labeled cells in rats subjected to BBA plus excision of the contralateral ION (Table 1). Taken together, the results from retrograde neuron labeling showed that, when compared to transection and suture alone (BBA), the lesion of the infraorbital nerve reduced the branching (or enhanced the elimination of branches) of transected facial axons. Surprisingly, the best recovery of function was detected after lesioning the trigeminal ganglion neurons contralateral to the lesioned facial nucleus. In search for an explanation, we decided to check anatomically whether the excision of the contralateral infraorbital nerve accelerated the elongation of transected facial axons.

3.1.2 No Evidence for an Increased Rate of Facial Axon Elongation After Combined Facial-Trigeminal Injury

Intact Control Rats

Injection of 100 µl 1% FB into the whisker pad of normal intact rats labeled 1,602±96 motoneurons (mean±SD, n=6 rats) localized exclusively in the lateral facial subnucleus.

Three days after tracer injection and 4 days after *BBA only*, we counted 1,503±102 retrogradely labeled motoneurons in the intact lateral facial nucleus on the control side. On the side where BBA was performed there were 308±57 (range 222–363) retrogradely labeled motoneurons (mean±SD; n=5 rats). All of them were localized in the lateral facial subnucleus. This value was significantly lower than the number found in intact control animals.

Three days after tracer injection and 4 days after *BBA plus excision of the ipsilateral infraorbital nerve*, there were 1,579±114 retrogradely labeled motoneurons in

the intact lateral facial nucleus on the control side. On the side of combined surgery we counted 218±130 (range 89–432) motoneurons projecting into the muscles of the whisker pad (n=4 rats). This number was significantly lower than the mean value in unoperated control animals and the mean value in animals that underwent BBA only.

Three days after tracer injection and 4 days after *BBA plus excision of the contralateral infraorbital* nerve we counted 1,605±141 motoneurons in the intact lateral facial nucleus on the control side. On the side of combined surgery there were 434±74 (range 357– 501) motoneurons whose axons had reached the whisker pad muscles (n=4 rats). This number is significantly lower than the mean value in unoperated control animals and not significantly higher than the mean value in animals which underwent BBA only. Compared to the mean value in animals which underwent BBA plus excision of the ipsilateral infraorbital nerve, this value was significantly higher.

These results did not provide evidence for an increased rate of facial axon elongation after combined facial-trigeminal injury: the number of motoneurons the axons of which succeeded to reinnervate the whisker pad in rats subjected to BBA plus excision of the contralateral ION was significantly higher only than that obtained in rats after BBA plus excision of the ipsilateral ION. When compared to the number obtained in animals subjected to BBA only, the increase was insignificant. Thus, considering rate of axonal elongation, the combination of facial axotomy plus excision of the contralateral infraorbital nerve turned out to be superior to BBA plus excision of the ipsilateral infraorbital nerve, but not to BBA only.

The combination of intramuscular tracer injection and subsequent counts of retrogradely labeled motoneurons has two main advantages: (1) it determines the source and amount of normal nerve supply and (2) it allows establishment of the time course of long-term muscle reinnervation. However, counts of retrogradely labeled motoneurons might be of relatively low precision when employed after nerve lesions performed close to the target muscle. Whereas it is established that even the earliest axonal branches after axotomy are capable of tracer incorporation (cf. Sparrow and Kiernan 1979; Olsson 1980), little is known as to what portion of these branches succeeds in establishing neuromuscular junctions later. Since in our model the distance between nerve transection site and target musculature is about 12 mm, the method chosen appears to be fairly crude. Pilot experiments to visualize the advancement of outgrowing axons from the site of transection are in progress.

3.1.3
Altered Trigeminal Input Slightly Improves the Accuracy of Target Muscle Reinnervation by Regenerating Facial Axons

Single Labeling in Intact Rats

The facial motoneurons of intact rats were labeled by either FG or FB to compare the *labeling efficiency* of these two retrograde fluorescent tracers. Injection of 100 µl

1% FG into the whisker pad (right or left) labeled the perikarya of 1,281±87 facial motoneurons (mean±SD, *n*=8 rats). Injection of 100 µl 1% FB into the whisker pad (right or left) labeled the perikarya of 1,302±96 motoneurons (mean±SD, *n*=8rats). Thus, there appeared to be no difference in the labeling efficiency of FG and FB in our experimental system. With both tracers, all labeled motoneurons were localized exclusively in the lateral facial subnucleus, which is in agreement with the previously described myotopic organization of the facial nucleus in normal rats (Aldskogius and Thomander 1986; Angelov et al. 1996; Streppel et al. 1998).

Sequential Labeling in Intact Rats

As a second methodological control, we tested whether the sequential injection of FG and FB into the selected muscle target would reliably distinguish between the FG (preoperatively labeled), FB (postoperatively labeled), and FG+FB (double-labeled) neurons. Employing the custom-made selective filter sets for FG and FB, we could differentiate and save separate digital images of FG (orange-red) and FB (blue) motoneuronal profiles. Our results showed that in intact rats the portion of double-labeled (FG+FB) motoneurons is about 90% (Table 2), which is reasonably close to the theoretical expectation of 100% double labeling.

Pre- and Postoperative Labeling

Our own experience shows that the best combination of fluorescent retrograde tracers to study the accuracy of post-transectional muscle reinnervation is a pre-operative labeling of the original motoneuronal pool by an injection of 1% FG into the target muscle, followed by a postoperative labeling of all motoneurons innervating the same target after surgery by an injection of 1% FB (Popratiloff et al. 2001). All numerical values of neurons labeled with FG, FB, and FG+FB are presented in Table 2.

Contralateral Intact Facial Nucleus

All retrogradely labeled neurons (FG, FB, and FG+FB) were localized exclusively in the lateral facial subnucleus (Fig. 11A–C). Thus, on the side of the brainstem contralateral to BBA, there were no detectable differences among all three types of operations either in location or in numbers of FG-, FB-, and FG+FB-labeled neurons (one way ANOVA; no significance).

Buccal–Buccal Anastomosis

Neuronal labeling 28 days after BBA showed that all FG-labeled neurons were located in the lateral facial subnucleus (Fig. 11D). However, the distribution pattern of the FB-labeled neurons innervating the whisker pad musculature after BBA was changed. We observed "ectopic" neurons, located in the intermediate facial subnucleus, projecting to the whisker pad musculature (Fig. 11E, F).

The quantitative estimates revealed no postoperative loss of neurons (Table 2, operated side, column "FB-labeled"). However, only 398±80 of these FB-labeled motoneurons were double-labeled (colored in pink to bright-purple in Fig. 11F),

Table 2 Accuracy of muscle target reinnervation by regenerating facial axons after altered afferent trigeminal input

Animals	Left side			Right side		
	FG-labeled original pool	FB-labeled original pool	FG+FB-labeled original pool	FG-labeled original pool	FB-labeled postoperatively regrown	FG+FB-labeled accurately regrown
Intact rats (subgroup $C_{1)}$; n=6	1,425±52	1,413±50	1,290±87 (91%)	1,264±114	1,305±137	1,169±224 (90%)
Rats treated with BBA (subgroup C_2); n=9	1,388±112	1,427±176	1,272±303 (89%)	1,119±109	1,456±132	398±80 (27%)
Rats treated with BBA plus excision of the ipsilateral infraorbital nerve (subgroup C_3); n=9	1,177±94	1,182±112	1,058±179 (90%)	1,147±95	1,362±162	436±68 (32%)
Rats treated with BBA plus excision of the contralateral infraorbital nerve (subgroup C_4); n=9	1,256±67	1,301±82	1,156±100 (89%)	1,245±76	1,406±81	580±63 (41%)

Mean numbers and standard deviations of retrogradely labeled motoneurons following preoperative intramuscular application of 100 µl 1% FG and postoperative injection of 100 µl 1% FB into the whisker pad of (1) intact rats and of rats 28 days after (2) buccal-buccal anastomosis (BBA), (3) BBA plus excision of the ipsilateral infraorbital nerve (ION), and (4) after BBA plus excision of the contralateral ION. The values in parentheses indicate what portion of the motoneurons that had innervated the whisker pad before FFA (FG-labeled) succeeded in reinnervating the original target and incorporating the second label

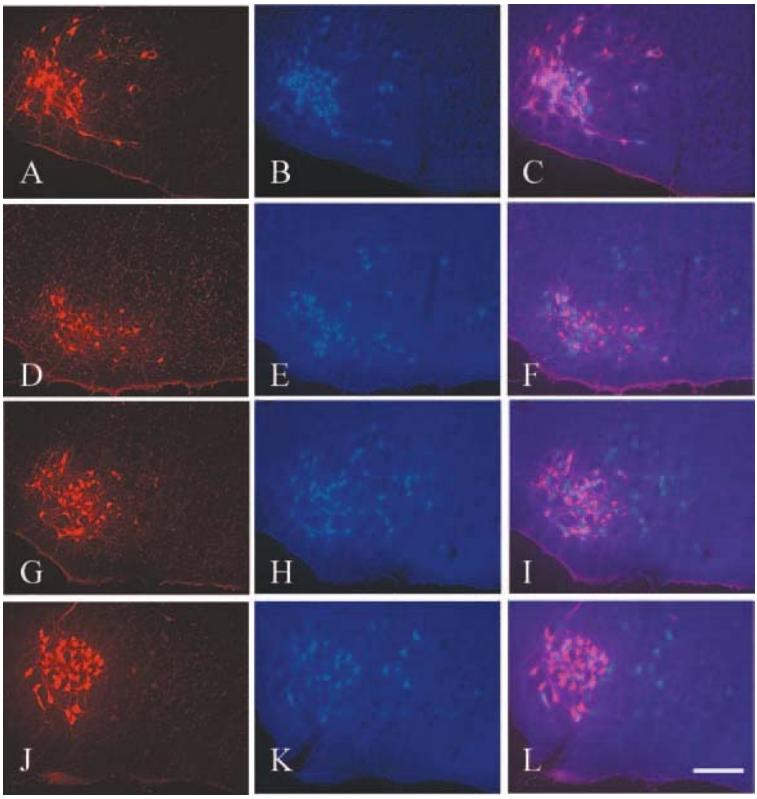

Fig. 11A–L Rat brainstem 28 days after surgery on the buccal branch of the facial nerve. The lateral facial subnucleus, indicated by the preoperative FG labeling is in the *left part* of each picture. All photographs in the *right column* were produced by double exposure. 50 μm thick vibratome sections. *Scale bar* 100 μm. **A–C** Intact facial nucleus with preserved myotopic organization of the motoneurons. Employing the selective filters, we depicted all preoperative FG-labeled (**A**) and all postoperative FB-labeled (**B**) motoneurons. **C** In the intact facial nucleus, the portion of double-labeled (FG+FB, *pink to bright purple in color*) motoneurons is about 90%. **D–F** Lesioned facial nucleus 28 days after BBA. Whereas all preoperatively FG-labeled motoneurons are localized in the lateral facial subnucleus (**D**), those labeled postoperatively with FB are observed also in the intermediate facial subnucleus (**E**). Our quantitative estimates show that only about 27% of these FB-labeled motoneurons are double-labeled (**F**) and belong to the original motoneuronal pool of the whisker pad. **G–I** Lesioned facial nucleus of a rat 28 days after BBA plus excision of the ipsilateral ION. All preoperatively FG-labeled motoneurons are localized in the lateral facial subnucleus (**G**). The postoperatively FB-labeled motoneurons are found in the lateral and intermediate facial subnuclei (**H**). The double-exposure picture (**I**) is similar to that in **f** showing that about 32% of the FB-labeled cells were also FG-labeled. **J–L** Lesioned facial nucleus of rat 28 days after BBA plus excision of the contralateral ION. All preoperatively FG-labeled motoneurons are localized in the lateral facial subnucleus (**J**) and some postoperatively FB-labeled cells are found in the intermediate facial subnucleus (**H**). Our counts show that after this type of combined surgery, the portion of the double-labeled motoneurons (**L**) increased significantly to 41%. (Reprinted from Skouras et al. 2002, with permission from IOS Press)

i.e., only 27% of them belonged to the original motoneuron pool; the rest were ectopic nerve cells.

The reinnervation of the whisker pad by "ectopic" motoneurons (Fig. 11E, F, H, I, K, L) localized in the dorsal, intermediate, medial, and ventromedial facial subnuclei is a well-known phenomenon after transection of the facial nerve (Angelov et al. 1996; Streppel et al. 1998). In unoperated rats, as well as in animals subjected to lesions of the buccal branch, the intact motoneurons in these subnuclei send their axons exclusively along the zygomatic, marginal mandibular, posterior auricular, and cervical branches of the facial nerve, respectively (Semba and Egger 1986). Whether the post-transectional misguidance of twin axons stemming from the intact facial branches occurred in the periphery as consequence of Schwann cell bridges (Love and Thompson 1999) or within the facial nerve trunk remains to be elucidated.

BBA Plus Excision of the Ipsilateral Infraorbital Nerve

All FG-labeled neurons were located in the lateral facial subnucleus (Fig. 11G). FB-labeled perikarya were found in the lateral, medial, and intermediate facial subnuclei (Fig. 11H, I). Four weeks after BBA and excision of the ipsilateral infraorbital nerve, we counted 436±68 double-labeled (pink-purple) motoneurons (Table 2), i.e., only about 32% of the motoneurons that innervated the whiskerpad post surgery belonged to the original pool. Compared to BBA alone, there was no statistically significant increase in the number of double-labeled motoneurons.

BBA Plus Excision of the Contralateral Infraorbital Nerve

Apart from preventing a transsagittal sprouting from the contralateral ION (Banfai 1976; Baumel 1974), the excision of the contralateral ION served to prove whether the removal of the contralateral vibrissae input to the axotomized facial motoneurons would attenuate the misguidance of regrowing facial sprouts. After this experimental approach, all FG-labeled motoneurons were located in the lateral facial subnucleus (Fig. 11J). These cells appeared larger than the perikarya observed in animals subjected to BBA only and BBA plus excision of the ipsilateral ION (compare Fig. 11J with Fig. 11G and D). FB-labeled motoneurons were found also in the intermediate facial subnucleus (Fig. 11K, L).

Four weeks after BBA plus excision of the contralateral infraorbital nerve we counted 580±63 double-labeled motoneurons (Table 2), i.e., about 41% of the motoneurons that innervated the whiskerpad muscles after this type of combined surgery sent an axon or an axonal branch to their original target. Compared to animals with BBA alone or to BBA plus excision of the ipsilateral ION, there is statistically significant increase in the number of double-labeled motoneurons (p=0.01).

Taken together, the results from retrograde neuron labeling showed that, when compared to transection and suture alone (BBA), or to BBA plus excision of the ipsilateral infraorbital nerve, the lesion of the contralateral infraorbital nerve resulted in less aberrant reinnervation, which correlates with the improved motor

function found after this operation (see Sects. 3.1.1. "Behavioral Observations" and 3.1.4. "Electrophysiological Measurements").

3.1.4
Electrophysiological Evidence that the Excision of the Contralateral ION Provided the Best Recovery of Synchronized Vibrissal Motor Performance

Unoperated Control Animals

In normal control rats, the suprathreshold stimulation of the buccal branch resulted in an obvious but variable sweep of the mystacial hairs. Following a supramaximal stimulation, the movements of the vibrissae were synchronized. The threshold for achieving maximal response was low (1.5–2.5 mA). This maximal response, termed the compound muscle action potential (CMAP), had a short latency of 1.55±0.09 ms; (n=5). However, both latency and threshold values were dependent on slight differences in electrode position, and were thus disregarded for statistical analysis.

The CMAP consisted of a fast 3-phasic positive-negative-positive wave, followed by a slow and not so prominent negative wave (Fig. 12A). With the recording procedure used here, the faster negative wave reflected the overlapping depolarizations of all innervated muscle fibers. The short duration (1.10±0.14 ms; n=5 rats) of the negative wave was due to the similar conductance velocities and excitability of the involved fibers. The peak amplitude was 4.53±0.55 mV (n=5). The Kolmogorov-Smirnov one sample test revealed that the distributions for both duration and amplitude met the criteria for normal distribution (asymmetric significance: duration, 0.89; amplitude, 0.76), which indicated a random sampling procedure.

Buccal-to-Buccal Anastomosis

In all animals after BBA, the latency, the threshold stimuli for achieving a CMAP, and the stimuli for generating maximal CMAP were elevated. The mean CMAP duration was obviously increased to 1.82±0.53 ms (n=5 rats). As shown in Fig. 12B, this increased duration was due to the prolonged time of the rising phase of the CMAP, which consisted of a fast and a slower component. This was in contrast to the CMAP in the controls, in which only a single fast rising phase was present. This phenomenon most likely reflects the variety of the conductance velocity in the regenerating buccal axons as well as the asynchronous depolarization of the whiskerpad muscles from synaptic input. The t-test for unpaired samples revealed that the mean duration was significantly different from the value obtained in the controls (Levene test: Sig <0.05; 2 tailed significance, equal variances not assumed = 0.035<0.05). The mean amplitude was lower than the mean value in control animals, but this difference was not significant (3.86±0.63 mV; n=5).

BBA Plus Excision of the Ipsilateral Infraorbital Nerve

Like the animals in the BBA group, the latency, threshold stimuli, and stimuli for generating maximal CMAP were increased (Fig. 12C). The CMAP typically consisted of a fast negative wave, the mean duration of which was shorter than in the animals subjected to BBA only. However, this mean duration (1.36±0.12; n=5)

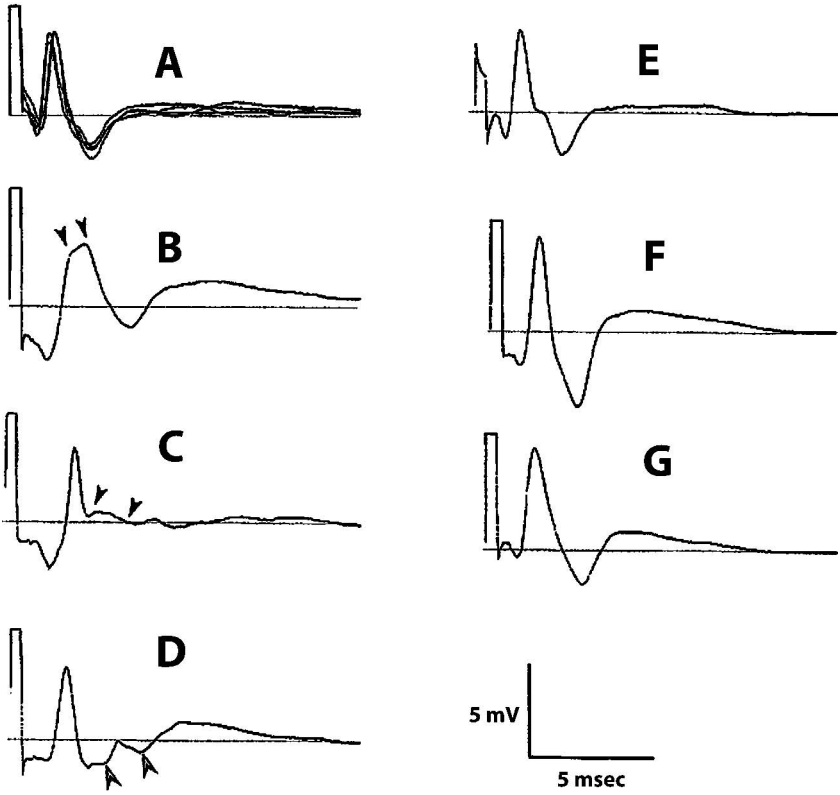

Fig. 12A–G Traces showing compound muscle action potential (CMAP) recorded from the whisker pad after supramaximal stimulation to the buccal facial branch. **A** Normal interindividual variability of CMAP demonstrated by four superimposed traces from four unoperated control animals. Recordings were made with a negative silver wire electrode inserted into the whisker pad. Typically, the CMAP consists of a faster negative wave, due to summation of depolarizations from numerous muscle fibers. This wave is followed by a positive wave of much smaller amplitude, resulting from the summation of the hyperpolarizations, and by a not so prominent and slow negative deflection due to the summation of after hyperpolarizations of the muscle fibers. **B** CMAP of identical amplitude, but prolonged duration at 28 days after BBA. The prolonged duration is due to the disintegration of CMAP's peaks (*arrowheads*). **C** A typical trace of CMAP taken from rats which underwent BBA plus excision of the ipsilateral ION. The fast negative wave is followed by smaller and slower depolarizations (*arrowheads*) superimposed to the hyperpolarization wave. The overall duration of the entire complex is shorter than in animals treated with BBA only. **D** Trace obtained from rats with BBA plus excision of the contralateral ION. The fast depolarization is followed by a positive hyperpolarization with an occasional negative activity superimposed on the positive wave. This negative activity, however, does not rise above the zero line (*open arrowheads*). **E–G** Traces of CMAP recorded from the left whisker pad of animals treated with BBA only, BBA combined with excision of the ipsilateral ION, and BBA combined with excision of the contralateral ION respectively. There are no obvious changes in the CMAP shape, duration and peak, when compared with those obtained from the control animals (see trace A). (Reprinted from Skouras et al. 2002, with permission from IOS Press)

was significantly longer than the respective value in control animals (Levene test significance >0.05; equal variances assumed; *t*-test significance <0.05). The amplitude of the CMAP (4.27±0.98; *n*=5) did not differ significantly from that obtained in control animals (Levene test significance >0.05; two independent sample *t*-test significance <0.05; 95% confidence interval of the difference contained "0").

BBA Plus Excision of the Contralateral Infraorbital Nerve

Like the animals that underwent BBA only, the latency, the threshold stimuli, and the stimuli for generating maximal CMAP were increased (Fig. 12D). The CMAP consisted of a fast wave, the mean duration of which was shorter than those measured in the groups animals treated with BBA only and BBA plus excision of the ipsilateral ION. This estimated mean duration (1.08±0.14 ms; *n*=5) was not significantly different from the control animals (Levene test significance >0.05; two independent sample equal variance *t*-test significance >0.05). The mean amplitude (3.81±0.5 mV; *n*=5) also did not differ significantly from the value measured in the control animals (Levene significance >0.05; two independent sample *t*-test equal variance presumed significance >0.05).

In conclusion, the reduced mean duration of CMAP in the group of animals subjected to BBA and excision of the contralateral ION reflects synchronized contractions of the whiskerpad muscles, which closely resemble those in control animals.

3.1.5
Altered Trigeminal Input Improves Motor Performance of the Vibrissal Muscles After Facial Nerve Transection and Suture (FFA)

The large caudal whiskers are associated with two types of striated musculature, one that moves the whole mystacial pad, and one that directly moves each sinus hair follicle; the most rostral vibrissae lack the latter muscle system (Dörfl 1985). The striated muscle fibers mediating protraction form a sling around the rostral aspect of each hair follicle: contraction of these muscles induced by activation of branches of the facial nerve pulls the base of the follicle caudally, moving the distal part of the whisker hair forward. By contrast, retraction of the vibrissae depends primarily upon passive elastic properties of deep connective tissue (Dörfl 1985; Wineski 1985).

3.1.5.1
Biometric Analysis of Whisking Behavior

In intact animals the vibrissae sweep back and forth during exploration with a frequency of about 6–8 Hz. The maximal protraction (the rostrally open angle between the vibrissa shaft and the median sagittal plane) is 60–70°. The amplitude of whisking (the difference between maximal retraction and maximal protraction in degrees) is 50–60° (Fig. 5). These movements are performed at a sagittal angular velocity of about 500°/s and a sagittal angular acceleration of 20,000°/s^2 (Tables 3–6).

Table 3 Recovery of vibrissal whisking 2 months after single and combined transection and suture of the facial nerve

Animals	Frequency (in Hz)	Angle at maximal protraction (in degrees)	Amplitude (in degrees)	Angular velocity during protraction (in degrees/s)	Angular acceleration during protraction (in degrees/s^2)
Intact rats (subgroup E_1); n=6	6±1	75±17 $^{E2-E4}$	44±14 $^{E2-E4}$	592±408 $^{E2-E4}$	23,417±17,984 $^{E2-E4}$
Animals subjected to FFA_{only} (subgroup E_2); n=6	6±0.8	98±11 ^{E1}	18±9 ^{E1}	114±56 ^{E1}	3,010±1,563 ^{E1}
Animals subjected to FFA plus excision of the ipsilateral infraorbital nerve (subgroup E_3); n=6	5.8±0.9	102±8 $^{E1, E4}$	16±5 ^{E1}	128±65 ^{E1}	3,534±2,425 ^{E1}
Animals subjected to FFA plus excision of the contralateral infraorbital nerve (subgroup E_4); n=6	6.5±0.5	81±20 ^{E1}	25±18 ^{E1}	216±128 ^{E1}	4,068±2,112 ^{E1}

Mean values and standard deviations of several parameters depicting the biometrics of whisking behavior in (1) intact Wistar rats and in animals 2 months after (2) transection and suture of the facial nerve (facial–facial anastomosis, FFA_{only}), (3) FFA plus excision of the ipsilateral infraorbital nerve (ION), and (4) FFA plus excision of the contralateral ION. Indices on the right side above some values indicate the subgroup with significantly different values according to a nonparametric analysis for unpaired (Mann-Whitney test) and paired values (Wilcoxon test)

Table 4 Recovery of vibrissal whisking 4 months after single and combined transection and suture of the facial nerve

Animals	Frequency (in Hz)	Angle at maximal protraction (in degrees)	Amplitude (in degrees)	Angular velocity during protraction (in degrees/s)	Angular acceleration during protraction (in degrees/s^2)
Intact rats (subgroup E_1); n=6	6.7±1	56±15 $^{E2\text{-}E4}$	53±12 $^{E2\text{-}E4}$	840±296 $^{E2\text{-}E4}$	30,316±18,340 $^{E2, E3}$
Animals subjected to FFA_{only} (subgroup E_2); n=6	6±0.8	103±9 ^{E1}	12±4 ^{E1}	88±34 ^{E1}	2,513±1,285 $^{E1, E4}$
Animals subjected to FFA plus excision of the ipsilateral infraorbital nerve (subgroup E_3); n=6	5.8±1.0	99±8.5 ^{E1}	13±6 ^{E1}	201±182 ^{E1}	2,531±1,898 $^{E1, E4}$
Animals subjected to FFA plus excision of the contralateral infraorbital nerve (subgroup E_4); n=6	6.4±0.7	87±16 ^{E1}	23±19 ^{E1}	352±302 ^{E1}	16,098±14,654 $^{E2, E3}$

Mean values and standard deviations of several parameters depicting the biometrics of whisking behavior in (1) intact Wistar rats and in animals 4 months after (2) transection and suture of the facial nerve (facial–facial anastomosis, FFA_{only}), (3) FFA plus excision of the ipsilateral infraorbital nerve (ION), and (4) FFA plus excision of the contralateral ION. Indices on the right side above some values indicate the subgroup with significantly different values according to a nonparametric analysis for unpaired (Mann-Whitney test) and paired values (Wilcoxon test)

Table 5 Recovery of vibrissal whisking 6 months after single and combined transection and suture of the facial nerve

Animals	Frequency (in Hz)	Angle at maximal protraction (in degrees)	Amplitude (in degrees)	Angular velocity during protraction (in degrees/s)	Angular acceleration during protraction (in degrees/s^2)
Intact rats (subgroup E_1); $n = 6$	6.8±0.7 ^{E2}	48±17 $^{E2\text{-}E4}$	58±30 $^{E2\text{-}E4}$	879±644 $^{E2\text{-}E4}$	37,637±29,981 $^{E2\text{-}E4}$
Animals subjected to FFA_{only} (subgroup E_2); n=6	5.4±0.5 ^{E1}	91±13 ^{E1}	14±5 ^{E1}	151±89 ^{E1}	3,810±1,291 $^{E1, E4}$
Animals subjected to FFA plus excision of the ipsilateral infraorbital nerve (subgroup E_3); n=6	6.0±0.5	98±10 $^{E1, E4}$	13±4 ^{E1}	138±21 ^{E1}	3,049±1,562 ^{E1}
Animals subjected to FFA plus excision of the contralateral infraorbital nerve (subgroup E_4);$n = 6$	5.8±1	83±9 $^{E1, E3}$	22±11 ^{E1}	273±202 ^{E1}	9,003±7,668 $^{E1, E2}$

Mean values and standard deviations of several parameters depicting the biometrics of whisking behavior in (1) intact Wistar rats and in animals 6 months after (2) transection and suture of the facial nerve (facial–facial anastomosis, FFA_{only}), (3) FFA plus excision of the ipsilateral infraorbital nerve (ION), and (4) FFA plus excision of the contralateral ION. Indices on the right side above some values indicate the subgroup with significantly different values according to a nonparametric analysis for unpaired (Mann-Whitney test) and paired values (Wilcoxon test)

Table 6 Recovery of vibrissal whisking 12 months after single and combined transection and suture of the facial nerve

Animals	Frequency (in Hz)	Angle at maximal protraction (in degrees)	Amplitude (in degrees)	Angular velocity during protraction (in degrees/s)	Angular acceleration during protraction (in degrees/s^2)
Intact rats (subgroup E_1); n = 6	6.6±0.5 ^{E2}	50±11 $^{E2- E4}$	52±15 $^{E2, E3}$	671±359 $^{E2, E3}$	28,661±18,645 $^{E2, E3}$
Animals subjected to FFA_{only} (subgroup E_2); *n*=6	5.3±0.8 $^{E1, E4}$	93±9 ^{E1}	11±3 $^{E1, E4}$	92±48 $^{E1, E4}$	2,126±896 $^{E1, E4}$
Animals subjected to FFA plus excision of the ipsilateral infraorbital nerve (subgroup E_3); *n*=6	6.1±0.4	93±12 ^{E1}	15±4 ^{E1}	147±63 ^{E1}	3,835±1,395 ^{E1}
Animals subjected to FFA plus excision of the contralateral infraorbital nerve (subgroup E_4); *n*=6	6.2±0.7 ^{E2}	79±16 ^{E1}	32±24 ^{E2}	397±369 ^{E2}	19,006±12,007 ^{E2}

Mean values and standard deviations of several parameters depicting the biometrics of whisking behavior in (1) intact Wistar rats and in animals 12 months after (2) transection and suture of the facial nerve (facial–facial anastomosis, FFA_{only}), (3) FFA plus excision of the ipsilateral infraorbital nerve (ION), and (4) FFA plus excision of the contralateral ION. Indices on the right side above some values indicate the subgroup with significantly different values according to a nonparametric analysis for unpaired (Mann-Whitney test) and paired values (Wilcoxon test)

Two months after surgery, the vibrissal hairs swept during exploration with a frequency of about 5–7 Hz. The mean angle during maximal protraction was 90–110°. The amplitude of whisking was 10–20°. These movements were performed at a sagittal angular velocity of about 50–150°/s and a sagittal angular acceleration of 1,500–4,500°/s^2. Thus, except for frequency, the four parameters were significantly worse after FFA only, after FFA plus excision of the ipsilateral ION, and after FFA plus excision of the contralateral ION than were those parameters measured in intact animals (Table 3).

Four months after surgery, no significant changes were detected in frequency, angle at maximal protraction, amplitude, and angular velocity during protraction. However, considering the angular acceleration during protraction, there was a tendency for improvement in the group of animals subjected to FFA plus excision of the contralateral ION: this parameter was significantly better than that in groups of animals treated with FFA only or FFA plus excision of the ipsilateral ION, and surprisingly did not differ from the value measured in intact rats (Table 4).

Six months after surgery, no improvement in any of the parameters was measured (Table 5).

Twelve Months After Surgery

With the exception of frequency, all parameters measured 1 year after FFA only remained significantly worse than in unoperated animals (Tomov et al., manuscript in preparation). Similar results were obtained if FFA was accompanied by a excision of the ipsilateral ION. If however, FFA had been combined with excision of the contralateral ION, the recovery of motor performance was very different. First, with the exception of the angle at maximal protraction, all parameters approached the values measured in intact animals and were not significantly different from them. Second, the values obtained for the animals treated with FFA plus excision of the contralateral ION 1 year after surgery were significantly better than those in animals subjected to FFA only (Table 6).

Taken together, the results of this experimental set show that:

1. There occurs virtually no improvement in the motor performance of the vibrissal muscles a whole year after FFA.
2. Alterations of the trigeminal afferent input from the axotomized facial motoneurons result in recovery of coordinated activity of the facial muscles.

3.1.6 Effect of Putatively Enlarged Cortical Representation of the Vibrissae in Blind Rats on the Quality of Target Reinnervation

This aspect has been investigated in visually normal SD rats and in blind SD/RCS rats. Using standard procedures, the fluorescent dyes FG and FB can be simultaneously visualized with the same Zeiss UV epi-fluorescence excitation filter set 01(Fig. 13A, B, C). Our previous experience, however, had shown that the blue

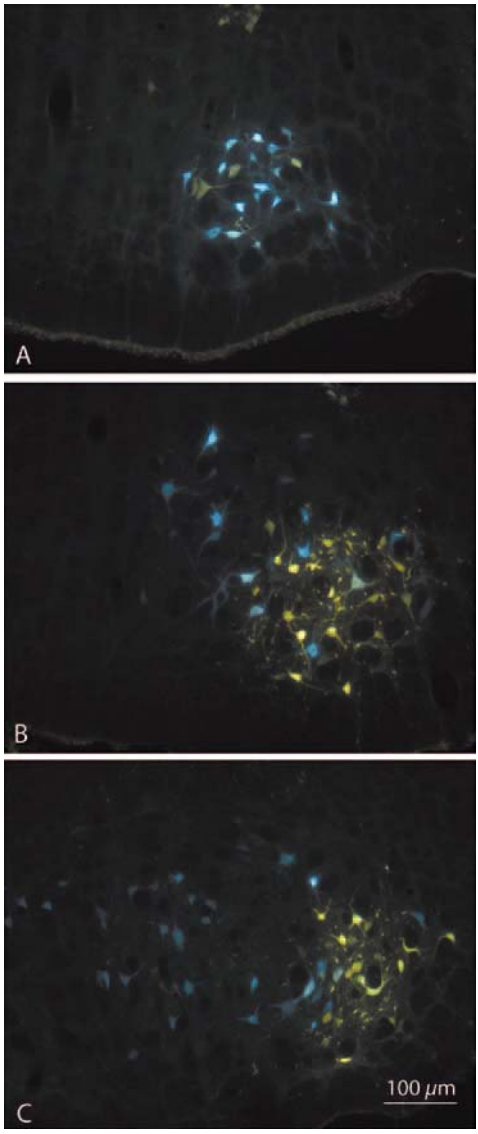

Fig. 13A–C Accuracy of reinnervation in visually normal SD and blind SD/RCS animals. **A** Pre- and postoperative neuronal labeling with FG (*yellow*) and FB (*blue*) in unoperated control rats shows that, in the intact facial nucleus, the portion of double-labeled (FG+FB) motoneurons is about 95% (cf. Table 3). **B** Visually normal SD rats 2 months after FFA. Whereas all FG-labeled motoneurons are localized in the lateral facial subnucleus, those labeled with FB are dispersed throughout the whole facial nucleus. Our quantitative estimates show that only about 30% these FB-labeled motoneurons are double-labeled and belong to the original motoneuronal pool of the whisker pad (cf. Table 3). **C** Blind SD/RCS rats 2 months after FFA. The pre- and postoperative retrograde labeling shows 30% double labeled motoneurons. (Reprinted from Tomov et al. 2002)

emission of FB obscures the white emission of FG, resulting in an artificially low number of FG-labeled neurons. The choice of the custom-made filter sets in the present investigation almost completely excludes the fluorescence "cross-talk" between FG and FB, albeit at the cost of reduced sensitivity (Popratiloff et al. 2001).

3.1.6.1 Pre- and Postoperative Retrograde Neuronal Labeling: Despite Neurotization, the Accuracy of Reinnervation Remains Insufficient in Both Visually Normal SD Rats and in Blind SD/RCS Rats

Unoperated Control SD Rats and SD/RCS Rats

Injection of 100 µl 1% FG into the whisker pad of visually normal SD rats labeled the perikarya of 1,401±111 facial motoneurons. FB, injected 2 months later as close as possible to the injection site of the earlier FG application, labeled the perikarya of 1,512±171 motoneurons (mean±SD, n=12 facial nuclei of six visually normal SD rats).

The numbers obtained for the blind RCS rats were similar: 1,252±72 perikarya were labeled by FG and 1,392±66 facial motoneurons by FB (mean±SD, n=12 facial nuclei of six blind SD/RCS rats). These numbers are practically identical and there is apparently no difference in the labeling efficiency of FG and FB. Both tracers labeled motoneurons that were localized exclusively in the lateral facial subnucleus, in agreement with the myotopic organization of the facial nucleus in normal rats (Aldskogius and Thomander 1986; Angelov et al. 1996).

Intact Facial Nucleus Contralateral to FFA

All retrogradely labeled neurons were localized exclusively in the lateral facial subnucleus (Fig. 13A). There were no detectable differences between visually normal SD and the blind SD/RCS rats either in location or in numbers of FG-, FB-, and FG+FB-labeled neurons (Table 7).

Facial Nucleus Ipsilateral to FFA

The distribution pattern of retrogradely labeled motoneurons dramatically changed in both groups: the myotopic organization of the facial nucleus was completely lost, i.e., the neurons projecting to the whisker pad musculature after surgery (labeled with FB) were scattered throughout the entire facial nucleus. All double labeled FG+FB neurons were observed only in the lateral facial subnucleus (Fig. 13B, C).

As indicated in Table 7, the number of postoperatively FB-labeled motoneurons on the operated side was 1,782±129 in the visually normal SD and 1,726±66 in the SD/RCS rats, indicating a distinct hyperinnervation (Angelov et al. 1996). In both animal groups, the percentage of double-labeled perikarya, i.e., those motoneurons that succeeded in reinnervating their original target did not exceed 40%.

Table 7 Insufficient accuracy of reinnervation in visually normal SD and in blind SD/RCS rats

Animals	Left side			Right side		
	FG-labeled original pool	FB-labeled original pool	FG+FB-labeled original pool	FG-labeled original pool	FB-labeled postoperatively regrown	FG+FB-labeled accurately regrown
Visually normal SD rats (subgroupF_1) n=6	1,380±111	1,428±134	1,296±93 (94%)	1,401±132	1,782±129	522±69 (37%)
Blind SD/RCS rats (subgroup F_2) n=6	1,522±75	1,422±101	1,349±99 (89%)	1,464±47	1,726±66	454±43 (31%)

Mean numbers and standard deviation of retrogradely labeled perikarya following injection of 100 µl 1% FG as a preoperative label and 100 µl 1% FB as a postoperative label in visually normal SD and blind SD/RCS rats 56 days after unilateral (right side) FFA. The values in parentheses indicate what portion of the motoneurons that had innervated the whisker pad before FFA (FG-labeled) succeeded in reinnervating the original target and incorporating the second label

3.1.6.2
Postoperative Triple Labeling: Identical Amount of Supernumerary Axonal Branches in Visually Normal SD Rats and Blind SD/RCS Rats

Unoperated Control SD Rats and SD/RCS Rats

Following simultaneous application of crystalline DiI, FG, and FB, respectively, to the freshly transected zygomatic, buccal, and marginal mandibular branches of the facial nerve in visually normal SD rats, we counted 303±51 DiI-labeled motoneurons projecting through the zygomatic branch and localized in the dorsal facial subnucleus, 1,503±186 FG-labeled motoneurons projecting through the buccal branch and localized in the lateral facial subnucleus, and 297±63 FB-labeled motoneurons projecting through the marginal mandibular branch and localized in the intermediate facial subnucleus. The values obtained for the blind SD/RCS rats were very similar: 316±49 motoneurons projected through the zygomatic branch, 1,450±145 through the buccal branch and 356±75 through the marginal mandibular branch (Table 8). No double-labeled motoneurons were observed. No cells were observed in the ventromedial facial subnucleus, whose motoneurons project through the posterior auricular branch, and which was not affected by our labeling procedures (Fig. 14A).

Facial–Facial Anastomosis

Eight weeks after unilateral FFA and another ten days after triple retrograde labeling, two changes were detected in the lesioned facial nucleus in both the visually normal SD rats, and in blind SD/RCS rats. First, a myotopic organization within subnuclei was no longer observed, i.e., all motoneurons retrogradely labeled by the three tracers were scattered throughout the whole nucleus. Second, numerous double-labeled (pink-orange or purple) motoneurons appeared, thus demonstrating that twin branches of parental axons projected into more than one ramus of the facial nerve (Fig. 14B, C). Counts of all motoneurons containing DiI (labeled by DiI only, DiI+FG, or by DiI+FB) showed that the double-projecting motoneurons whose axons regrew a branch into the zygomatic ramus comprised about 35% of all motoneurons (Table 8).

3.1.6.3
Functional Analysis of Vibrissae Movement: Poor Motor Performance in Visually Normal SD Rats, but Perfect Recovery of Whisking Behavior in Blind SD/RCS Rats

Behavioral Observations

Following FFA in visually normal SD rats, the vibrissae drooped and acquired a caudal inferior orientation. At 10–14 days post operation (DPO), the vibrissae rose again to the level of the mouth and acquired a posterior orientation. No signs of restoration of rhythmical whisking were observed.

Following FFA in blind SD/RCS rats, the vibrissae drooped and became motionless but rose to the level of the mouth at 10–14 DPO. Initial signs of restoration of rhythmical whisking occurred at 21–28 DPO. An almost complete recovery of function was detected 2 months after surgery.

Table 8 Identical amount of supernumerary axonal branches in visually normal SD rats and blind SD/RCS rats

Animals	Neurons with axons only in the zygomatic branch (DiI-only)	Neurons with axon sprouts in the zygomatic and buccal branches (DiI+FG)	Neurons with axon sprouts in the zygomatic and marginal mandibular branches (DiI+FB)	Total of branched and unbranched neurons projecting in the zygomatic nerve (DiI, DiI+FG, DiI+FB)	Neurons with axons only in the buccal branch (FG-only)	Neurons with axons only in the marginal mandibular branch (FB-only)
Intact visually normal SD rats (subgroup F_1); n=6	303±51 (100%)	0	0	303±51 (100%)	1,503±186	297±63
Intact blind SD/RCS rats (subgroup F_2); n=6	316±49 (100%)	0	0	316±49 (100%)	1,450±145	356±75
Visually normal SD rats treated with FFA (subgroup F_1); n=6	212±49 (65%)	60±27 (18%)	54±29 (17%)	326±98 (100%)	2,185±239	1,780±230
Blind SD/RCS rats treated with FFA (subgroup F_2); n=6	282±53 (65%)	100±27 (23%)	52±16 (12%)	434±41 (100%)	1,702±98	416±49

Mean numbers and standard deviations of retrogradely labeled motoneurons, the axons of which project through the zygomatic, buccal, and marginal mandibular branches in intact rats and after unilateral transection and suture of the facial nerve (FFA). The portions of motoneurons projecting through the zygomatic nerve with branched axons (DiI+FG or DiI+FB) and unbranched axons (DiI-only) are indicated in percents below the absolute numbers

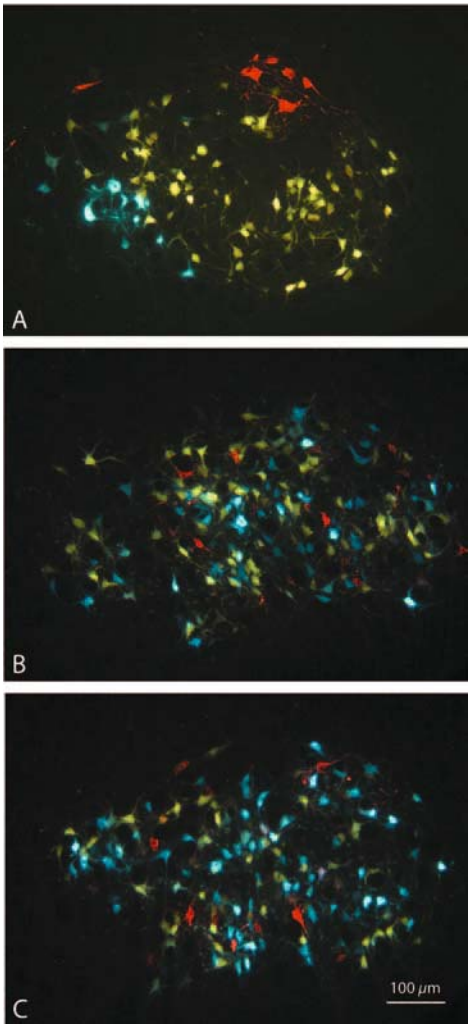

Fig. 14A–C Retrograde labeling in the facial nucleus after application of crystalline DiI to the zygomatic, FG to the buccal and FB to the mandibular nerves. **A** Triple labeling in an unoperated control rat. Note the myotopic organization of the nucleus: the DiI-labeled motoneurons (*red*) are localized in the dorsal, the FG-labeled (*yellow*) mainly in the lateral, and the FB-labeled (*blue*) motoneurons mainly in the intermediate facial subnucleus. **B** Facial nucleus of a visually normal SD rat 2 months after FFA and 10 days after triple retrograde labeling . Note the complete lack of myotopic organization and the presence of double-labeled neurons. **C** Blind SD/RCS rats 2 months after FFA. The triple retrograde labeling reveals a lack of myotopic organization and the presence of double-labeled neurons. (Reprinted from Tomov et al. 2002)

Biometric Analysis of Whisking Behavior

In intact visually normal SD rats and in blind SD/RCS rats, the mystacial vibrissae were erect with an anterior orientation. During exploration, they swept back and forth with a frequency of about 6 Hz. The maximal protraction was 70°. The amplitude of whisking measured 50° (Fig. 15A). These movements were performed at a mean maximal sagittal angular velocity of about 500°/s and a mean maximal sagittal angular acceleration of 20,000°/s^2 (Table 9). There were practically no detectable differences in the whisking behavior of intact visually normal SD rats and intact but blind SD/RCS rats (Table 9). This shows that the biometrics of whisking in rats is stable. Despite the obviously increased importance of vibrissae whisking in blind rats, our measurements revealed no significant differences in all five parameters studied between blind and visually normal rats.

Operated Visually Normal SD Rats

Two months after FFA, the vibrissal hairs swept during exploration with a frequency of about 6–7 Hz. The mean angle during maximal protraction was 80°–90°. The amplitude of whisking was 17°–23°. These movements were performed at a sagittal angular velocity of about 300°–400°/s and a sagittal angular acceleration of 8,000–12,000°/s^2. Thus, except for frequency, all other four parameters remained significantly altered at 2 months after FFA (Table 9). The changes in angle at maximal protraction and in amplitude are graphically illustrated in Fig. 15B.

Operated Blind SD/RCS Rats

The group of blind SD/RCS animals showed complete recovery in almost all biometrical parameters (Table 9). This is very well demonstrated for the angle at maximal protraction and for the amplitude in Fig. 15C.

3.2 Attempts to Reduce Collateral Axonal Branching at the Lesion Site

3.2.1 Application of Extracellular Matrix Proteins Does Not Alter Axonal Branching

3.2.1.1 Behavioral Observations

As already indicated at the beginning of the "Results" section, the "facial-nerve-lesion model" supplies the valuable opportunity to observe postoperative vibrissae paralysis and recovery of rhythmical whisking. Being totally aware of the fact that, in our observations, this type of motor activity represents a relatively crude and nonspecific ballistic movement, we believe that its restoration is in any case superior to the motionless spastic state.

Following any surgery on the facial nerve, the vibrissae drooped and acquired a inferior orientation. In the operated animals the vibrissae "rose" again to the level of the mouth and acquired a posterior orientation at 10–14 days post operation

Table 9 Biometrics of normal and recovering whisking behavior in visually normal SD rats and blind SD/RCS rats.

Animals	Frequency (in Hz)	Angle at maximal protraction (in degrees)	Amplitude (in degrees)	Angular velocity during protraction (in degrees/s)	Angular acceleration during protraction (in degrees/s^2)
Intact visually normal SD rats (subgroup F_1); n=6	5.4±0.7	71±12	48±8	627±213	19,874±11,103
Intact blind SD/RCS rats (subgroup F_2); n = 6	6.0±0.6	63±11	54±17	521±343	24,544±7,737
Visually normal SD rats treated with FFA (subgroup F_1); n=6	6.0±0.7	80±6	20±3	373±61	10,791±1,785
Blind SD/RCS rats treated with FFA (subgroup F_2); n=6	6.0±0.1	66±7.1	50±21	581±254	24,395±11,360

Mean values and standard deviations of several parameters depicting the biometrics of whisking behavior in (1) intact visually normal Sprague-Dawley (SD) rats, (2) intact blind SD/RCS rats, (3) visually normal SD rats subjected to unilateral facial–facial anastomosis (FFA), and (4) blind SD/RCS rats subjected to FFA. The postoperative survival time was 8 weeks

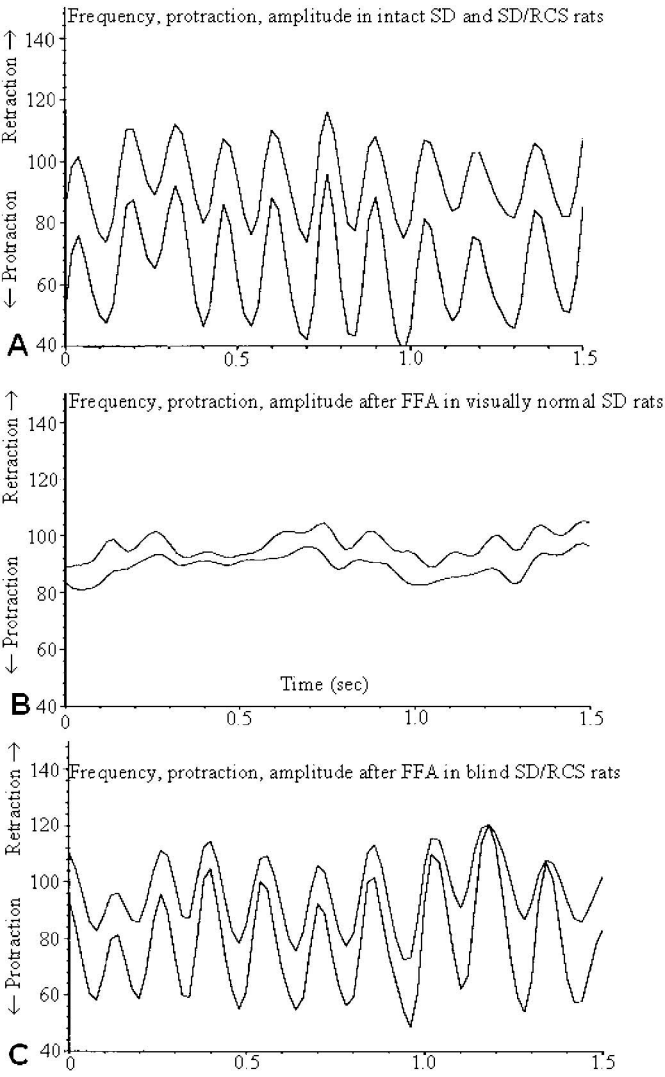

Fig. 15A–C Vibrissae motor performance in intact rats and in rats after FFA. **A** Graphical representation of the changes in angles of two large C-row vibrissae during explorative cyclic whisking in intact rats reconstructed from at least 50 successive frames. The parallel course of the curves indicates the synchronous movements of the two vibrissae. In this case, the frequency was 8 Hz, the protraction between 55° and 75°, and the amplitude between 30° and 60°. **B** Faint whisker movements (protraction and retraction with very small amplitude) during an active exploration of a representative visually normal SD rat 2 months after FFA. **C** Typical synchronous movement of the two large vibrissae of a blind SD/RCS animal during active exploration 2 months after FFA. Frequency of whisking was 6 Hz, protraction about 60°, and amplitude approximately 50°. (Reprinted from Tomov et al. 2002)

(DPO). Initial vibrissae movements were detected at 21–28 DPO. Restoration of rhythmical whisking, however, did not occur.

3.2.1.2 Determination of Axonal Branching

Control Group of Unoperated Rats

In normal Wistar rats (strain HsdCpb:WU), the zygomatic ramus contained axons of 204±88 motoneurons localized in the dorsal facial subnucleus (stained red in Fig. 14A), the buccal ramus the axons of 1,324±29 motoneurons in the lateral facial subnucleus (yellow in Fig. 14A), and the mandibular ramus those of 274±31 motoneurons in the intermediate facial subnucleus (blue in Fig. 14A). No double-labeled motoneurons were observed (Fig. 14A; Table 10).

Facial–Facial Anastomosis

The qualitative changes in the facial nucleus of Wistar rats are identical to those already described for Sprague-Dawley (SD) and the blind SD/RCS rats (Sect. 3.1.6) Counts of motoneuronal perikarya labeled by DiI (labeled by DiI_{only}, DiI+FG, or by DiI+FB) showed that (1) the zygomatic nerve contained axons of significantly more motoneurons than under normal conditions and (2) the perikarya that regrew an axonal branch into the zygomatic and buccal ramus comprised about 20% and those with an axonal branch in the zygomatic and marginal mandibular ramus about 8% of all motoneurons (Table 10).

Entubulation of the Transected Facial Nerve Trunk

In this experimental paradigm, the proximal and distal stump of the transected nerve were inserted into a silicone tube and the interstump space was carefully filled with either phosphate-buffered saline (PBS) or with PBS containing the extracellular matrix (ECM) proteins collagen type I (100 μg/ml), laminin, fibronectin, or tenascin-R (all three at 20 μg/ml). After identical postoperative survival time and triple retrograde labeling as that described for FFA, none of the ECM components used showed a significant impact on the portion of double projecting neurons (Table 10).

Statistical Evaluation

The comparison between unoperated animals and operated rats showed:

1. No significant difference in the number of motoneurons whose axons project through the zygomatic ramus only (see “DiI only” column in Table 10)
2. A significant difference in the number of double-labeled motoneurons, whose axons project through the zygomatic and the buccal ramus or through the zygomatic and the marginal mandibular ramus (see “DiI+FG” and “DiI+FB” columns in Table 10)
3. A significant difference in the total number of motoneurons projecting with one axonal branch through the zygomatic ramus (see “DiI only” and “DiI+FG” and “DiI+FB” columns in Table 10)

Table 10 Application of extracellular matrix proteins does not alter axonal branching

Animals and treatment	Zygomatic nerve (DiI only)	Zygomatic and buccal nerves (DiI+FG)	Zygomatic and mandibular nerves (DiI+FB)	Total zygomatic (DiI and DiI+FG and DiI+FB)
Intact rats (subgroup G_1); n=6	204±88 100%	0	0	204±88 100%
Facial nerve suture (FFA) (subgroup G_2); n=6	238±57 72%	65±36 20%	25±57 8%	328±50* 100%
Entubulation of the facial nerve with 0.9% NaCl (subgroup G_3); n=6	187±32 72%	35±32 13%	39±60 15%	262±68* 100%
Entubulation with 3 mg/ml collagen (subgroup G_4); n=6	208±67 72%	67±37 24%	10±7 4%	285±94* 100%
Entubulation of the facial nerve with 0,002% laminin (subgroup G_5); n=6	173±37 62%	80±25 28%	29±24 10%	282±66* 100%
Entubulation with 20 µg/ml fibronectin F (subgroup G_6); n=6	250±51 69%	32±13 9%	86±15 23%	368±74* 100%
Entubulation with 20 µg/ml tenascin-R (subgroup G_7); n=6	223±49 65%	45±26 13%	76±29 22%	344±35* 100%

Mean numbers and standard deviations of retrogradely labeled motoneurons, the axons of which project into the zygomatic, zygomatic plus buccal, and zygomatic plus marginal mandibular nerve in intact rats, in rats after unilateral FFA, and after entubulation of a transected facial nerve into regeneration chambers with various extracellular matrix proteins. Postoperative survival time, 8 weeks. The portions of motoneurons projecting through the zygomatic nerve with branched axons (DiI+FG or DiI+FB) and unbranched axons (DiI-only) are indicated in percents below the absolute numbers *Indicates statistically significant (P<0.05) difference from the value in intact rats (subgroup G_1)

The statistical comparison of neuron numbers in the various groups of operated rats showed no significant difference in any parameter among rats that underwent transection of the facial nerve.

3.2.2 NGF, BDNF, FGF-2, IGF-I, and GDNF Are Differentially Expressed in the Proximal and Distal Stumps of the Transected Buccal Branch of the Facial Nerve

Despite the sound knowledge indicating that, with the exception of CNTF, which is synthesized by myelinating Schwann cells, the other factors are target-derived (see Sect. 1.5.2) we had to analyze the local presence of neurotrophic factors at the lesion site. As already described in detail (Sect. 2.2.2), the m. masseter with the nerves on it (i.e., the nerve–muscle plate) and the m. levator labii superioris were cut tangentially into 20-µm-thick sections, which were processed for immunocytochemistry. In this way, we also tested the specificity of the selected antibodies, to be used also as therapeutic agents (see Sect. 3.2.3).

NGF Immunoreactivity (IR)

Following resection of 1 mm from the buccal facial branch (BFB), NGF-IR was first detected in the proximal nerve stump at 3 days post axotomy (DPA), reached a maximum at 5 DPA, and declined at 6 DPA (Fig. 16A, B). In the distal nerve stump, NGF-IR appeared at 1 DPA, reached a maximum at 4–5 DPA, and was no longer observed at 12 DPA (Fig. 17). A parallel immunostaining for S-100 protein, considered as a general marker of Schwann cells, showed that the majority of the cells labeled by NGF-IR were Schwann cells. NGF-IR was also found in the target musculature of the whisker pad at 4–5 DPA (Streppel et al. 2002).

BDNF immunoreactivity (IR) was detected in the Schwann cells of the proximal nerve stump at 3–4 DPA, reached a maximum at 5 DPA, and steeply declined after 6 DPA. In the Schwann cells of the distal nerve stump, BDNF-IR became evident at 4 DPA, reached its maximum at 5 DPA, and was no longer observed at 12 DPA (Fig. 16C, D; Fig. 18). These findings support, though indirectly, earlier observations that the retrogradely transported BDNF prevents injury-induced death of facial motor neurons in neonatal rats (Hughes et al. 1993; Koliatsos et al. 1993; Yan et al. 1993). No BDNF immunoreactivity was detected in the target musculature of the whisker pad.

FGF-2-immunoreactivity (IR) was detected in the proximal stump at 1 DPA, reached a first peak at 2 DPA, and declined at 4 DPA in three out of four rats. At 5–6 DPA there occurred a second peak in the FGF-2-IR (in four of four rats), which was followed by a gradual decline to zero at 18 DPA. Identical changes in the FGF-2-IR were detected in the Schwann cells of the distal nerve stump (Fig. 16E, Fig. 19). There was a faint FGF-2-IR in the target muscles of the whisker pad. Similar findings have been reported by Chen et al. (1999).

IGF-I immunoreactivity (IR) followed a pattern of localization and expression identical to that of FGF-2. However, the IGF-I-IR in the target muscles (detected

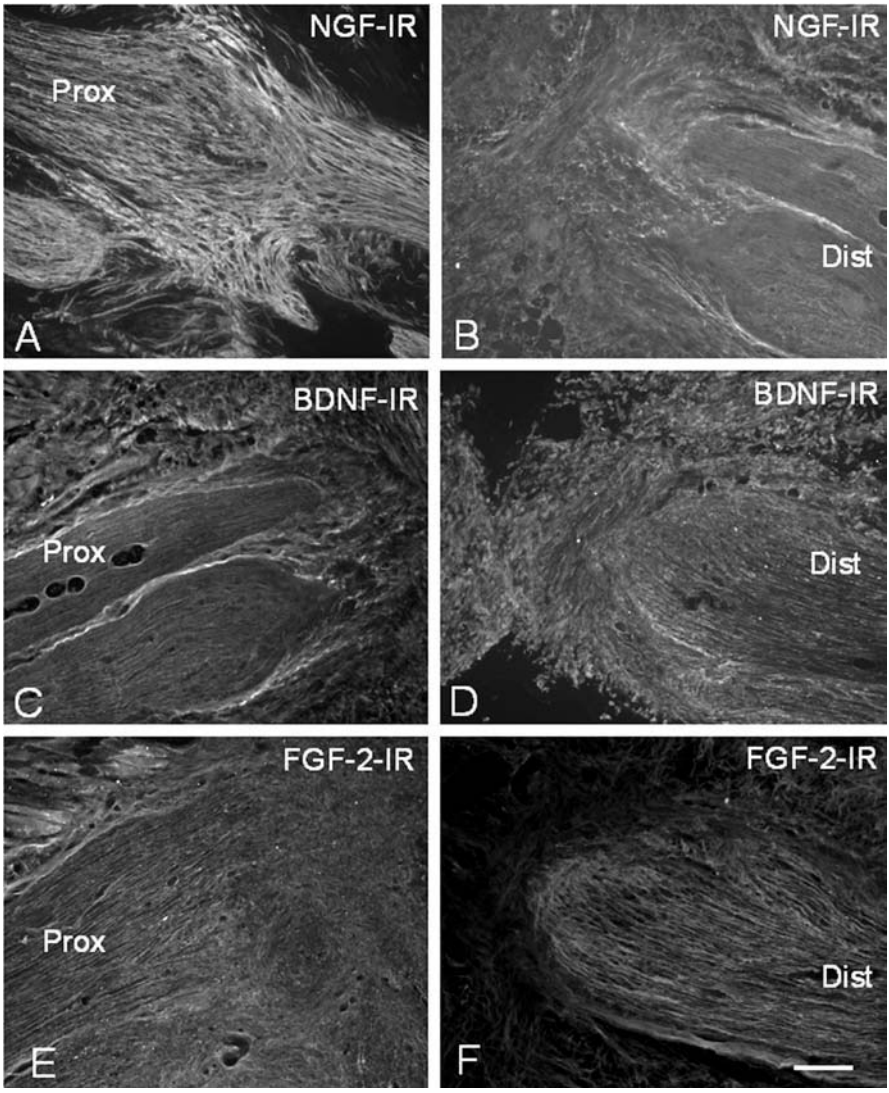

Fig. 16A–F Patterns of expression of NGF (**A**, **B**), BDNF (**C**, **D**) and FGF-2 (**E**, **F**). Longitudinal section through transected buccal branch of rat facial nerve showing immunofluorescence in small cells (Schwann cells) with long and slender processes running parallel to the long axis of the nerve. Immunopositive structures are observed in both proximal (*Prox*) and distal *(Dist*) nerve segments; 20-µm-thick frozen sections. *Scale bar*=200 µm

at 1 DPA) was stronger and persisted till 5 DPA (Fig. 20). This result is in line with earlier data showing that IGF-I immunoreactivity is mainly found in Schwann cells in the first week after the lesion, i.e., before strongly IGF-1 positive macrophages invade the lesioned nerve (Glazner et al. 1994; Ishii et al. 1994; Cheng et al. 1996).

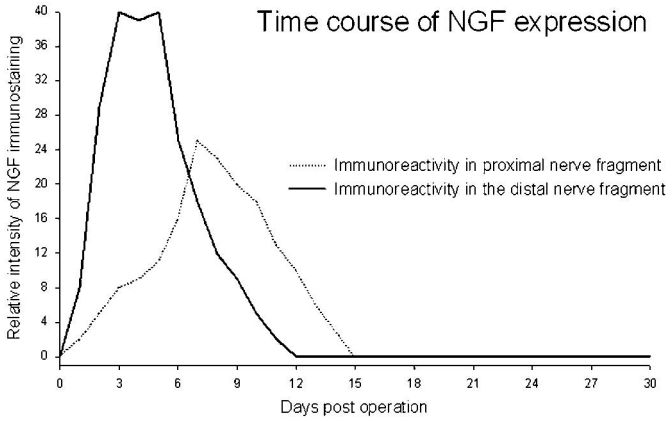

Fig. 17 Time course of the expression of NGF-immunoreactivity in the proximal and distal stumps of the transected buccal branch of the facial nerve. Both the presence and the intensity of the immunofluorescence were estimated by two independent observers who were "blind" to the previous treatment of the rat. A *scale* with a minimum of 0 and maximum of 40 was used

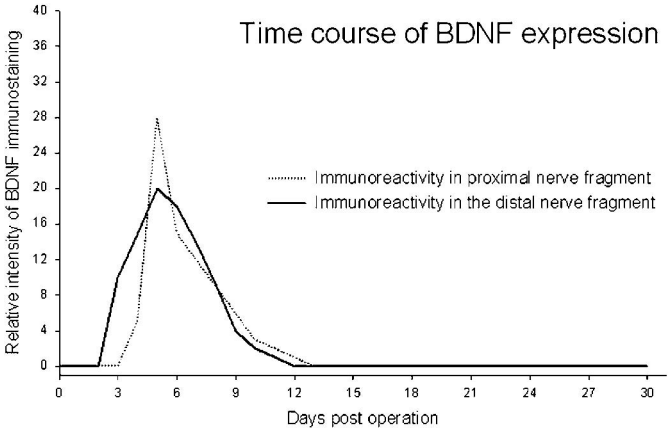

Fig. 18 Time course of the expression of BDNF-immunoreactivity in the proximal and distal stumps of the transected buccal branch of the facial nerve. For methodological details see Fig. 17

GDNF immunoreactivity (IR) in the proximal nerve stump appeared at 1–2 DPA, reached a maximum at 6 DPA, and disappeared at 16 DPA. In the distal nerve stump, GDNF-IR appeared at 3 DPA, reached a maximum at 5 DPA, and was no longer observed at 10 DPA (Fig. 21). These results are in accord with earlier data on the expression of GDNF-IR by the facial motoneurons (Yan et al. 1995). There was no GDNF-IR in the target musculature of the whisker pad.

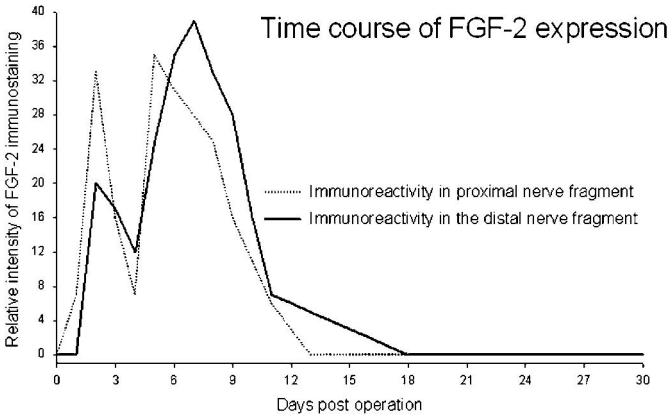

Fig. 19 Time course of the expression of FGF-2-immunoreactivity in the proximal and distal stumps of the transected buccal branch of the facial nerve. For methodological details see Fig. 17

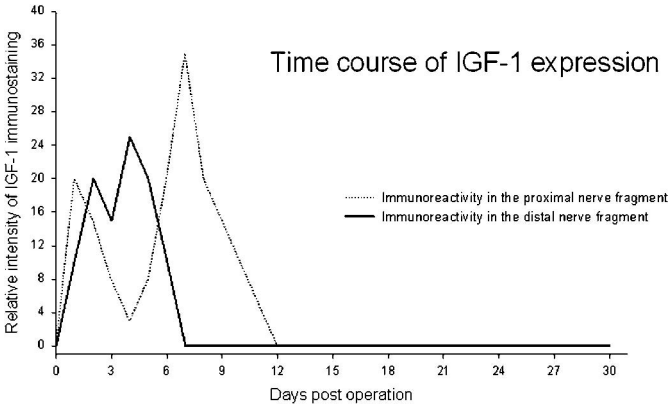

Fig. 20 Time course of the expression of IGF-immunoreactivity in the proximal and distal stumps of the transected buccal branch of the facial nerve. For methodological details see Fig. 17

CNTF Immunoreactivity (IR)

There were no detectable amounts of CNTF in the whole nerves and muscle plates after transection of the buccal branch of the facial nerve (not shown). This finding is consistent with previous results showing that the expression of CNTF mRNA and protein in the peripheral nerve decreases following nerve lesion (Friedman et al. 1992; Sendtner et al. 1992b; Smith et al. 1993).

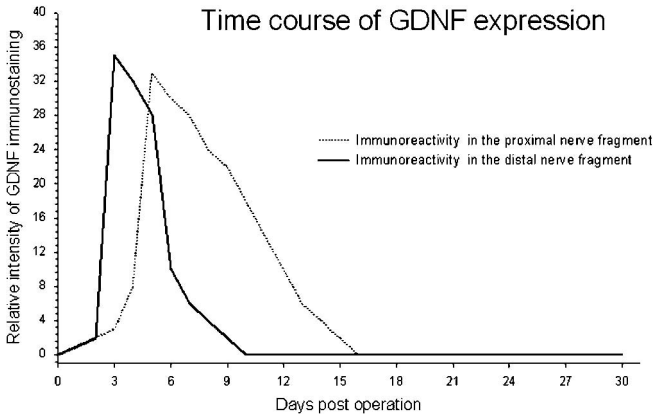

Fig. 21 Time course of the expression of GDNF-immunoreactivity in the proximal and distal stumps of the transected buccal branch of the facial nerve. For methodological details see Fig. 17

3.2.3
Focal Application of Neutralizing Antibodies to Soluble Neurotrophic Factors Reduces Collateral Axonal Branching After Peripheral Nerve Lesion

3.2.3.1
Unoperated Rats

The zygomatic, buccal, and marginal mandibular branches of the facial nerve contained the axons of myotopically organized motoneurons whose number was similar to that described in Sect. 3.2.1 (Table 11, Fig. 14A). No double-labeled motoneurons were observed and all motoneurons projecting through the zygomatic branch contained only DiI. No fluorescent perikarya were ever found in the medial or ventromedial facial subnucleus, the motoneurons of which project through the posterior auricular and cervical branch respectively—neither nerve was an object of transection and labeling.

3.2.3.2
General Features of the Facial Nucleus After Transection of the Facial Nerve

Eight weeks after unilateral FFA/entubulation and another 10 days after triple retrograde labeling, three general changes were detected in the lesioned facial nucleus. First, the myotopic organization into subnuclei was no longer observed, i.e., all retrogradely labeled motoneurons were scattered throughout the facial nucleus (Fig. 14B).

Second, as a rule there were always more retrogradely labeled motoneuronal cell somata than in unoperated animals (last two columns in Tables 11–14). The reason for this postoperative "hyperinnervation of targets" (Angelov et al. 1996) is the labeling of motoneurons which, under normal conditions, do not send

axons into the three facial fascicles under study. After transection of the facial nerve, however, these motoneurons developed axonal branches which adjoined the "wrong" fascicles and thus reached the sites of tracer application. The effects of neutralizing antibodies to neurotrophic factors on the increased number of axons projecting through the regenerated ramus marginalis mandibulae (instilled with crystals of FB), ramus buccalis (labeled by crystals of FG), and ramus zygomaticus (labeled with crystals of DiI) are described below in more detail.

Third, numerous double-labeled motoneurons occurred after the lesion (appearing pink-orange or purple in Fig. 14B), which demonstrated that twin axons projected into more than one branch of the facial nerve. All double- and single-labeled motoneurons labeled were counted. The mean values were statistically analyzed (columns 2–5 in Tables 11–14). The effects of the neutralizing antibodies on the number of axons that postoperatively branched and projected through the ramus zygomaticus (instilled with crystals of DiI) are described also below after the effects on hyperinnervation.

Table 11 Degree of axonal branching as established by triple retrograde labeling after transection of the facial nerve and varying treatments

Animals and treatments	Neurons sending axons only through the zygomatic nerve (DiI-only)	Neurons with axon sprouts in the zygomatic and buccal nerves (DiI+FG)	Neurons with axon sprouts in the zygomatic and marginal mandibular nerves (DiI+FB)
Intact rats (subgroup I_1); n=9	306±81*[2–5,13,15,16,18,19] 100%	0*[2–20]	0*[2–20]
Facial nerve suture (FFA) (subgroup I_2); n=9	132±33*[1,6,7,9,10] 45%	99±12*[1,5,12–20] 34%	63±9*[1,5,12–18] 21%
Entubulation of the facial nerve (subgroup I_3); n=9	183±33*[1,6,10] 53%	78±24*[1,5,12–20] 23%	84±9*[1,5,12–18] 24%
Entubulation with collagen (subgroup I_4); n=9	192±24*[1,5,6,10,15] 62%	93±24*[1,5,12–20] 30%	24±7*[1,5,12–18] 8%
Entubulation with mouse IgG (subgroup I_5); n=9	80±66*[1,4,6,7,9,10] 14%	305±100*[1–4,6–11] 52%	196±80*[1–4,6–11] 34%

Table 11 (continued)

Animals and treatments	Total of branched and unbranched neurons projecting through the zygomatic nerve (DiI, DiI+FG DiI+FB)	Neurons sending axons only through the buccal nerve (FG-only)	Neurons sending axons only through the marginal mandibular nerve (FB-only)
Intact rats (subgroup I_1); n=9	306±81*[12,15–17] 100%	1,422±39*[2,4,5,12–20]	288±42*[2–20]
Facial nerve suture (FFA) (subgroup I_2); n=9	294±33*[12,14–18] 100%	1,833±120*[1,3,5–9,12–20]	402±36*[1,4,5,10,12–20]
Entubulation of the facial nerve (subgroup I_3); n=9	345±66*[12,15–17] 100%	1,521±111*[2,5,12–20]	462±99*[1,5,10,12–20]
Entubulation with collagen (subgroup I_4); n=9	309±36*[12,15–17] 100%	1,890±141*[1,3,5,6–9,12–20]	501±30*[1,2,5,10,12–20]
Entubulation with mouse IgG (subgroup I_5); n=9	581±203 100%	2,470±292*[1–4,6–11]	2,332±236*[1–4,6–11]

Mean numbers and standard deviations of retrogradely labeled motoneurons whose axons project through the zygomatic, buccal, or marginal mandibular branches of the facial nerve in intact rats, in rats after unilateral FFA, and after entubulation of a transected facial nerve into a silicone tube containing varying control substances. Survival time was 56 days post surgery and 10 days post triple-retrograde labeling. Small numbers indicate the subgroups of group I with significantly different values The portions of motoneurons projecting through the zygomatic nerve with branched axons (DiI+FG or DiI+FB) and unbranched axons (DiI-only) are indicated in percents below the absolute numbers *The level of significance is $P < 0.05$

Table 12 Degree of axonal branching after entubulation of the facial nerve with neutralizing antibodies to trophic factors

Animals and treatments	Neurons sending axons only through the zygomatic nerve (DiI-only)	Neurons with axon sprouts in the zygomatic and buccal nerves (DiI+FG)	Neurons with axon sprouts in the zygomatic and marginal mandibular nerves (DiI+FB)
Entubulation with anti-NGF (40 µg/ml) (subgroup I_6); n=9	302±66*[2–5] 77%	65±36*[1,5,12–20] 16%	27±16*[1,5,12–20] 7%
Entubulation with anti-BDNF (160 µg/ml) (subgroup I_7); n=9	270±82*[2,5] 82%	47±25*[1,5,12–20] 14%	14±10*[1,5,12–20] 4%
Entubulation with anti-FGF-2 (100 µg/ml) (subgroup I_8); n=9	196±101*[10] 78%	35±26*[1,5,12–20] 14%	19±9*[1,5,12–20] 8%
Entubulation with anti-IGF-I (30 µg/ml) (subgroup I_9); n=9	282±77*[2,5] 73%	74±45*[1,5,12–20] 20%	28±16*[1,5,12–20] 7%
Entubulation with anti-GDNF (3 µg/ml) (subgroup I_{10}); n=9	392±74*[2–5,8] 70%	131±69*[1,5,12–20] 23%	40±22*[1,5,12–20] 7%
Entubulation with anti-CNTF (100 µg/ml) (subgroup I_{11}); n=9	252±98 77%	55±28*[1,5,12–20] 17%	20±8*[1,5,12–20] 6%

Table 12 (continued)

Animals and treatments	Total of branched and unbranched neurons projecting through the zygomatic nerve (DiI, DiI+FG DiI+FB)	Neurons sending axons only through the buccal nerve (FG-only)	Neurons sending axons only through the marginal mandibular nerve (FB-only)
Entubulation with anti-NGF (40 µg/ml) (subgroup I_6); n=9	394±85*[12,15–17] 100%	1,168±502*[2,4,5,12–20]	572±206*[1,5,12–20]
Entubulation with anti-BDNF (160 µg/ml) (subgroup I_7); n=9	331±107*[12,15–17] 100%	1,152±357*[2,4,5,12–20]	434±179*[5,12–20]
Entubulation with anti-FGF-2 (100 µg/ml) (subgroup I_8); n=9	250±127*[12,15–17] 100%	1,040±314*[2,4,5,12–20]	675±282*[1,5,12–20]
Entubulation with anti-IGF-I (30 µg/ml) (subgroup I_9); n=9	386±127*[12,15–17] 100%	1,365±270*[2,4,5,12–20]	480±162*[5,12–20]
Entubulation with anti-GDNF (3 µg/ml) (subgroup I_{10}); n=9	563±128*[12,15–17] 100%	1,466±444*[5,12–20]	818±281*[1–5,12–20]
Entubulation with anti-CNTF (100 µg/ml) (subgroup I_{11}); n=9	327±121*[12,15–17] 100%	1,501±344*[5,12–20]	542±121*[1,5,12–20]

Mean numbers and standard deviations of retrogradely labeled motoneurons whose axons project through the zygomatic, buccal, or marginal mandibular branches 56 days after entubulation of a transected facial nerve into a silicone tube containing antibodies to trophic factors in neutralizing concentrations. Small numbers indicate the subgroups of group I with significantly different values. The portions of motoneurons projecting through the zygomatic nerve with branched axons (DiI+FG or DiI+FB) and unbranched axons (DiI-only) are indicated in percents below the absolute numbers *The level of significance is $P<0.05$

Table 13 Degree of axonal branching after entubulation of the facial nerve with high concentrations of neutralizing antibodies to trophic factors

Animals and treatments	Neurons sending axons only through the zygomatic nerve (DiI-only)	Neurons with axon sprouts in the zygomatic and buccal nerves (DiI+FG)	Neurons with axon sprouts in the zygomatic and marginal mandibular nerves (DiI+FB)	Total of branched and unbranched neurons projecting through the zygomatic nerve (DiI, DiI+FG DiI+FB)	Neurons sending axons only through the buccal nerve (FG-only)	Neurons sending axons only through the marginal mandibular nerve (FB-only)
Entubulation with anti-NGF (200 µg/ml) (subgroup I_{12}); n=4	198±56 34%	214±75*[1–4,6–11] 37%	166±73*[1–4,6–11] 29%	578±121*[1–11] 100%	2,524±572*[1–4,6–11]	2,058±252*[1–4,6–11]
Entubulation with anti-BDNF (800 µg/ml) (subgroup I_{13}); n=4	152±28*[1,10] 32%	200±50*[1–4,6–11] 42%	125±68*[1–4,6–11] 26%	477±118 100%	2,680±84*[1–4,6–11]	2,109±98*[1–4,6–11]
Entubulation with anti-FGF-2 (500 µg/ml) (subgroup I_{14}); n=4	136±103*[10] 24%	254±156*[1–4,6–11] 44%	190±97*[1–4,6–11] 32%	580±340*[2] 100%	2,194±125*[1–4,6–11]	1,710±714*[1–4,6–11]
Entubulation with anti-IGF-I (150 µg/ml) (subgroup I_{15}); n=4	85±58*[1,4,6,7,9,10] 5%	626±364*[1–4,6–11] 56%	412±255*[1–4,6–11] 39%	1,123±362*[1–11,13,14,18–20] 100%	2,643±150*[1–4,6–11]	1,966±274*[1–4,6–11]

Table 13 (continued)

Animals and treatments	Neurons sending axons only through the zygomatic nerve (DiI-only)	Neurons with axon sprouts in the zygomatic and buccal nerves (DiI+FG)	Neurons with axon sprouts in the zygomatic and marginal mandibular nerves (DiI+FB)	Total of branched and unbranched neurons projecting through the zygomatic nerve (DiI, DiI+FG DiI+FB)	Neurons sending axons only through the buccal nerve (FG-only)	Neurons sending axons only through the marginal mandibular nerve (FB-only)
Entubulation with anti-GDNF (15 μg/ml) (subgroup I_{16}); n=4	143±63*[1,10] 25%	248±76*[1–4,6–11] 44%	172±57*[1–4,6–11] 31%	563±88*[1–4,6–11] 100%	3,214±857*[1–4,6–11]	2,339±437*[1–4,6–11]
Entubulation with anti-CNTF (500 μg/ml) (subgroup I_{17}); n=4	267±105 43%	225±46*[1–4,6–11] 36%	133±22*[1–4,6–11] 20%	616±128*[1–4,6–11] 100%	2,773±171*[1–4,6–11]	1,972±194*[1–4,6–11]

Mean number and standard deviations of retrogradely labeled motoneurons whose axons project through the zygomatic, buccal, or marginal mandibular branches 56 days after entubulation of a transected facial nerve into a silicone tube containing antibodies to trophic factors exceeding the neutralizing concentration fivefold. Small numbers indicate the subgroups of group I with significantly different values. The portions of motoneurons projecting through the zygomatic nerve with branched axons (DiI+FG or DiI+FB) and unbranched axons (DiI-only) are indicated in percents below the absolute numbers *The level of significance is $P<0.05$

Table 14 Degree of axonal branching after entubulation of the facial nerve with combinations of neutralizing antibodies to trophic factors

Animals and treatments	Neurons sending axons only through the zygomatic nerve (DiI-only)	Neurons with axon sprouts in the zygomatic and buccal nerves (DiI+FG)	Neurons with axon sprouts in the zygomatic and marginal mandibular nerves (DiI+FB)	Total of branched and unbranched neurons projecting through the zygomatic nerve (DiI, DiI+FG DiI+FB)	Neurons sending axons only through the buccal nerve (FG-only)	Neurons sending axons only through the marginal mandibular nerve (FB-only)
Entubulation with anti-NGF and anti-BDNF (subgroup I_{18}); n=6	91±56*[1,6,7,9,10] 17%	306±195*[1–4,6–11] 56%	206±127*[1–4,6–11] 38%	544±232*[2] 100%	2,582±352*[1–4,6–11]	2,602±424*[1–4,6–11]
Entubulation with anti-BDNF and anti-bFGF (subgroup I_{19}); n=6	175±21*[1,10] 35%	202±91*[1–4,6–11] 41%	121±67 24%	496±152 100%	2,770±314*[1–4,6–11]	1,966±229*[1–4,6–11]
Entubulation with anti-bFGF and anti-NGF (subgroup I_{20}); n=6	191±88*[10] 42%	196±107*[1–4,6–11] 43%	72±39 15%	460±216 100%	2,690±406*[1–4,6–11]	1,791±208*[1–4,6–11]

Mean numbers and standard deviations of retrogradely labeled motoneurons whose axons project through the zygomatic, buccal, or marginal mandibular branches 56 days after entubulation of a transected facial nerve into a silicone tube containing combinations of antibodies to neurotrophic factors in neutralizing concentrations. Small numbers indicate the subgroups of group I with significantly different values. The portions of motoneurons projecting through the zygomatic nerve with branched axons (DiI+FG or DiI+FB) and unbranched axons (DiI-only) are indicated in percents below the absolute numbers *The level of significance is $P<0.05$

3.2.3.3 Varying Effects of the Neutralizing Antibodies on the Increased Number of Axons and Neurons in the Three Main Branches (Rami) of the Regenerating Facial Nerve

Effects on the Increased Number of Axons and Neurons Projecting Through Ramus Marginalis Mandibulae

As just explained above, following any surgical treatment more motoneurons labeled by FB appeared than in intact rats (last two columns in Tables 11–14).

Our counts after the control entubulations (subgroups I_3–I_5) showed that the values for the groups surgically treated with FFA only (402±36), an empty tube (462±99), and with a tube filled with collagen (510±130) did not differ from those obtained after application of antibodies in neutralizing concentrations (Tables 11, 12).

The counts after application of antibodies in neutralizing concentrations (subgroups I_6–I_{11}) showed that the numbers of FB-labeled motoneurons after treatment with anti-NGF (572±206), anti-BDNF (434±179), anti-FGF-2 (675±282), anti-IGF-I (480±162), and anti-CNTF (542±121) did not significantly differ from that counted after FFA (402±36).

The numbers of FB retrogradely labeled motoneurons in subgroups I_2–I_{11} (last column of Table 12) were significantly higher than the number counted in intact rats. At the same time, however, they were significantly lower than the numbers counted after treatment of the nerve stump with fivefold higher concentrations (Table 13) and after combined treatments (Table 14).

Taken together, we may conclude that the application of neutralizing antibodies to trophic factors to the transected facial nerve trunk had no effect on the increased number of axons or axonal branches projecting into the ramus marginalis mandibulae.

Effect on the Increased Number of Axons and Neurons Projecting Through the Ramus Buccalis

In general, all rats that underwent transection of the facial nerve trunk, e.g., FFA (1,833±120), entubulation in collagen (1,890±111), or in mouse IgG (2,470±292) had significantly more retrogradely labeled motoneurons than intact rats (Table 11). Compared to the number obtained after application of antibodies in neutralizing concentrations (see below, Table 12), these values (in animals subjected to FFA, entubulation with collagen or treatment with mouse IgG) were significantly higher. However, compared to those obtained after fivefold higher concentrations (Table 13), and after combined treatments (Table 14), these numbers were significantly lower.

The counts after the application of antibodies in neutralizing concentrations (subgroups I_6–I_{11}) showed that, in general, the numbers of motoneurons retrogradely labeled by FG after treatment with anti-NGF (1,168±502), anti-BDNF (1,152±357), anti-FGF-2 (1,040±314), and anti-IGF-I (1,365±270) were significantly lower than were counted after simple transection and suture of the facial nerve (FFA; 1,833±120). None of these values (Table 12) were significantly higher

than the number counted in intact rats (Table 11). At the same time, however, they were significantly lower than when counted after treatment of the nerve stump with fivefold higher concentrations (Table 13) and after combined treatments (Table 14).

Thus we may conclude that the application of antibodies that neutralize trophic factors to the transected facial nerve trunk decreased the number of axons projecting into the ramus buccalis. Why this effect did not occur in the ramus marginalis mandibulae (as described in the previous subsection) is unknown.

Effects on the Number of Axons and Neurons Projecting Through the Ramus Zygomaticus

To our surprise, the counts after control entubulations (subgroups I_3–I_5) showed no increase in the total number of neurons whose axons projected through the zygomatic nerve between intact rats (306±81) and rats subjected to FFA (294±33), to implantation of an empty tube (345±66), to entubulation with collagen (309±36), or to entubulation with mouse IgG (581±203). All these values were, however, significantly lower than the numbers obtained after treatment with fivefold higher concentrations of some neutralizing antibodies (Table 13).

The counts after the application of antibodies in neutralizing concentrations (subgroups I_6–I_{11}) showed that, compared to all values in the control entubulations groups (Table 11), the numbers of neurons counted after treatment of the animals with anti-NGF (394±85), anti-BDNF (331±107), anti-FGF-2 (250±127), anti-IGF-I (386±127), anti-GDNF (563±128), anti-CNTF (327±121) were not significantly different (Table 12). These values were, however, significantly lower than the numbers of neurons counted after treatment with fivefold higher concentrations of some neutralizing antibodies (Table 13).

We may summarize that, taken together, the application of neutralizing antibodies to trophic factors to the transected facial nerve trunk had no effect on the number of axons projecting into the ramus zygomaticus.

Furthermore, we may conclude that, in general, the therapy with neutralizing antibodies to neurotrophic factors had no dramatic effect on the overall number in axons in the three main branches (rami) of the rat facial nerve following its transection and regeneration.

3.2.3.4 Effects of Neutralizing Antibodies on Axonal Branching as Estimated by the Portions of Double- and Single-Labeled Motoneuronal Perikarya

We selected the zygomatic branch as a representative of the whole facial nerve plexus to evaluate the degree of axonal branching after surgery. The reason for this was the relatively small number of motoneurons projecting through the zygomatic branch before and after surgery. Thus, the distribution of the tracer DiI was of special interest and we carefully differentiated the portions of motoneuronal perikarya labeled by DiI_{only}, by DiI+FG, or by DiI+FB. Each percentage is indicated below the absolute mean number in the first four columns of all tables. A beneficial

effect of a particular treatment was recognized only if a given value was close to the distribution pattern in intact rats (first row in Table 11).

Effects on the Portion of Double-Labeled Motoneurons Projecting Through the Zygomatic Branch (DiI+FG and DiI+FB)

The counts after control entubulations (subgroups I_3–I_5) showed that the portion of DiI+FG- and DiI+FB-labeled perikarya in the groups surgically treated with FFA only (34% Dil+FG and 21% Dil+FB), with an empty tube (23% and 24%), and with a tube filled with collagen (30% and 8%) did not differ significantly among each other (Table 11). In general, all values were significantly lower than the numbers obtained after treatment with fivefold higher concentrations of all neutralizing antibodies (Table 13) and after combined treatment (Table 14).

The subsequent counts after application of antibodies in neutralizing concentrations (subgroups I_6–I_{11}) showed that, compared to values in the control entubulations (Table 11), the portions of neurons estimated after treatment of the animals with anti-NGF (16% Dil+FG and 7% Dil+FB), anti-BDNF (14% and 4%), anti-FGF-2 (14% and 8%), anti-IGF-I (20% and 7%), anti-GDNF (23% and 7%), anti-CNTF (17% and 6%) were generally decreased, but not significantly different (Table 12). These values (subgroups I_6–I_{11}) were, however, significantly lower than the numbers of neurons counted after treatment with fivefold higher concentrations of some neutralizing antibodies (Table 13) and after combined treatments (Table 14).

Thus, despite a well expressed tendency to diminish the portion of double-labeled perikarya, the application of antibodies to neurotrophic factors failed to reduce significantly the number of motoneurons whose axons gave off branches.

Effects on the Number of Single-Labeled Motoneurons Projecting Through the Zygomatic Branch (DiI-Only)

There were no differences among the control entubulations (subgroups I_3–I_5). In general, the treatment with neutralizing concentrations of anti-NGF (77%), anti-BDNF (82%), anti-IGF-I (78%), and anti-GDNF (70%) significantly increased the number of motoneurons sending a single axon only through the zygomatic branch (Table 12). Treatment with fivefold higher concentration of the same antibodies (Table 13), however yielded worse results. Due to the massive collateral axonal branching probably caused by this dosage, the number of neurons labeled by DiI-only turned out to be lower not only than that after treatments with neutralizing concentrations, but even than that found in the surgical controls (Table 11).

We may thus conclude that the treatment with antibodies to neurotrophic factors significantly increased the portion of unbranched axons in the ramus zygomaticus when compared with the control entubulations and FFA (subgroups I_2–I_5). If we combine this result with the clear trend to diminish the number of double-labeled perikarya, we may summarize that, in general, the application of neutralizing antibodies to a transected nerve trunk reduces axonal branching.

3.2.4
Transplantation of Olfactory Ensheathing Cells, Schwann Cells, and Bone Marrow Stromal Cells Does Not Alter Axonal Branching of Regenerating Facial Motoneurons

3.2.4.1
Determination of the Degree of Axonal Branching

Eight weeks following unilateral facial nerve transection, it was determined how cell suspensions—highly enriched with olfactory ensheathing cells (OECs), Schwann cells (SCs) or bone marrow stroma cells (BMSCs), and transplanted in between the stumps of the transected facial nerve—affect the degree of axonal branching from facial motoneurons.

The myotopic organization of the facial subnuclei as revealed by triple retrograde tracing was completely lost after nerve transection with or without entubulation (Fig. 14A). None of the cell preparations applied (OEC, SC, BMSC) restored the original organization pattern and all of the experimental conditions resulted in the emergence of double-labeled motoneurons sending twin branches into different nerve rami (Fig. 14B, C). Moreover, no differences were observed in the number of double-labeled motoneurons between animals receiving a cellular transplant and animals receiving the collagen-filled control tube alone. This suggests it is the entubulation alone and not the transplanted cells that stimulate axonal branching (Table 15).

3.2.4.2
Biometric Analysis of Whisking Behavior

Biometric analysis was performed to test whether the experimental manipulations caused changes in whisking behavior. Entubulation of the facial nerve in collagen and application of OECs, SCs, and BMSCs in Sprague Dawley rats did not significantly alter the parameters compared to those after FFA (Table 16). Significant differences were found neither in the frequency, angle at maximal protraction, and amplitude, nor in the angular velocity and angular acceleration during protraction between any cell-suspension-treated rats and FFA. Contrary to the morphological evaluation, the biometric analysis did not reveal differences between FFA and entubulation.

3.2.5
Transplantation of Autologous Olfactory Mucosa Does Not Increase the Accuracy of Reinnervation but Promotes Functional Recovery of Vibrissal Motor Performance

3.2.5.1
Transplantation of Olfactory Mucosa Reduces the Collateral Axonal Branching

Transplantation of olfactory mucosa (OM) to the site of facial–facial anastomosis (FFA) significantly ($P<0.05$) reduced axonal collateral branching, as determined

Table 15 Degree of axonal branching after entubulation of the facial nerve of Sprague-Dawley rats with suspensions of cultured cells

Animals and treatments	Neurons with axons only in the zygomatic branch (DiI-only)	Neurons with axon sprouts in the zygomatic and buccal branches (DiI+FG)	Neurons with axon sprouts in the zygomatic and marginal mandibular branches (DiI+FB)	Total of branched and unbranched neurons projecting in the zygomatic nerve (DiI, DiI+FG, DiI+FB)	Neurons with axons only in the buccal branch (FG-only)	Neurons with axons only in the marginal mandibular branch (FB-only)
Intact rats (subgroup J_1); n=6	303±51*[4] (100%)	0*[2–6]	0*[2–6]	303±51*[5] (100%)	1503±186*[2–6]	297±63*[2–6]
Rats treated with FFA (subgroup J_2); n=6	212±49 (65%)	60±27*[1,3,6] (18%)	54±29*[1,3,6] (17%)	326±98*[3,5] (100%)	2,185±239*[1]	1,780±230*[1]
Entubulation with 33 μg/ml collagen (subgroup J_3); n=6	323±67 (48%)	202±58*[1,2] (29%)	161±60*[1,2] (23%)	696±192*[1,2,4] (100%)	2,387±256*[1]	1,976±243*[1]
Entubulation with 200000 OEC in 33 μg/ml collagen type I; (subgroup J_4); n=8	93±57*[1] (31%)	118±58*[1,2] (39%)	94±60*[1] (30%)	300±66*[3,5] (100%)	2,689±672*[1]	1,998±300*[1]

Table 15 (continued)

Animals and treatments	Neurons with axons only in the zygomatic branch (DiI-only)	Neurons with axon sprouts in the zygomatic and buccal branches (DiI+FG)	Neurons with axon sprouts in the zygomatic and marginal mandibular branches (DiI+FB)	Total of branched and unbranched neurons projecting in the zygomatic nerve (DiI, DiI+FG, DiI+FB)	Neurons with axons only in the buccal branch (FG-only)	Neurons with axons only in the marginal mandibular branch (FB-only)
Entubulation with 200000 SC in 33 µg/ml collagen type I (subgroup J_5); n=8	318±169*[4] (49%)	184±103*[1,2] (28%)	147±96*[1] (23%)	650±56*[1,2,4] (100%)	1,933±199*[1]	1,675±219*[1]
Entubulation with 200000 BMSC in collagen; (subgroup J_6); n=6	239±89 (46%)	166±68*[1,2] (30%)	132±55*[1,2] (24%)	547±220 (100%)	2,384±544*[1]	2,115±459*[1]

Mean numbers and standard deviations of retrogradely labeled motoneurons whose axons project through the zygomatic, buccal, or marginal mandibular branches of the facial nerve in intact rats, in rats after unilateral facial–facial anastomosis (FFA), and after entubulation of a transected facial nerve into a silicone tube containing OEC, SC, or BMSC. Small numbers indicate the subgroups of group J with significantly different values. The portions of motoneurons projecting through the zygomatic nerve with branched axons (DiI+FG or DiI+FB) and unbranched axons (DiI-only) are indicated in percents below the absolute numbers *The level of significance is $P<0.05$

Table 16 Recovery of vibrissal whisking after entubulation of the facial nerve with suspensions of cultured cells

Animals	Frequency (in Hz)	Angle at maximal protraction (in degrees)	Amplitude (in degrees)	Angular velocity during protraction (in degrees/s)	Angular acceleration during protraction (in degrees/s^2)
Intact rats (subgroup J_1); n =6	6.7±0.5	59±14*J2-J6	56±16*J2-J6	874±354*J2-J6	36,517±17.519*J2-J6
Rats treated with FFA (subgroup J_2); n=6	6.0±0.7	80±6*J1	20±3*J1-J5	373±61*J1, J3-J6	10,791±1,785*J1
Entubulation with 33 µg/ml collagen (subgroup J_3); n =6	6.0±0.8	91±17*J1	14±5*J1	114±38*J1, J2	3,099±1,481*J1
Entubulation with 20,0000 OECs in 33 µg/ml collagen type I; (subgroup J_4); n=8	5.6±0.8	92±7*J1, J2	18±11*J1	156±159*J1, J2	4,951±6,129*J1, J2
Entubulation with 200,000 SCs in 33 µg/ml collagen type I; (subgroup J_5); n=8	4.4±1.2*1,2	88±9*J1	10±5*J1, J2	91±38*J1, J2	1,615±498*J, J2
Entubulation with 200000 BMSC in collagen; (subgroup J_6); n=6	5.92±1.03	90±12*J1	14±6*J1	92±28*J1, J2	2,376±914*J1

Mean numbers and standard deviations of several parameters depicting the biometrics of whisking behavior in intact SD rats, in animals after transection and suture of the facial nerve (facial–facial anastomosis, FFA), and after entubulation of the transected facial nerve in suspensions of cultured cells. The postoperative survival time was 8 weeks. Indices on the right side above some values indicate the subgroups with significantly different values according to a nonparametric analysis for unpaired (Mann-Whitney test) and paired values (Wilcoxon test)

by counting the motoneurons that sent an axon through the zygomatic facial nerve branch and through twin branches in the buccal or marginal mandibular facial nerve branches (Table 17). After transplantation of OM, 312±88 motoneurons sent an axon or an axonal branch through the zygomatic ramus compared to 482±50 after FFA-only and 301±25 in the intact animal. OM-transplants also significantly ($P<0.05$) reduced the number of double-labeled motoneurons to about 39% compared to 76% after FFA. This was accompanied by a significant ($P<0.05$) increase in the number of motoneurons (61%) that sent a single unbranched axon through the zygomatic ramus (Table 17).

Triple retrograde labeling of motoneurons in the intact animals revealed the myotopic organization of the facial nucleus. No double-labeled perikarya were observed, i.e., under normal physiological conditions, motoneurons do not send twin branches to different nerve rami (cf. Fig. 14A). Fluorescent perikarya were never found in the medial or ventromedial facial subnuclei, the motoneurons of which project through the posterior auricular and cervical branch respectively—neither nerve was an object of transection and labeling. This is in accordance with our previous studies (Dohm et al. 2000; Guntinas-Lichius et al. 2001).

Transection and suture of the facial nerve completely abolished the myotopic organization (cf. Fig. 14B). Furthermore, about 75% of the motoneurons sending an axon to the zygomatic branch gave rise to a twin branch and got double-labeled (Fig. 14B, Table 17). The total number of retrogradely labeled motoneurons in all operated animals was higher than in the control intact rats.

This post-transectional hyperinnervation of targets (Angelov et al. 1996) was reflected by a three- to fourfold increase in the number of motoneurons single-labeled by FB (Table 17, last column). The majority of axons which took up the retrograde tracer originated from motoneurons projecting to the cervical branch of the facial nerve in intact animals (Fig. 1). Since this branch was not traced in intact animals (Fig. 5), the corresponding motoneurons were not visible until the post-transectional misguidance "led" their axons into the FB-traced marginal mandibular branch. Transplantation of OM did not restore the myotopic organization.

Taken together, our data clearly demonstrate that transplantation of OM significantly reduced collateral branching compared to FFA only, but did not completely restore the original innervation pattern as observed in the intact animal. Interestingly, transplantation of OM significantly increased the number of single-labeled motoneurons projecting into the marginal mandibular branch.

3.2.5.2
Transplantation of Olfactory Mucosa Does Not Increase the Accuracy of Reinnervation

Following transplantation of OM to the suture site, a mean of 1,625±553 motoneurons was found to reinnervate the whisker pad compared to 2,024±103 after FFA and 1,540±94 in the intact animal (Table 18). However, the reduction of 33% compared to FFA was statistically not significant. Using preoperative labeling with

Table 17 Effect of autologous olfactory mucosa transplanted to transected and sutured facial nerve on the degree of axonal branching

Animals and treatments	Neurons with axons only in the zygomatic branch (DiI-only)	Neurons with axon sprouts in the zygomatic and buccal branches (DiI+FG)	Neurons with axon sprouts in the zygomatic and marginal mandibular branches (DiI+FB)	Total of branched and unbranched neurons projecting in the zygomatic nerve (DiI, DiI+FG, DiI+FB)	Neurons with axons only in the buccal branch (FG-only)	Neurons with axons only in the marginal mandibular branch (FB-only)
Intact Lewis SSN rats (subgroup K_1); n=6	301±25$^{*K2, K3}$ (100%)	0$^{*K2, K3}$	0$^{*K2, K3}$	301±25^{*K2} 100%	1,345±115	445±74^{*K3}
Animals treated with FFA-only (subgroup K_2); n=6	116±15$^{*K1, K3}$ (24%)	239±42$^{*K1, K3}$ 50%	123±13$^{*K1, K3}$ 26%	482±50$^{*K1, K3}$ 100%	1,734±183	315±62^{*K3}
Animals treated with FFA + olfactory mucosa (subgroup K_3); n=6	190±33$^{*K1, K2}$ (61%)	71±34$^{*K1, K2}$ 23%	40±22$^{*K1, K2}$ 16%	312±88^{*K2} 100%	1,726±234	1,306±140$^{*K1, K2}$

Mean numbers and standard deviations of retrogradely labeled facial perikarya, the axons of which project through the zygomatic, buccal, and marginal mandibular branches in intact rats, in rats that underwent unilateral facial–facial anastomosis (FFA) only, or unilateral FFA+OM (olfactory mucosa). The postoperative survival time was 8 weeks. Indices on the right above indicate the subgroups with significantly different values. The portions of motoneurons projecting through the zygomatic nerve with branched axons (DiI+FG or DiI+FB) and unbranched axons (DiI-only) are indicated in percents below the absolute numbers *The level of significance is $P<0.05$

FG and postoperative labeling with FB after transplantation of OM, an increased portion of motoneurons was observed that succeeded in reinnervating their original target: 597±283 motoneurons (49%) compared to 320±50 (22%) after FFA and 1,367±96 (93%) in the intact animal. This increase was also statistically not significant compared to FFA.

Injection of FG into the whisker pad of intact rats was found to label 1,472±71 facial motoneurons. Two months later, injection of FB as close as possible to the primary injection site, labeled 1,515±78 motoneurons. This demonstrates that there is no difference in the labeling efficiency for FG and FB (Table 18). Moreover, both tracers labeled only motoneurons that were localized in the lateral facial subnucleus, which is in agreement with the myotopic organization of the facial nucleus in intact rats (Fig. 13A). Control experiments, including the injection of tracers on the left side (contralateral to FFA), revealed again no differences in labeling efficiency between both tracers. The data were comparable to those of the intact animal (Table 18).

After FFA, no mytopic organization into subnuclei was evident and the bulk of motoneurons (about 80%), which were postoperatively labeled by FB, were scattered throughout the other facial subnuclei (Fig. 13B, C; Table 18). Due to the posttransectional axonal branching, the number of retrogradely labeled motoneurons in all operated animals was higher than that in the control intact rats.

3.2.5.3 Transplantation of Olfactory Mucosa Promotes Functional Recovery of Vibrissal Motor Performance

The detailed biometric analysis of whisking behavior showed that all animals that underwent FFA and transplantation of OM displayed a significantly ($P<0.05$) better recovery of the biometrical parameters than the rats with FFA-only (Table 19). This is well demonstrated by the curves representing the angle at maximal protraction and amplitude (cf. Fig. 15). Furthermore, the values for angular velocity and angular acceleration did not differ significantly from those of the intact animals. Following surgery and implantation of OM, the vibrissae drooped motionlessly and "rose" at 10–14 DPO. Initial signs of restoration of rhythmical whisking occurred at 21–28 DPO. An almost complete recovery of function was detected 2 months after surgery.

After FFA-only or FFA combined with transplantation of buccal mucous membrane devoid of OECs (FFA+BMM) the vibrissae drooped and acquired an inferior orientation. At 10–14 days post operation (DPO), the vibrissae "rose" again to the level of the mouth and acquired a posterior orientation. No signs of restoration of rhythmical whisking were observed.

This is the first demonstration indicating that transplanted tissue exerts beneficial effects on facial nerve regeneration. Since there was no evident functional improvement after transplantation of BMM, we feel confident that this beneficial effect is not due to an unspecific mechanical effect of any given transplanted tis-

Table 18 Effect of autologous olfactory mucosa transplanted to transected and sutured facial nerve on the accuracy of reinnervation

Animals treatments	Left side			Right side		
	FG-labeled original pool	FB-labeled original pool	FG+FB-labeled original pool	FG-labeled original pool	FB-labeled postoperatively regrown	FG+FB-labeled accurately regrown
Intact Lewis SSN rats (subgroupK_1) n=6	1,472±71	1,515±78	1,410±79 (96%)	1,472±100	1,540±94	1,367±96 $^{*K2, K3}$ (93%)
Animals treated with FFA only (subgroup K_2); n=6	1,396±61	1,563±44	1,370±57 (98%)	1,440±78	2,024±103	320±50^{*K1} (22%)
Rats treated with FFA + olfactory mucosa (subgroup K_3); n=6	1,459±53	1,571±34	1,403±34 (96%)	1,220±302	1,625±553	597±283^{*K1} (49%)

Mean numbers and standard deviation of retrogradely labeled perikarya following injection of 100 µl 1% FG as a preoperative label and 100 µl 1% FB as a postoperative label in intact rats and in rats that underwent unilateral (on the right side) FFA only, or unilateral (on the right side) FFA+OM. The postoperative survival time was 8 weeks. Indices on the right above indicate the subgroup with significantly different values. The values in parentheses indicate what portion of the motoneurons that had innervated the whisker pad before FFA (FG-labeled) succeeded in reinnervating the original target and incorporating the second label *The level of significance is $P<0.05$

Table 19 Effect of autologous olfactory mucosa transplanted to transected and sutured facial nerve on recovery of vibrissal whisking

Animals and treatments	Frequency (in Hz)	Angle at maximal protraction (in degrees)	Amplitude (in degrees)	Angular velocity during protraction (in degrees/s)	Angular acceleration during protraction (in degrees/s^2)
Intact Lewis SSN rats (subgroup K_1); n=6	5.4±1.0	44.6±10.7$^{*K2, K3}$	69.4±15.3$^{*K2, K3}$	803±247^{*K2}	25,485±10,842^{*K2}
Animals treated with FFA-only (subgroup K_2); n=6	5.2±0.8	84.8±7.90$^{*K1, K3}$	17.0±3.80$^{*K1, K3}$	159±63$^{*K1, K3}$	3,308±1,593$^{*K1, K3}$
Animals treated with FFA + olfactory mucosa (subgroup K_3); n=6	5.7±0.8	72.0±11.0$^{*K1, K2}$	44.0±15.0$^{*K1, K2}$	559±385^{*K2}	16,024±8,508^{*K2}

Mean values and standard deviations of several parameters depicting the biometrics of recovering whisking behavior in rats after facial–facial anastomosis (FFA) only and FFA+olfactory mucosa (OM). Indices indicate the subgroups with significantly different values *The level of significance is $P<0.05$

sue, but reflects a specific impact of the transplanted OM. Thus, our present results are relevant not only for the basic processes underlying axonal regeneration and pathfinding, which are important for developing novel cell-based therapeutical strategies of nerve injury, but also for the general use of olfactory ensheathing glia in restoration studies.

4 Discussion

The present synopsis of our experiments yielded two main conclusions: First, the collateral axonal branching that occurs after transection of a peripheral motor nerve has deleterious effects on recovery of coordinated muscle activity. Second, this excessive branching can be reduced by experimental procedures affecting both the lesioned motoneuronal perikarya as well as the axons and Schwann cells in the proximal nerve stump.

4.1 The Combined Approach to Evaluate the Quality of Peripheral Nerve Regeneration

When an axon is severed, the proximal cut end rapidly closes with a membrane seal (Fishman et al. 1990; Spira et al. 1993) and soon afterward forms a terminal swelling or "end-bulb" (Friede and Bischhausen 1980; Fried et al. 1991). Within the following 3 h, numerous axonal branches begin to emerge from the end-bulb and start to elongate (Bisby and Pollock 1983) at a rate of 1–4 mm/day (Tetzlaff and Bisby 1989; Fawcett and Keynes 1990). Under ideal conditions, only one of these branches actually reach its original target. The navigation of these immature axons is under the control of short-range-acting guidance cues, most of them deriving from the distal nerve stump. Thus, post-lesional axonal branching is considered to represent the search of axons for local guidance cues necessary for their navigation (Al-Majed et al. 2000). In general, however, exactly these "actively searching" axons not only choose the wrong way, but also branch and project simultaneously along several different fascicles (subdivisions, rami) of a transected nerve trunk (Angelov et al. 1999). Thus, the process of branching, originally aimed at both neuronal and target survival, turns out to be responsible for the failure of axons to reinnervate solely their original domain (Fu and Gordon 1997).

During the recent years we established *simultaneous multiple neuronal labeling to study axonal branching* (Angelov et al. 1999). In several earlier experimental sets, we conceptually divided the process of axonal regrowth into "axonal elongation" and "axonal branching." We hypothesized that an axonal elongation, which had been fostered by local application of extracellular matrix proteins or olfactory ensheathing cells (OECs), might reduce axonal branching and thus improve recovery of function. The subsequent neuron counts showed that despite their

sue, but reflects a specific impact of the transplanted OM. Thus, our present results are relevant not only for the basic processes underlying axonal regeneration and pathfinding, which are important for developing novel cell-based therapeutical strategies of nerve injury, but also for the general use of olfactory ensheathing glia in restoration studies.

4 Discussion

The present synopsis of our experiments yielded two main conclusions: First, the collateral axonal branching that occurs after transection of a peripheral motor nerve has deleterious effects on recovery of coordinated muscle activity. Second, this excessive branching can be reduced by experimental procedures affecting both the lesioned motoneuronal perikarya as well as the axons and Schwann cells in the proximal nerve stump.

4.1 The Combined Approach to Evaluate the Quality of Peripheral Nerve Regeneration

When an axon is severed, the proximal cut end rapidly closes with a membrane seal (Fishman et al. 1990; Spira et al. 1993) and soon afterward forms a terminal swelling or "end-bulb" (Friede and Bischhausen 1980; Fried et al. 1991). Within the following 3 h, numerous axonal branches begin to emerge from the end-bulb and start to elongate (Bisby and Pollock 1983) at a rate of 1–4 mm/day (Tetzlaff and Bisby 1989; Fawcett and Keynes 1990). Under ideal conditions, only one of these branches actually reach its original target. The navigation of these immature axons is under the control of short-range-acting guidance cues, most of them deriving from the distal nerve stump. Thus, post-lesional axonal branching is considered to represent the search of axons for local guidance cues necessary for their navigation (Al-Majed et al. 2000). In general, however, exactly these "actively searching" axons not only choose the wrong way, but also branch and project simultaneously along several different fascicles (subdivisions, rami) of a transected nerve trunk (Angelov et al. 1999). Thus, the process of branching, originally aimed at both neuronal and target survival, turns out to be responsible for the failure of axons to reinnervate solely their original domain (Fu and Gordon 1997).

During the recent years we established *simultaneous multiple neuronal labeling to study axonal branching* (Angelov et al. 1999). In several earlier experimental sets, we conceptually divided the process of axonal regrowth into "axonal elongation" and "axonal branching." We hypothesized that an axonal elongation, which had been fostered by local application of extracellular matrix proteins or olfactory ensheathing cells (OECs), might reduce axonal branching and thus improve recovery of function. The subsequent neuron counts showed that despite their

known effect of supporting neurite elongation, these procedures failed to suppress axonal branching in the facial nerve plexus (Dohm et al. 2000; Guntinas-Lichius et al. 2001).

Pre- and Postoperative Neuronal Labeling as a Tool to Study the Accuracy of Target Reinnervation

A wealth of experimental studies has shown that intramuscular injection of a tracer (e.g., horseradish peroxidase, HRP) and counts of retrogradely labeled motoneurons provide a powerful and reliable method to evaluate muscle reinnervation (Angelov et al. 1993, 1996, 1997; Streppel et al. 1998; Guntinas-Lichius et al. 2000). Unfortunately, quantitative estimation after single tracing with HRP provides information solely about the reinnervation status of a muscle target since the one-tracer approach cannot elucidate the relationship between pre- and postoperative innervation of target muscles. This is why we switched to sequential application of retrograde labels which allows an optimal evaluation of pre- and postoperative distribution of motoneurons in the same animal, avoiding counting errors due to inter-individual variability (Brushart et al. 1998; Harsh et al. 1991; Molander and Aldskogius 1992; Madison et al. 1996).

The biometrics of whisking behavior provides a very sensitive analysis we recently introduced as a tool to study facial nerve regeneration (Guntinas-Lichius et al. 2001; Tomov et al. 2002). Under normal physiological conditions, the mystacial vibrissae of the rat are erect with anterior orientation. Apart from the fine tremor of about 9 bursts per second in still-standing animals (Semba et al. 1980), the vibrissae perform two additional types of controlled movements during exploration. The first one is the simultaneous sweep of all vibrissae known as "whisking" or "sniffing" (Welker 1964; Semba et al. 1980) repeated 5–11 times per second (Komisaruk 1970; Carvell et al. 1991). The second aspect of motor behavior is the individual action of a single vibrissa in specific palpating fashion upon encountering a novel object (Carvell and Simons 1990; Bermejo et al. 1996). The key movements for both types of motor activity are the protraction and retraction of the vibrissal hairs by the piloerector muscles. The striated muscle fibers mediating protraction form a sling around the rostral aspect of each hair follicle: contraction of these muscles via branches of the facial nerve pulls the base of the follicle caudally, moving the distal aspects of the whisker hair forward. In contrast, retraction of the vibrissae depends primarily upon passive elastic properties of deep connective tissue (Dörfl 1985; Wineski 1985).

4.2 Sensory–Motor Integrity as a Factor in Motor Regeneration

The principal finding of the first experimental set is that a peripheral lesion to the contralateral trigeminal nerve improves the motor reinnervation of the whisker pad in animals whose buccal facial nerve was transected and sutured. This finding is supported by electrophysiological and morphological observations, indicating

that after this type of combined lesion, approximately 41% of all axotomized facial motoneurons reinnervated their original target group of muscles.

So far, we do not know the exact mechanism through which lesions of the trigeminal system affect the axotomized facial motoneurons and we can only speculate on its role in the improved accuracy of reinnervation. From clinical experience after reconstructive surgery on the facial nerve, it is well known that conditioning rehabilitation improves the speed and specificity of reinnervation, which results in only infrequent occurrence of synkinesia (Barbara et al. 2003).

Activation of the low-threshold mechanoreceptors in the corresponding region of the face has been frequently used as a conditioning stimulus (Cronin and Steenerson 2003). Accordingly, increased sensory input may exert a twofold effect on the regenerating facial motoneurons: (1) it may speed up axonal elongation and (2) it may decrease aberrant innervation. Our present experiments provide data that fit well with this concept. The rat facial nucleus receives a dense projection from second-order somatosensory neurons situated throughout the spinal trigeminal complex. This projection is mainly ipsilateral, so we expected that the ipsilateral trigeminal nerve would play the most important role for the sensory-motor integration at the level of the facial nucleus. However, our data show a significantly better regeneration if the facial buccal nerve transection and suture is accompanied by a lesion of the contralateral trigeminal nerve.

4.2.1
Rationale for Using the Combined Trigemino-Facial Lesion Model to Study Neuronal Regeneration

For our experiments we selected the vibrissal area as representative of the morpho-functional entity "facial muscles" → "trigeminal nerve" → "trigeminal nucleus" → "facial nucleus"→ "facial nerve"→ "facial muscles" and performed surgery on the buccal facial nerve branch. Employing this model, we took advantage of:

1. Readily observable verification of postoperative paralysis and recovery by the rhythmical vibrissae movements (Kujawa and Jones 1990).
2. Single and well-established sensory innervation by the infraorbital nerve (Munger and Renehan 1989; Jacquin et al. 1993; Rice et al. 1993).
3. Single and well-established motor nerve supply by the buccal facial nerve branch (Hinrichsen and Watson 1984; Dörfl 1985; Klein and Rhoades 1985; Semba and Egger 1986). This is why following any surgery on the buccal facial nerve the vibrissae drooped and acquired inferior orientation.

The major advantage of the "facial nerve-lesion model" is the possibility to observe post-operative vibrissae paralysis and the recovery of rhythmical whisking. Our behavioral observations reveal that the best recovery of vibrissal motor performance occurs after combined facial–trigeminal lesions. Following transection and suture of the buccal facial nerve plus excision of the contralateral ION, full restoration of rhythmical whisking becomes evident at 7-10 DPO, which is

14–18 days earlier than in rats undergoing only BBA (full restoration of function at 21–28 DPO). This finding is supported by anatomical proofs and electrophysiological measurements showing a faster recovery of the whisker pad muscles after suture of the buccal facial nerve branch combined with excision of the contralateral infraorbital nerve.

4.2.2 Axonal Branching as a Component of Misdirected Target Reinnervation

It is well known that the post-transectional "misdirected" or "aberrant" reinnervation of muscles (Sumner 1990) may occur in three ways.

The first way is that axons are simply misrouted, due to malfunctioning axon guidance, along "false" endoneural tubes through "wrong" fascicles toward "wrong" muscles (Thomander 1984; Aldskogius and Thomander 1986; Brushart and Seiler 1987; Zhao et al. 1992).

The second way is that, in contrast with the precise target-directed pathfinding through single motor neurites during embryonic development (Liu and Westerfield 1990), several (not one single) branches regrow from one transected axon (Shawe 1954; Esslen 1960; Brushart and Mesulam 1980; Baker et al. 1994). Due to the abundance of branches from the transected and misguided axons (Al Majed et al. 2000; Mackinnon et al. 1991; Morris et al. 1972), a given muscle fiber is reinnervated by several axonal branches originating from different motoneurons (Ito and Kudo 1994), a state known as "polyneuronal innervation" (Brown et al. 1981; Rich and Lichtman 1989).

The third way of misdirection occurs through the intramuscular or terminal sprouting of axons within the target (Son et al. 1996). Although thought to be transient (Hennig and Dietrichs 1994), this aberrant innervation may persist for extended periods (Mackinnon et al. 1991; Madison et al. 1999) with deleterious effects on function.

4.2.3 Lesion of the Contralateral Trigeminal Nerve Attenuates the Branching of Transected Facial Axons and Improves the Accuracy of Target Reinnervation

The results obtained after BBA only, BBA plus excision of the ipsilateral ION, and BBA plus excision of the contralateral ION support the following general conclusions:

1. Neither operation leads to an obvious neuronal loss in the lateral facial subnucleus. The total neuron number remains in the range 1,500–2,000 (Table 1).
2. Neither operation succeeds in completely restoring the myotopic organization within the lateral facial subnucleus (compare Figs. 8A, 9A, 10A with Figs. 8B, 9B, 10B).
3. The results after BBA plus excision of the contralateral ION are definitely superior to those obtained after BBA only or BBA plus excision of the ipsilateral ION.

The portions of single- (with unbranched axons) and double-labeled perikarya (with branched axons) were significantly closer to the normal values in intact rats in subgroup A_4 than those obtained after the other two types of surgery (Table 1). This, in turn, means that the degree of collateral axonal branching was the lowest after BBA plus excision of the contralateral ION.

A careful analysis of the data listed in Table 1 shows that the portion of double-labeled (with branched axons) motoneurons displayed the most dynamic changes in response to various types of surgery: Beginning with a zero in intact rats, their percentage reaches 23% after BBA-only and provides a good explanation for the slow recovery of function in this experimental group. After BBA combined with excision of the ipsilateral infraorbital nerve, the portion of double-labeled motoneurons decreases to 13%, and after BBA plus excision of the contralateral infraorbital nerve—to 8% of the whole motoneuronal pool.

The importance of axonal branching and its effect on restoration of function became even more evident after an additional experiment. Under narcosis, we transected and sutured the main trunk of the facial nerve in two Wistar rats of the same strain. As there was no recovery of vibrissal whisking till 56 DPO [at which time there were 1,430±36 motoneurons projecting into the whisker pad muscles (Angelov et al. 1996)], we supposed that an unknown portion of these motoneurons could have regrown axonal branches not only within the buccal nerve, but also within the adjacent zygomatic and/or marginal mandibular nerves. To accept or reject this hypothesis, we reoperated the animals and removed the zygomatic and marginal mandibular nerves totally. Within the following week (5–7 DPO) the vibrissae began rhythmical whisking (own unpublished results). This additional experiment provides strong evidence for the harmful effect of axonal branching and suggests that the leading pathogenetic factor in the misdirected reinnervation is not the simple misrouting of axons, but the redundant axonal branching enabling a single neuron to project to several targets simultaneously.

4.2.4
Nature of the Beneficial Effect of the Accompanying Lesion

Unfortunately, whereas the pathophysiology and the clinical consequences of the post-transectional misdirected reinnervation of muscles are extensively documented, little is known about how the occurrence of this phenomenon might be prevented. Two contradictory therapeutical strategies exist to date.

The first strategy is based on the assumption that the chances of a correct post-transectional axonal routing rise in proportion (1) to the number of growth cones from the axons in the proximal stump and in inverse proportion (2) to the time required by the growth cones to cross the injured zone, grow down the nerve, and reach the muscle targets (Brown et al. 1981; Fu and Gordon 1995a, b).

The second strategy assumes that, despite the established abundance of cues able to guide axons, the growth cones themselves choose their own way by releasing proteases that modify their immediate environment. Consequently, only a perfect

synchronization between the degenerative changes in the distal nerve stump and the sprouting from the proximal nerve stump allows a recovery of the original reinnervation (Dodd and Jessel 1988; Ochi et al. 1994). Our present results fully support this second strategy and show that injury-triggered alterations of the trigeminal input to the axotomized facial motoneurons improve the accuracy of reinnervation, although this procedure does not merely accelerate the outgrowth rate of growth cones.

Our behavioral observations conform to results obtained by other authors after various single or combined lesions on the facial nerve in rats (see Huston et al. 1990 for a review) and are consistent with some known benefits of physical therapy in human patients (Baumel 1974; Taub et al. 1993; Diels 1994). Unfortunately, the mechanisms underlying such improvements are still unknown, but we would like to offer some speculative theories that might explain why a trigeminal lesion reduces facial axonal branching.

The first theory assumes that the observed changes of axonal growth are driven by the abnormal excitability of the spinal trigeminal nucleus as a consequence of the injury to the ipsilateral infraorbital nerve. This abnormal excitability is the result of complex changes. First, the proximal ION stump develops a neuroma, which is a source of sustained long term ectopic impulses (Devor et al. 1989). Second, 15%–20% of the injured sensory cells and fibers degenerate, whereby the small-caliber afferents are preferentially affected (Arvidsson et al. 1986; Wilson and Kitchener 1996). Meanwhile thicker A-delta fibers occupy the "vacant room" of the degenerated A-beta and C-fibers (Woolf et al. 1992). Third, in the corresponding spinal trigeminal nucleus, inhibitory control decreases due to a selective degeneration of GABA-ergic cells (Castro-Lopes et al. 1993). All these changes underlie an unnatural, injury-triggered hyperexcitation of the trigeminal nucleus neurons.

This abnormal activity in the spinal trigeminal nucleus ipsilateral to the lesioned ION can be transmitted to the facial motoneurons via the well established trigemino-facial projection. Thus, the facial motoneurons are reached by trigeminal efferents releasing an excess of glutamate, which is known to suppress neurite outgrowth (Owen and Bird 1997). Since the projection to the ipsilateral facial nucleus is much denser than that to the contralateral one, the facial motoneurons ipsilateral to the lesioned ION are affected much stronger than those on the contralateral one.

Alternatively, since the crossing trigemino-facial projection is definitely less developed than the ipsilateral one (Hinrichsen and Watson 1983), the neurotoxic effect of glutamate is merely not strong enough to cause sufficient glutamate-mediated damage. Furthermore, the crossed trigemino-facial connection may be indirect and may involve interneurons employing GABA (Li et al. 1997; Dauvergne et al. 2001; Popratiloff et al. 2001 b), shown to enhance neurite outgrowth (Barbin et al. 1993). In summary, this first theory assumes that the slower regrowth and more abundant branching of axons on the side ipsilateral to the combined (facial and trigeminal) surgery is due to hyper-stimulation in the ipsilateral trigeminal nucleus.

The second theory assumes that unilateral excision of the infraorbital nerve deprives the facial motoneurons from physiological trigeminal input and "forces" the rat to use the side with intact sensory innervation.

Although the BBA-only itself does not affect the sensory innervation, the rat preferentially uses the intact side of the face. This partially deprives the lesioned facial motoneurons of the trophic effects exerted by the powerful ipsilateral sensory afferents.

The transection of the buccal nerve and the excision of the ipsilateral ION further worsens the trophic environment of the facial motoneurons, because they are not provided with any normal sensory impulses, but are targeted by trigeminal efferents that release an excess of glutamate. Consequently, regeneration proceeds at lower speed and with more abundant axonal branching.

In contrast, if the infraorbital nerve is resected contralateral to the facial nerve transection, then the rat preferentially uses the side with the intact sensory innervation, i.e., the side with the transected facial axons. Receiving, in this way, an excessive rehabilitation and use-dependent neuroprotection very early after the lesion, the axotomized motoneurons are strongly stimulated to elongate axons, to re-innervate the piloerector muscles and to provide the motor basis for the rhythmical whisking of the vibrissae. This increase in the speed of reinnervation in turn reduces the excessive collateral axonal branching and indirectly improves the accuracy of reinnervation. Thus it might be that the mighty ipsilateral afferent input strongly stimulates the axotomized motoneurons to regrow axons.

Further, both factors—the abnormal sensory input and the overuse of an intact trigeminal nerve—may work in concert to provide an optimal tune-up for the facial motoneurons to regenerate properly to their original target. A clue can be found in the marginal changes that we have seen after BBA plus excision of the ipsilateral ION. Although the increased number of accurately regenerated neurons is not significantly higher than in animals with BBA alone, their number is somewhere between BBA and BBA plus excision of the contralateral ION. This could mean that an ipsilateral trigeminal lesion yields an effect which in principle, is similar to that caused by a contralateral lesion, but much less pronounced. Despite the unresolved problems deriving from this experimental paradigm, a theoretical postulate is evolving: the change in the sensory input during the process of regeneration of facial motoneurons may play a beneficial role in their post-lesional pathfinding.

4.2.5 Clinical Implications

The method of combined transection of both the facial and trigeminal nerves finds absolutely no application in human patients. Still, the surprisingly good restoration of facial function after excision of the contralateral trigeminal nerve in rats may suggest that a temporary blockade of the trigeminal fascicles (e.g., by paraneural injections of various anesthetics) during the post-facial-surgery period might yield beneficial results in humans. This assumption needs to be tested in clinical trials.

4.2.6
Recovery of Whisker Movement in Blind Rats Is Probably Due to an Extraordinary Plasticity of the Facial Motoneurons Induced by Putative Behavioral Demand and Early Forced Overutilization

The principal finding of this part of our work is that, despite the poor accuracy of target reinnervation and excessive axonal branching, the recovery of whisking function in blind SD/RCS rats is better than that in visually normal SD animals.

It is well known that in rodents the mystacial vibrissae play an important role in the survival of the individual. In rats they are involved in many types of behavior, including surface discrimination, maze running, and depth perception (Barneoud et al. 1991). Neuroanatomical studies have shown that the mystacial vibrissae together with their large CNS representation area (barrel cortex) constitute a major part of the tactile apparatus of rodents (Rice et al. 1985).

This is why we checked whether the behavioral demand and the forced over-use of the vibrissae after axotomy of the facial nerve are key issues for recovery of vibrissae rhythmical whisking in blind SD/RCS rats.

Since the morphological correlates of nerve regrowth and target reinnervation in both groups of animals (visually normal SD rats and blind SD/RCS rats) were equally poor, we conclude that the present report has revealed a prominent example of motoneuronal plasticity. We suggest that the ectopic facial motoneurons (labeled by FB in Fig. 13B, C), that did not innervate the whisker pad muscles before surgery changed their electrophysiological properties in response to a strong behavioral cortical demand.

Although it cannot be excluded that the differences in recovery between blind and visually normal rat strains may have been due to other, as yet unknown factors, this part of our work shows that (1) poor anatomical specificity can sometimes be compatible with excellent recovery of function, and that (2) behavioral conditions are crucial factors in determining the degree of functional plasticity in the CNS.

4.3
Manipulations of the Conditions at the Lesion Site Cause Changes in the Quality of Axonal Regeneration and Recovery of Function

4.3.1
The Use of Extracellular Matrix Proteins to Improve Reinnervation

The principal finding of these experiments is that regardless of subsequent surgical treatment, the transection of a peripheral motor nerve is always followed by a rather constant amount of axonal branching. This branching capacity of lesioned motoneurons is so strongly determined that even significant changes in the local microenvironment of the lesion site are not able to suppress it.

After nerve transection most of the regenerating axons respond with branching at the injury site, i.e., each parental axon divides into daughter axons or branches, the number of which may reach 25 (Shawe 1954; Jeng et al. 1988). Axonal branching

begins within 3 h after injury (Bisby and Pollock 1983; Sjoberg and Kanje 1990) and is considered to represent the search for local guidance cues necessary for axonal navigation. Still, the factors responsible for the outgrowth and elimination of post-transectional axonal branches are poorly understood (Horch and Lisney 1981; Murphy et al. 1990; Mackinnon et al. 1991).

A key process that occurs after transection of the facial nerve is the appearance of an abnormal activity pattern of the axotomized motoneurons. On one side, the increase in resting potential and the existence of still functioning axo-dendritic synapses (Sumner and Watson 1971; Lux and Schubert 1975) render them hyperexcitable upon intracellular current injections (Eccles et al. 1958; Ferguson 1978). On the other side, the decreased synthesis of transmitter-related compounds (Lieberman 1971) and reduced axo-somatic synaptic input (Blinzinger and Kreutzberg 1968) render the axotomized facial motoneurons less excitable upon afferent stimulation and unable to discharge (Titmus and Faber 1990). This altered excitability of the facial motoneurons, the trans-axonal exchange of intensive nerve impulses between axons (Sadjapour 1975), the alterations in synaptic input to facial motoneurons (Bratzlavsky and vander Eecken 1977; Graeber et al. 1993; Moran and Neely 1996), and the axonal branching are often associated with occurrence of a "post-paralytic syndrome" including mass movements and altered blink reflexes (Kimura et al. 1975; Montserrat and Benito 1988; Sumner 1990).

We hypothesized that the number of branches arising from a transected axon is likely to reflect the complexity of the microenvironment that a regenerating axon faces during its growth down into the distal nerve stump (Brown and Hopkins 1981) prior to reaching a target with important trophic support. To this end, we conceptually subdivided "axonal regrowth" into "axonal elongation" and "axonal branching." As axonal branching appears adverse to functional recovery, we tried to reduce it by improving the rate of axonal elongation in two major ways.

First, it is well known that if the cut nerve ends are tightly reapproximated, a major portion of the severed axons become trapped at the suture site: Since the rate of proceeding Wallerian degeneration is lower than that of axonal elongation, directed axonal growth is impaired (i.e., there is no room for growth because the axons still fill the space). The resprouting axonal branches either turn back to grow in reverse direction, or form a tangled terminal mass, i.e., a neuroma (Horch and Lisney 1981; Ashur et al. 1987). For this reason, instead of facial–facial anastomosis we connected the proximal and distal nerve stump with a silicone tube filled with PBS to allow for an undisturbed axonal regrowth across the gap.

The results obtained favor two conclusions: One: regeneration of transected rat facial nerve across a 5-mm gap in a silicone chamber is as successful as facial nerve suture (Table 10). Our results confirm earlier observations on other peripheral nerves (Lundborg et al. 1982; Williams et al. 1987; Navarro and Kennedy 1989; Danielsen 1990; Seckel 1990; Spector et al. 1992 1993; Labrador et al. 1995; Buti et al. 1996; Gomez et al. 1996; Valero-Cabre et al. 2004). Two: the portion of facial motoneurons with axonal branches projecting synchronously into two fascicles remained unchanged, i.e. despite the putatively improved synchronization between

the degenerative changes in the distal nerve stump and the axonal regrowth from the proximal nerve stump by the locally applied ECM proteins, massive axonal branching still occurred (Table 10).

Second, since the silicone chamber allows manipulation of the regeneration process (Madison et al. 1985, 1987, 1988; Madison and Archibald 1994), we tried to promote axonal elongation without branching by application of ECM proteins known to foster neurite outgrowth. Each myelinated axon and its ensheathing Schwann cell are enclosed in a basal lamina tube, built up by collagen, laminin, heparan sulfate proteoglycan(s), and fibronectin (Tohyama and Ide 1984). Tenascin-R, which is amply detectable in the postnatal and adult mammalian central nervous system (Pesheva et al. 1989; Martini et al. 1990; Bartsch et al. 1993; Angelov et al. 1998), has recently been found to be expressed by Schwann cells in the peripheral nervous system during early development and after nerve injury (R. Probstmeier and P. Pesheva, unpublished observations). All transection injuries disrupt the continuity of these basal lamina tubes, which degenerate and are consequently cleared by phagocytosis. We thus hypothesized that the immediate application of the ECM proteins collagen, laminin (Siironen et al. 1992), fibronectin (Lefcort et al. 1992), or tenascin-R (Erickson 1993; Pesheva et al. 1989 1994), a member of the tenascin family (Martini 1994), may be sufficient to promote a rapid axonal elongation during a period preceding the de novo synthesis of basal lamina components by Schwann cells, as required for tube repair (Hall 1989). Unfortunately, none of the ECM molecules applied was capable of interfering with axonal branching in our experimental system.

One reason for this may be that the ECM molecules employed did not foster axonal elongation in the facial nerve model. On the other hand, it may be that the employed concentration of collagen (100 µg/ml) and laminin (20 µg/ml) was too low to foster neurite outgrowth, even though these concentrations were chosen because of our earlier observations of axonal growth in vitro (Pesheva et al. 1993). Alternatively, the use of the commercially available "Matrigel" might not allow discrimination between the effect(s) of the numerous individual ECM components in this mixture. Anyway, additional experiments with varying concentrations of single ECM proteins in larger animal groups are needed to clarify this point. Moreover, we cannot exclude the possibility that the applied proteins diffused out of the silicone tubes. Although the fostering effect of ECM proteins is assumed to be at its maximum during the first 3 post-transectional hours (period of branching initiation), such a leakage might have reduced the concentration of the neurotrophic agents to ineffective levels.

At the end of this part of our work we may conclude that although isolated growth cones have been shown to respond to alterations in their environment independently (Bixby and Harris 1991; Letourneau and Cypher 1991; Lin and Forscher 1993; Gordon-Weeks 1997), there is no clinical evidence for any specificity in growth cone response to its microenvironment during motor nerve regeneration. The ECM proteins which may confer specificity to the regrowth of axons are unknown. Thus, if mechanisms exist in the adult mammal to recover specific

motor reinnervation, they might not be strong enough to promote a rapid axonal elongation and thus prevent excessive axonal branching.

4.3.2 Role(s) of Trophic Factors in Axonal Regrowth and Effect of Their Neutralization

In our previous set of experiments, we forwarded the hypothesis that accelerated axonal elongation through extracellular matrix proteins fostering neurite outgrowth might reduce axonal branching and improve recovery of function. The subsequent neuron counts showed that, despite their known effect to support neurite elongation, the tested extracellular matrix proteins failed to suppress axonal branching in the facial nerve plexus (Dohm et al. 2000). In this part of our work we approached the problem in a completely different, actually in an exactly opposite way, i.e., by blocking the entire process of neurite regrowth we hoped to achieve a reduction in axonal branching.

Focal application of neutralizing antibodies to neurotrophic factors in a suitable dose shows that collateral axonal branching from the proximal stump of the lesioned peripheral nerve can be experimentally reduced. This treatment diminished the number of axonal branches without any notable harmful affect on neuronal survival and axonal elongation.

The beneficial effect was only observed if antibodies to neurotrophic factors were used in neutralizing concentrations. Following this treatment, the numbers of neurons projecting through each of the investigated branches were found to be very close to those in intact rats. Application of mouse IgG, or antibodies against NGF, BDNF, FGF-2, IGF-I, GDNF, and CNTF in fivefold higher concentrations as well as the combinations of antibodies against NGF+BDNF, BDNF+FGF-2, FGF-2+NGF did not seem to support neurite elongation. Massive axonal branching followed.

Most of the neurotrophic agents are produced by the target tissue and reach the intact facial motoneurons via retrograde axonal transport. Accordingly, after axotomy trophic factors are taken up by regenerating axons to keep the neurons trophically satisfied until the axons regain their target-derived source (DiStefano et al. 1992; Unsicker et al. 1992; Yan et al. 1992; Friedman et al. 1995; Sendtner et al. 1997).

Apart from this "central effect" on neuronal cell bodies (promoting survival), however, numerous reports show an additional "peripheral effect" of the trophic factors, mediated by receptors for NGF, BDNF, FGF-2, GDNF, CNTF, and IGF-I, which are up-regulated at the lesion site following axotomy (Meyer et al. 1992; Raivich and Kreutzberg 1993; McMahon and Priestley 1995; MacLennan et al. 1999). For example, neurotrophins and FGF-2 have been shown to stimulate and hypermodulate neurite outgrowth, enlarge axon caliber and induce sprouting of neurons in vitro and in vivo (Aebischer et al. 1989; Unsicker et al. 1993; Laquerriere et al. 1994; Fujimoto et al. 1997; Gallo and Letourneau 1998; Batchelor et al. 2000; Davies 2000; Deng et al. 2000; Mamounas et al. 2000). On the other hand, the expression of $p75^{NTR}$ in Schwann cells following facial nerve surgery was not found

necessary to promote motoneuron survival or to prompt regeneration (Ferri et al. 1998). This was a major reason for our attempt to neutralize the trophic agents themselves and not their receptors.

In the following paragraphs we will try to interpret the results on the quantitative changes in post-transectional axonal branching after neutralization of this "peripheral effect" and correlate them with other already established events at the lesion site.

The ciliary neurotrophic factor (CNTF) increases the rate of axonal elongation, axonal sprouting, and number of reinnervated muscle end plates, and improves functional recovery (Gurney et al. 1992; Curtis et al. 1993; Sahenk et al. 1994; Ulenkate et al. 1994; Newman et al. 1996; Oyesiku and Wigston 1996). Treatment with 100 μg/ml anti-CNTF decreased the number of double-labeled neurons with branched axons when compared to the control animals that received mouse IgG, but not versus the other controls (Table 12). Based on these results we cannot ascribe any obvious effect to the anti-CNTF-treatment (100 μl/ml) on the branching of axons stemming from a transected rat facial nerve.

The glial-cell-line-derived neurotrophic factor (GDNF) has a marked stimulatory effects on neurite outgrowth (Ebendal et al. 1995; Rosenblad et al. 1996; Sinclair et al. 1996; Wang et al. 1996; Wilby et al. 1999). It has been shown that its neutralization inhibits branching and reduces sprouting (Batchelor et al. 2000). Our present results, however, do not support these earlier data. Treatment with 3 μg/ml anti-GDNF caused a significant increase in the total number of motoneurons projecting through the zygomatic branch of the facial nerve when compared to the values obtained after FFA and after neutralization of FGF-2 (Table 12). This suggests that the neutralization of GDNF potentiated rather than inhibited axonal branching from motoneurons.

The insulin-like growth factors (IGFs) control Schwann cell viability (Meier et al. 1999; Syroid et al. 1999), promote neurite outgrowth of motoneurons (Caroni and Grandes 1990; Lewis et al. 1993; Vergara et al. 1993), increase regeneration rate in vivo after lesions of the sciatic nerve (Sjoberg and Kanje 1989; Pu et al. 1999), and enhance axonal regeneration in chronically injured neurons (Houle et al. 1996). It has been shown that their neutralization causes a sustained reduction in the regeneration rate (Glazner et al. 1993) as well as inhibition of epithelial cell proliferation (Zheng et al. 1997) and spontaneous regeneration (Kanje et al. 1989; Near et al. 1992). In our experiments, treatment with 30 μg/ml anti-IGF-I decreased the number of double-labeled neurons when compared to the control animals treated with mouse IgG (Table 12). Based on these data we can state that the neutralization of IGF-I with 30 μg/ml anti-IGF-I reduced the post-transectional axonal branching.

The basic fibroblast growth factor (FGF-2) stimulates in vivo neurite outgrowth from the proximal stump of transected peripheral nerves and contributes to the enlargement of axon caliber (Aebischer et al. 1989; Unsicker et al. 1993; Laquerriere et al. 1994; Fujimoto et al. 1997). Its neutralization causes a significant decrease in the number of regenerating axons (Chen et al. 1999). Our results, however,

fail to confirm these recent data. Treatment with 100 µg/ml anti-FGF-2 decreased the number of double-labeled neurons only when compared to the animals treated with mouse IgG. Thus, we may conclude that an inhibition of FGF-2 by neutralizing concentrations of antiserum had no significant effect on the post-transectional branching of motoneurons.

The brain-derived neurotrophic factor (BDNF) influences the dynamic branching of axonal arbors (Sawai et al. 1996; Inoue and Sanes 1997; Cohen-Cory 1999; Lom and Cohen-Cory 1999) and effectively promotes axonal outgrowth (Novikov et al. 1997; Novikova et al. 1997; Bamber et al. 2001). Its neutralization reduces the arborizations of axons (Cohen-Cory and Fraser 1995), retards the length of regenerated nerves (Zhang et al. 2000) and decreases the average axon length (Ghosh et al. 1994; Nawa et al. 1994). Our results are generally in line with these findings (Tables 11, 12). The significant increase in the portion of motoneurons sending one single axon through the zygomatic branch (82% of DiI_{only}-labeled cells) when compared to animals treated with FFA (45%) leads to a relative reduction of the portion of neurons with branched axons (there were no differences in the total number of axons comprising the ramus zygomaticus). Reducing the chances for abnormally associated movements (synkinesis; see second way of misdirection in Sect. 4.2.2), this treatment provided conditions for qualitatively better reinnervation of the target muscles.

The nerve growth factor (NGF) can preserve the Schwann cells, whereupon they facilitate regeneration from the proximal stump and modulate neurite outgrowth and axon branching (Aloe et al. 1985; Heumann et al. 1987; Lindsay 1988; Snider and Johnson 1989; Gloster and Diamond 1992; Kimpinski et al. 1997; Galo and Letourneau 1998; McAllister et al. 1999; Mohiuddin et al. 1999). When introduced into silicone tubes bridging the ends of transected sciatic and facial nerves, NGF increases the regeneration rate (Chen et al. 1989; Derby et al. 1993; Spector et al. 1993). Its neutralization by antibodies or antisense oligonucleotides reduced the maladaptive axonal branching and the detrimental sprouting (Yip et al. 1984; Mearow and Kril 1995; Krenz et al. 1999). The results of our work confirm these earlier data (Tables 11, 12). As in the case with application of anti-BDNF, there was a significant increase in the portion of cells with unbranched axons labeled by DiI_{only} (77%) when compared to animals after FFA (45%), after mere entubulation (53%), and after entubulation with mouse IgG (14%). As already described above, this provided conditions for better reinnervation.

Taken together, the results show that treatment of a transected rat facial nerve with anti-NGF or anti-BDNF in suitable neutralizing concentrations significantly reduces the post-transectional axonal branching. In this way focal intraoperative antibody treatment, which should be carefully controlled in human patients, may open new perspectives in the surgical strategies to improve the quality of reinnervation.

4.3.3
The Use of Cell Transplantation for Improving Reinnervation

Transplantation of glial cells into the lesioned PNS is most frequently used to bridge larger nerve gaps that axons lacking support are not able to cross. Previous work has shown that application of supportive cells, like Schwann cells, within guidance channels significantly increased the extent of regeneration (Harvey et al. 1995). However, the effects of transplanted glial cells on the number of newly formed axonal sprouts and their pathfinding has so far not been analyzed in detail.

Since we observed reduced axonal sprouting after application of blocking antibodies (see Sect. 3.2.3.) and olfactory mucosa (see Sect. 3.2.5.), we tested whether the application of a glial cell suspension also interfered with collateral formation. OECs were used in order to test whether the glial cell type thought to be responsible for beneficial effects of olfactory mucosa was also effective as a dissociated cell population. Li et al. (1994; 1997, 1998) reported that OECs but not Schwann cells reduced axonal sprouting that occurred in the lesioned spinal cord. Schwann cells were included in the experimental setup since the cells are known to be supportive to axonal growth and only little is known about putative differential effects of both cell types. The third cell type used in this model, stromal cells from bone marrow, has been shown recently to mediate remyelination in the spinal cord following transplantation (Akiyama et al. 2002a) and intravenous delivery (Akiyama et al. 2002b).

Transplantation of Schwann cells, OECs and BMSCs increased axonal sprouting and reduced functional restoration in comparison with FFA. Comparing the effects of transplanted cell suspensions with control animals treated with collagen only, no significantly different effects were observed. In functional terms, the Schwann-cell-induced changes were most pronounced, although not significantly different. This suggests it is the implantation of the collagen-filled silicon tube that makes the difference, and that the cellular material used within the matrix is of minor importance. Two explanations for the lack of effects of transplanted cells are conceivable:

First, injury to the nervous system is known to trigger the synthesis of trophic factors (Nieto-Sampedro et al. 1983). Entubulation of a transected (e.g., sciatic) nerve is known to increase the trophic factor concentration at the lesion site (Longo et al. 1983, Williams et al. 1983). Among the identified regeneration-promoting molecules are extracellular matrix proteins (Longo et al. 1984) as well as neurotrophic factors (Danielson and Varon 1995). Thus, one may argue that entubulations stimulate the production of trophic factors more strongly than the transplantation of glial cells. The second explanation refers to rat-strain-specific differences in nerve repair. Comparing different inbred and outbred rat strains, we noted recently that there are dramatic differences in the endogenous sprouting capacity (Grosheva et al., manuscript in preparation). Sprague-Dawley rats used for the transplantation experiments displayed a striking and unique increase in axonal collateral formation compared to other strains used in the different experiments. Thus, it is tempting to speculate that the high endogenous sprouting

capacity of Sprague-Dawley rats made it impossible to detect any cell-type-specific effects. Transplantation experiments with different rat strains will show whether the rat strain is of decisive importance.

4.3.4 The Beneficial Effect of Transplanted Olfactory Mucosa May Involve a Moderate but Long-Lasting Secretion of Trophic Molecules at the Lesion Site

The major finding of this part of our work is that transplantation of olfactory mucosa to the transected facial nerve reduces axonal branching and improves vibrissal motor performance. Implying a direct link between diminished axonal branching and recovery of motor function, our results also show that reinnervation of muscle targets by "foreign" motoneurons can yield good functional recovery, thus revealing the vast possibilities of neuronal plasticity.

We showed that transplanted olfactory mucosa improves peripheral nerve regeneration after facial nerve injury. This effect as measured by functional and morphological analysis appears to be mainly based on the reduction of axonal collateral formation. Whether the observed effect was directly due to the olfactory ensheathing glia present in the lamina propria or to other cells of the transplanted olfactory tissue cannot be decided by the present data. What can be said, however, is that the transplant was still in place at the lesion site at the end of the experiments, as shown by *in situ hybridization* using a Y-chromosome-specific DNA probe. Another important point is whether the transplant itself directly exerted the regeneration-promoting effects or whether it may have stimulated beneficial secondary processes. Again, the presented data cannot answer this question unequivocally, mainly because only the outcome of the transplantation was monitored. Immunostaining for trophic factors demonstrated that an increased immunoreaction for NGF, BDNF, and FGF-2 occurred at the lesion site of OM-transplanted animals but not of the operated controls (FFA). Thus, it is conceivable to speculate that the transplant prevented the down-regulation of trophic factors, and therefore that such factors may be responsible for the observed reduction in collateral sprouting and the good functional recovery. It remains to be demonstrated to what extent the OECs in the transplant contributed to the trophic factor expression.

OECs have been shown to promote axon regeneration and remyelination in a variety of model systems (Li et al. 1997, 1998; Ramon-Cueto et al. 1998). It was found that OECs, contrary to Schwann cells, reduced sprouting of central neurons and stimulated the growth into the distal part of the experimentally transected spinal cord. In sharp contrast, transplantation of pure cultures of neonatal OECs to the transected facial nerve, using the same model system as in the present study, resulted in a dramatic increase in axonal sprouting (Guntinas-Lichius et al. 2001).

How can the apparent discrepancy with the present data on OM transplantation be explained? For OEC transplantations we used cultured cells of the *neonatal* rat instead of *adult* olfactory tissue. The expression profile may differ between neonatal and adult tissue and between cultured cells and intact tissue, and may

thus account for the differing effects. Recent evidence implies that trophic factors and their receptors become up-regulated upon dissociation and cultivation of OECs. The expression of the CNTFR α subunit, for example, cannot be found in the developing olfactory bulb (Lee et al. 1997) but is robust in cultured OECs (Wewetzer et al. 2001). The differences in collateral sprouting upon transplantation of cultured OECs and olfactory tissue may, therefore, reflect differing levels of trophic factors. This, in turn, would suggest that the amount of trophic factor is the critical factor that determines the degree of sprouting at the lesion site. This speculation is underscored by our own recent findings demonstrating that application of antibodies against trophic factors reduces collateral sprouting in the same model (Streppel et al. 2002).

The application of olfactory mucosa, which very likely contained fewer cells than the implanted suspensions of OECs, may have induced more moderate effects. Since expression of trophic factors was noted in structures outside the implant itself, it is likely that the transplant induced and maintained trophic factor expression outside the implant.

Thus, we suggest that this forced axonal branching was most likely due to excessive amounts of trophic molecules provided by the cultured OECs. In contrast, our present results show that the transplanted olfactory mucosa may provide a weaker but long-lasting secretion of neurotrophins and FGF-2 at the lesion site.

In conclusion, we showed that transplantation of autologous olfactory mucosa to the sutured perineurium of a peripheral motor nerve significantly improved the quality of target innervation. The reduced axonal branching promoted better axonal pathfinding, which, in turn, provided excellent recovery of function.

4.4
Collateral Branching Versus Terminal Sprouting of Axons

Throughout this study we always tried to differentiate collateral branching of axons at or close to the lesion site from terminal sprouting of axons in the target muscles. Terminal axonal sprouting is a remarkable neural regenerative phenomenon that comes into play after motoneuron trauma: surviving motoneurons expand the size of their motor units to reinnervate as many muscles as possible and in this way to compensate for reduced functional capacity (Grimby et al. 1989; Trojan et al. 1991; Tam and Gordon 2003). Since both phenomena inevitably occur after transection of a peripheral nerve, it is very important to know the impact of collateral branching and that of terminal intramuscular sprouting on the recovery of function. Since some of our preliminary unpublished results show that a diminished collateral branching promotes neither reduction of terminal sprouting nor improvement of coordinated muscle activity, we advance the hypothesis that the intramuscular sprouting is of decisive importance. In this way we support the conclusions of some reports showing that the increased neuromuscular activity improves the quality of target reinnervation by inhibiting terminal axonal sprouting and bridge formation of perisynaptic Schwann cell processes (Brown et al. 1977; Brown and Holland 1979; Tam et al. 2001; Love et al. 2003; Tam and Gordon 2003).

4.5
Prospects for the Future: Role of the Cytoskeleton

As already mentioned, the majority of recent reports assume that both collateral and terminal branching of axons are part of the neurons' responses to extracellular guidance cues. Since most of the receptor-mediated signal transduction pathways converge onto the Rho family of small GTPases, both responses are associated with substantial reorganization of the cytoskeleton (McHale et al. 1995; King et al. 2001; Guan and Rao 2003). This is why an attempt to reduce branching by altering the dynamics of the cytoskeletal reorganization looks plausible. There are three major intracellular cytoskeletal components responsible for the cytomechanical forces in the leading edge of the axon: actin microfilaments, myosin, and microtubules (Challacombe et al. 1996).

It is generally accepted that the actin-based motility causes the movement of microtubules towards the actin-rich peripheral domains of the growth cones (Santos Da Silva and Dotti 2002; Schaefer et al. 2002; Vignjevic et al. 2003). The retraction of F-actin from the leading edge of the growth cone after cytochalasin treatment (inhibition of actin polymerization) causes a complete loss of the guidance capabilities (Bentley and Torojan-Raymond 1986), although microtubules can still extend to the leading edge (Marsh and Letourneau 1984; Forscher and Smith 1988).

Whereas numerous earlier studies indicate that tubulin is involved mainly in the process of axonal elongation (Yamada et al. 1970, 1971; Hoffman and Cleveland 1988; Hoffman et al. 1992; Moskowitz et al. 1993), recent direct observations show that at axonal branching points, the focal accumulation of F-actin is always accompanied by splaying of looped or bundled microtubules, i.e., these dynamic microtubules colocalize and copolymerize with F-actin at the branching points. Interestingly, F-actin is excluded from regions of stable microtubules (Dent and Kalil 2001). These findings are consistent with observations in fixed growth-cones (Tanaka et al. 1995). Accordingly, Schaefer et al. (2002) and Fukata et al. (2002) show that the population of microtubules that invade the peripheral domain via filopodia are highly dynamic, suggesting functional specializations, perhaps in an exploratory and/or signaling capacity. Finally, drugs that attenuate either microtubule or actin dynamics (inhibition of actin polymerization with cytochalasin, stabilization of microtubules with taxol, or damping of microtubule dynamics with vinblastine) have been shown to inhibit axonal branching but not elongation (Baas and Ahmad 1993; Tanaka et al. 1995; Williamson et al. 1996; Challacombe et al. 1997). Treatment with vincristine, an inhibitor of microtubule formation, blocks the outgrowth of some axons and delays the regeneration of others (Pan et al. 2003).

Reorganization of microtubules from bundled to splayed forms at axonal branch points has been documented (Gallo and Letourneau 1998). This might be caused by local attenuation of F-actin flow associated with growth cone–target interactions (Suter and Forscher 2000), or dynamic microtubule ends may be actively captured by actin filaments (Bentley and O'Connor 1994). It has been suggested that microtubules continually explore the growth cone periphery.

Based on the key role(s) of the cytoskeletal proteins actin and tubulin during neurite elongation, axonal branching at the growth cone edge and collateral axon-shaft branch formation, we suggest the following prospect for future studies: pharmacological alterations in the cytoskeletal assembly (polymerization and depolymerization) may diminish in vivo the number of axonal branches after transection of a peripheral motor nerve. Such a treatment would reduce the misdirected reinnervation of targets and improve the recovery of synchronized function of muscles. This project is not only highly relevant to everyday clinical practice, but also could be applied very rapidly; some pharmacological agents that affect microtubule dynamics are registered and established drugs for use in human patients.

5 Summary

Facial nerve surgery inevitably leads to pareses, abnormally associated movements, and pathologically altered reflexes. The reason for this "post-paralytic syndrome" is the misdirected reinnervation of targets, which consists of two major components. First, due to malfunctioning axonal guidance, a muscle gets reinnervated by a "foreign" axon, that has been misrouted along a "wrong" fascicle. Second, the supernumerary collateral branches emerging from all transected axons simultaneously innervate antagonistic muscles and cause severe impairment of coordinated activity. Since it is hardly possible to influence the first major component and improve the guidance of several thousands of axons, we concentrated on the second major component and tried to reduce the collateral axonal branching. The efficiency of various treatments was evaluated in rats by determining: (1) the degree of post-operative axonal branching as estimated by the number of double- or triple-labeled perikarya after application of crystalline DiI, Fluoro-Gold (FG), and Fast Blue (FB) to the zygomatic, buccal, and marginal mandibular branch of the facial nerve respectively; (2) the accuracy of reinnervation as estimated by the number of double-labeled perikarya innervating the whisker pad muscles before and after surgery as shown by intramuscular injections of FG and FB respectively; (3) the recovery of vibrissal motor performance, estimated by a video based motion analysis. So far, we have tried to reduce branching by alteration of the afferent trigeminal input to the axotomized facial motoneurons and by focal application of: (1) neurite outgrowth fostering ECM proteins; (2) neutralizing antibodies to NGF, BDNF, CNTF, GDNF, IGF-I, and FGF-II; (3) suspensions of olfactory ensheathing cells, Schwann cells, and bone marrow stroma cells; and (4) pieces of autologous olfactory mucosa to the transection site. Although most of these manipulations do influence peripheral nerve regeneration to some extent, only the application of autologous olfactory mucosa yielded a major improvement, i.e., better function.

Based on the key role(s) of the cytoskeletal proteins actin and tubulin during neurite elongation, axonal branching at the growth cone edge and collateral axon-shaft branch formation, we suggest the following prospect for future studies: pharmacological alterations in the cytoskeletal assembly (polymerization and depolymerization) may diminish in vivo the number of axonal branches after transection of a peripheral motor nerve. Such a treatment would reduce the misdirected reinnervation of targets and improve the recovery of synchronized function of muscles. This project is not only highly relevant to everyday clinical practice, but also could be applied very rapidly; some pharmacological agents that affect microtubule dynamics are registered and established drugs for use in human patients.

5 Summary

Facial nerve surgery inevitably leads to pareses, abnormally associated movements, and pathologically altered reflexes. The reason for this "post-paralytic syndrome" is the misdirected reinnervation of targets, which consists of two major components. First, due to malfunctioning axonal guidance, a muscle gets reinnervated by a "foreign" axon, that has been misrouted along a "wrong" fascicle. Second, the supernumerary collateral branches emerging from all transected axons simultaneously innervate antagonistic muscles and cause severe impairment of coordinated activity. Since it is hardly possible to influence the first major component and improve the guidance of several thousands of axons, we concentrated on the second major component and tried to reduce the collateral axonal branching. The efficiency of various treatments was evaluated in rats by determining: (1) the degree of post-operative axonal branching as estimated by the number of double- or triple-labeled perikarya after application of crystalline DiI, Fluoro-Gold (FG), and Fast Blue (FB) to the zygomatic, buccal, and marginal mandibular branch of the facial nerve respectively; (2) the accuracy of reinnervation as estimated by the number of double-labeled perikarya innervating the whisker pad muscles before and after surgery as shown by intramuscular injections of FG and FB respectively; (3) the recovery of vibrissal motor performance, estimated by a video based motion analysis. So far, we have tried to reduce branching by alteration of the afferent trigeminal input to the axotomized facial motoneurons and by focal application of: (1) neurite outgrowth fostering ECM proteins; (2) neutralizing antibodies to NGF, BDNF, CNTF, GDNF, IGF-I, and FGF-II; (3) suspensions of olfactory ensheathing cells, Schwann cells, and bone marrow stroma cells; and (4) pieces of autologous olfactory mucosa to the transection site. Although most of these manipulations do influence peripheral nerve regeneration to some extent, only the application of autologous olfactory mucosa yielded a major improvement, i.e., better function.

References

Aebischer P, Salessiotis AN, Winn SR (1989) Basic fibroblast growth factor released from synthetic guidance channels facilitates peripheral nerve regeneration across long nerve gaps. J Neurosci Res 23:282–289

Ahmad FJ, Baas PW (1995) Microtubules released from the neuronal centrosome are transported into the axon. J Cell Sci 108:2761–2769

Akiyama Y, Radtke C, Kocsis JD (2002 a) Remyelination of the rat spinal cord by transplantation of identified bone marrow stromal cells. J Neurosci 22:6623–6630

Akiyama Y, Radtke C, Honmou O, Kocsis JD (2002 b) Remyelination of the spinal cord following intravenous delivery of bone marrow cells. Glia 39:29–236

Aldskogius H, Thomander L (1986) Selective reinnervation of somatotopically appropriate muscles after facial nerve transection and regeneration in the neonatal rat. Brain Res 375:126–134

Aletta JM, Greene LA (1988) Growth cone configuration and advance: a time-lapse study using video-enhanced differential interference contrast microscopy. J Neurosci 8:1425–1435

Al-Majed AA, Neumann CM, Brushart TM, Gordon T (2000) Brief electrical stimulation promotes the speed and accuracy of motor axonal regeneration. J Neurosci 20:2602–2608

Aloe L, Cozzari C, Levi-Montalcini R. (1985) Cyclocytidine-induced release of nerve growth factor from mouse submandibular glands enhances regeneration of sympathetic fibers in adult mice. Brain Res 332, 259–265

Angelov DN, Gunkel A, Stennert E, Neiss WF (1993). Recovery of original nerve supply after hypoglossal-facial anastomosis causes permanent motor hyperinnervation of the whisker-pad muscles in the rat. J Comp Neurol 338:214–224

Angelov DN, Neiss WF, Gunkel A, Guntinas-Lichius O, Stennert E (1994) Axotomy induces intranuclear immunolocalization of neuron-specific enolase (NSE) in facial and hypoglossal neurons of the rat. J Neurocytol 23:218–233

Angelov DN, Neiss WF, Streppel M, Andermahr J, Mader K, Stennert E (1996) Nimodipine accelerates axonal sprouting after surgical repair of rat facial nerve. J Neurosci 16:1041–1048

Angelov DN, Neiss WF, Gunkel A, Streppel M, Guntinas-Lichius O, Stennert E (1997) Nimodipine-accelerated hypoglossal sprouting prevents the postoperative hyperinnervation of target muscles after hypoglossal-facial anastomosis in the rat. Restor Neurol Neurosci 11:109–121

Angelov DN, Walther M, Streppel M, Guntinas-Lichius O, Neiss WF, Probstmeier R, Pesheva P (1998) Tenascin-R is antiadhesive for activated microglia that induce downregulation of the protein after peripheral nerve injury—a new role in neuronal protection. J Neurosci 18:6218–6229

Angelov DN, Skouras E, Guntinas-Lichius O, Streppel M, Popratiloff A, Walther M, Klein J, Stennert E, Neiss WF (1999) Contralateral trigeminal nerve lesion reduces polyneuronal muscle innervation after facial nerve repair in rats. Eur J Neurosci 11:1369–1378

Anonsen CK, Trachy RE, Hibbert J, Cummings CW (1986). Assessment of facial reinnervation by use of chronic electromyographic monitoring. Otolaryngol Head Neck Surg 94:32–36

Arenas E, Persson H (1994) Neurotrophin-3 prevents the death of adult central noradrenergic neurons in vivo. Nature 367:368–371

Arvidsson J (1982) Somatotopic organization of vibrissae afferents in the trigeminal sensory nuclei of the rat studied by transganglionic transport of HRP. J Comp Neurol 211:84–92

Arvidsson J, Ygge J, Grant G (1986) Cell loss in lumbar dorsal root ganglia and transganglionic degeneration after sciatic nerve resection in the rat. Brain Res 373:15–21

Ashur H, Vilner Y, Finsterbush A, Rousso M, Weinberg H, Devor M (1987) Extent of fiber regeneration after peripheral nerve repair: Silicone splint vs. suture, gap repair vs. graft. Exp Neurol 97:365–374

Azisi SA, Stokes D, Augelli BJ, Di Girolamo C, Prockop DJ (1998) Engraftment and migration of human bone marrow stromal cells implanted in the brains of albino rats-similarities to astrocyte grafts. Proc Natl Acad Sci USA 95:3908–3913

Baas PW (1997) Microtubules and axonal growth. Curr Opin Cell Biol 9:29–36

Baas PW (1999) Microtubules and neuronal polarity: lessons learned from mitosis. Neuron 22:23–31

Baas PW, Ahmad FJ (1993) The transport properties of axonal microtubules establish their polarity orientation. J Cell Biol 120:1427–1437

Baas PW, Deitch JS, Black MM, Banker GA (1988) Polarity orientation of microtubules in hippocampal neurons: uniformity in the axon and nonuniformity in the dendrite. Proc Natl Acad Sci USA 85:8335–8339

Baker RS, Stava MW, Nelson KR, May PJ, Huffman MD, Porter JD (1994). Aberrant reinnervation of facial musculature in a subhuman primate: a correlative analysis of eyelid kinematics, muscle synkinesis, and motoneuron localization. Neurology 44:2165–2173

Bamber NI, Li H, Lu X, Oudega M, Aebischer P, Xu XM (2001) Neurotrophins BDNF and NT-3 promote axonal re-entry into the distal host spinal cord through Schwann cell-seeded mini-channels. Eur J Neurosci 13:257–268

Bamburg JR, Bray D, Chapman K (1986) Assembly of microtubules at the tip of growing axons. Nature 321:788–790

Banfai P (1976) Die angewandte klinische Anatomie des Nervus Facialis. II. Die Anastomosen. HNO 24:289–294

Barbara M, Monini S, Buffoni A, Cordier A, Rochetti F, Harguindey A, Di Stadio A, Cerruto R, Filipo R (2003) Early rehabilitation of facial nerve deficits after acoustic neuroma surgery. Acta Otolaryngol 123:932–935.

Barbin G, Pollard H, Gaiarsa J, Ben-Ari Y (1993). Involvement of GABA A receptors in the outgrowth of cultured hippocampal neurons. Neurosci Lett 152:150–154

Barneoud P, Gyger M, Andres F, van der Loos H (1991) Vibrissa-related behavior in mice: transient effect of ablation of the barrel cortex. Behav Brain Res 44:87–99

Bartolomei JC, Greer CA (2000) Olfactory ensheathing cells: Bridging the gap in spinal cord injury. Neurosurgery 47:1057–1069

Bartsch U, Pesheva P, Raff M, Schachner M (1993) Expression of janusin (J1–160/180) in the retina and optic nerve of the developing and adult mouse. Glia 9:57–69

Bastmeyer M, O'Leary DDM (1996) Dynamics of target recognition by interstitial axon branching along developing cortical axons. J Neurosci 16:1450–1459

Batchelor PE, Liberatore GT, Porritt MJ, Donnan GA, Howells DW (2000) Inhibition of brain-derived neurotrophic factor and glial cell line-derived neurotrophic factor expression reduces dopaminergic sprouting in the injured striatum. Eur J Neurosci 12:3462–3468

Baumel JJ (1974) Trigeminal-facial nerve communications. Their function in facial muscle innervation and reinnervation. Arch Otolaryngol 99:34–44

Baumgartner BJ, Shine, HD (1997) Targeted transduction of CNS neurons with adenoviral vectors carrying neurotrophic factor genes confers neuroprotection that exceeds transduced population. J Neurosci 17:6504–6511

Bedi K, Winter J, Berry M, Cohen J (1992) Adult rat dorsal root ganglion neurons extent neurites on predegenerated but not on normal peripheral nerves in vitro. Eur J Neurosci 4:193–200

Bentley D, Torojan-Raymond A (1986) Disoriented pathfinding by pioneer neuron growth cones deprived of filopodia by cytochalasin treatment. Nature 323:712–715

Bentley D, O'Connor TP (1994) Cytoskeletal events in growth cone steering. Curr Opin Neurobiol 4:43–48

Bento RF, Miniti A (1993). Anastomosis of the infratemporal facial nerve using fibrin tissue adhesive. Ear Nose Throat J 72:663

Bermejo R, Harvey M, Gao P, Zeigler HP (1996) Conditioned whisking in the rat. Somatosens Mot Res 13:225–233

Bisby MA (1995) Regeneration of peripheral nervous system axons. In: Waxman SG, Kocsis JD, Stys PK (eds) The Axon. Oxford University Press, Inc., New York, pp 553–578

Bisby MA, Pollock B (1983) Increased regeneration rate in peripheral nerve axons following double lesions: Enhancement of the conditioning lesion phenomenon. J Neurobiol 14:467–472

Bisby MA, Tetzlaff W (1992) Changes in cytoskeletal protein synthesis following axon injury and during regeneration. Mol Neurobiol 6:107–123

Bixby JL, Harris WA (1991) Molecular mechanisms of axon growth and guidance. Annu Rev Cell Biol 7:117–159

Blinzinger K, Kreutzberg G (1968) Displacement of synaptic terminals from regenerating motoneurons by microglial cells. Z Zellforsch Mikrosk Anat 85:145–157

Borgens RB (1988) Voltage gradients and ionic currents in injured and regenerating axons. Adv Neurol 47:51–66.

Bowe CM, Kocsis JD, Waxman SG (1985) Differences between mammalian ventral and dorsal spinal roots in response to blockade of potassium channels during maturation. Proc R Soc Lond 224:355–366

Bratzlavsky M, vander Eecken H (1977) Altered synaptic organization in facial nucleus following facial nerve regeneration: an electrophysiological study in man. Ann Neurol 2:71–73

Bray GM, Aguayo AJ (1974) Regeneration of peripheral unmyelinated nerves. Fate of the axonal sprouts which develop after surgery. J Anat 117:517–529

Bray D, Bunge MB (1981) Serial analysis of microtubules of cultured rat sensory neurons. J Neurocytol 10:589–605

Bray D, Thomas C, Shaw G (1978) Growth cone formation in cultures of sensory neurons. Proc Natl Acad Sci USA 75:5226–5229

Brecht M, Preilowski B, Merzenich MM (1997) Functional architecture of the mystacial vibrissae. Behav. Brain Res 84:81–97

Brown MC, Holland RL (1979) A central role for denervated tissues in causing nerve sprouting. Nature 282:724–726

Brown MC, Hopkins WG (1981) Role of degenerating axon pathways in regeneration of mouse soleus motor axons. J Physiol (Lond) 318:365–373

Brown MC, Jansen JK, Van Essen DC (1976) Polyneuronal innervation of skeletal muscle in new-born rats and its elimination during maturation. J Physiol 261:387–422

Brown MC, Goodwin GM, Ironton R (1977) Prevention of motor nerve sprouting in botulinum toxin poisoned mouse soleus muscles by direct stimulation of the muscle. J Physiol (Lond) 267:42P-43P

Brown MC, Holland RL, Hopkins WG, Keynes RJ (1981)) An assessment of the spread of the signal for terminal sprouting within and between muscles. Brain Res 210:145–151

Brushart TM (1993). Motor axons preferentially reinnervate motor pathways. J Neurosci 13:2730–2738

Brushart TM, Mesulam MM (1980). Alteration in connections between muscle and anterior horn motoneurons after peripheral nerve repair. Science 208:603–605

Brushart TM, Seiler WA (1987) Selective reinnervation of distal motor stumps by peripheral motor axons. Exp Neurol 97:289–300

Brushart TM, Gerber J, Kessens P, Chen Y-G, Royall RM (1998) Contributions of pathway and neuron to preferential motor reinnervation. J Neurosci 18:8674–8681

Büngner O (1891) Ueber die Degenerations- und Regenerationsvorgänge am Nerven nach Verletzungen. Beitr pathol Anat allg Pathol 10:21–393

Burton PR, Hinkley RE, Pierson GB (1975) Tannic acid stained microtubules with 12, 13, and 15 protofilaments. J Cell Biol 65:227–233

Buti M, Verdu E, Labrador RO, Vilches JJ, Fores J, Navarro X (1996) Influence of physical parameters of nerve chambers on peripheral nerve regeneration and reinnervation. Exp Neurol 137:26–33

Caroni P, Grandes P (1990) Nerve sprouting in innervated adult skeletal muscle induced by exposure to elevated levels of insulin-like growth factors. J Cell Biol 110:1307–1317

Carvell GE, Simons DJ (1990) Biometric analyses of vibrissal tactile discrimination in the rat. J Neurosci 10:2638–2648.

Carvell GE, Simons DJ, Lichtenstein SH, Bryant P (1991) Electromyographic activity of mystacial pad musculature during whisking behavior in the rat. Somatosens Mot Res 8:159–164

Castro-Lopes JM, Tavares I, Coimbra A (1993). GABA decreases in the spinal cord dorsal horn after peripheral neurectomy. Brain Res 620:287–291

Challacombe JF, Snow DM, Letourneau PC (1996) Actin filament bundles are required for microtubule reorientation during growth cone turning to avoid an inhibitory guidance cue. J Cell Sci 109:2031–2040

Challacombe JF, Snow DM, Letourneau PC (1997) Dynamic microtubule ends are required for growth cone turning to avoid an inhibitory guidance cue. J Neurosci 17:3085–3095

Chang S, Rodionov VI, Borisy GG, Popov SV (1998) Transport and turnover of microtubules in frog neurons depend on the pattern of axonal growth. J Neurosci 18:821–829

Chen YSH, Wang-Bennet LT, Coker NJ (1989) Facial nerve regeneration in the silicone chamber: the influence of nerve growth factor. Exp Neurol 103:52–60

Chen Y-S, Murakami S, Gyo K, Wakisaka H, Matsuda S, Sakanaka M (1999) Effects of basic fibroblast growth factor (FGF-2)-neutralizing antibody and platelet factor-4 on facial nerve regeneration. Exp Neurol 155:274–283

Cheng H, Cao YH, Olson L (1996 a). Spinal cord repair in adult paraplegic rats: Partial restoration of hind limb function. Science 273:510–513

Cheng HL, Randolph A, Yee D, Delafontaine P, Tennekoon G, Feldman EL (1996 b) Characterisation of insulin-like growth factor-I and its receptor and binding proteins in transected nerves and cultured Schwann cells. J Neurochemistry 66:525–536

Choi D, Raisman G (2002) Somatotopic organization of the facial nucleus is disrupted after lesioning and regeneration of the facial nerve: the histological representation of synkinesis. Neurosurgery 50:355–362

Clatterbuck RE, Price DL, Koliatsos VE (1994) Further characterization of the effects of BDNF and CNTF on axotomized neonatal and adult mammalian motor neurons. J Comp Neurol 342:45–56

Cohen-Cory S (1999) BDNF modulates but does not mediate activity dependent branching and remodelling of optic axon arbours in vivo. J Neurosci 19:9996–10003

Cohen-Cory S, Fraser SE (1995) Effects of brain-derived neurotrophic factor on optic axon branching and remodelling in vivo. Nature 378:192–196

Cronin GW, Steenerson RL (2003) The effectiveness of neuromuscular facial training combined with electromyography in facial paralysis rehabilitation. Otolaryngol Head Neck Surg 128:534–538

Cuevas P, Carceller F, Gimenez-Gallego G (1995) Acidic fibroblast growth factor prevents post-axotomy neuronal death of the newborn rat facial nerve. Neurosci Lett 197:183–186

Curtis R, Adryan KM, Zhu Y, Harkness PJ, Lindsay RM, DiStefano PS (1993) Retrograde axonal transport of ciliary neurotrophic factor is increased by peripheral nerve injury. Nature 365:253–255

Daniloff JK, Levi G, Grumet M, Rieger F, Edelman GM (1986) Altered expression of neuronal cell adhesion molecules induced by nerve injury and repair. J Cell Biol 103:929–945

D'Cruz PM, Yasumura D, Weir J, Matthes M T, Abderrahim H, La Vail MM, Vollrath D (2000) Mutation of the receptor tyrosine kinase gene Mertk in the retinal dystrophic RCS rat. Hum Mol Genet 9:645–651

Danielsen N (1990) Regeneration of the sciatic nerve in the silicone chamber model. Restor Neurol Neurosci 1:253–259

Danielson N, Varon S (1995) Characterization of neurotrophic activity in the silicone-chamber model for nerve regeneration. J Reconstr Microsurg 11:231–235

Dauvergne C, Pinganaud G, Buisseret P, Buisseret-Delmas C, Zerari-Mailly F (2001) Reticular premotor neurons projecting to both facial and hypoglossal nuclei receive trigeminal afferents in rats. Neurosci Lett 311:109–112

Davies AM (2000) Neurotrophins: Neurotrophic modulation of neurite growth. Curr Biol 10:198–200

Deng YS, Zhong JH, Zhou XF (2000) Effects of endogenous neurotrophins on sympathetic sprouting in the dorsal root ganglia and allodynia following spinal nerve injury. Exp Neurol 164:344–350

Dent EW, Kalil K (2001) Axon branching requires interactions between dynamic microtubules and actin filaments. J Neurosci 21:9757–9769

Dent EW, Callaway JL, Szebenyi G, Baas PW, Kalil K (1999) Reorganization and movement of microtubules in axonal growth cones and developing interstitial branches. J Neurosci 19:8894–8908

Derby A, Englemen VW, Friedrich GE, Neises G, Rapp SR, Roufa DG (1993) Nerve growth factor facilitates regeneration across nerve gaps: morphological and behavioural studies in rat sciatic nerve. Exp Neurol 119:176–191

Devor M, Keller CH, Deerinck TJ, Ellisman MH (1989) Na^+ channel accumulation on axolemma of afferent endings in nerve end neuromas in Apteronotus. Neurosci Lett 102:149–154

Diamond J, Coughlin M, Macintyre L, Holmes M, Visheau B (1987) Evidence that endogenous B nerve growth factor is responsible for the collateral sprouting, but not for regeneration of nociceptive axons in adult rats. Proc Natl Acad Sci U S A 84:6596–6600

Diamond J, Holmes M, Coughlin M (1992) Endogenous NGF and nerve impulses regulate the collateral sprouting of sensory axons in the skin of the adult rat. J Neurosci 12:1454–1466

Diels HJ (1994) Treatment of facial paralysis using electromyographic feedback – a case study. Eur J Otorhinolaryngol Suppl S129-S132

Ding M, Hart RP, Shadiack AM, Jonakait GM (1994) The interleukin-1-induced increase of substance P in sympathetic ganglia is not mediated by ciliary neurotrophic factor. J Neurosci Res 38:640–647

DiStefano PS, Friedman B, Radziejewski C, Alexander C, Boland P, Schick CM, Lidsay RM, Wiegand SJ (1992) The neurotrophins BDNF, NT-3 and NGF display distinct patterns of retrograde axonal transport in peripheral and central neurons. Neuron 8:983–993

Dodd J, Jessel TM (1988) Axon guidance and the patterning of neuronal projections in vertebrates. Science 242:692–699

Dörfl J (1985). The innervation of the mystacial region of the white mouse. A topographical study. J Anat 142:173–184

Dohm S, Streppel M, Guntinas-Lichius O, Pesheva P, Probstmeier R, Neiss WF, Angelov DN (2000) Local application of extracellular matrix proteins fails to reduce the number of axonal branches during regeneration. Restor Neurol Neurosci 16:117–126

Duberley RM, Johnson IP (1996) Increased expression of the alpha subunit of the CNTF receptor by rat facial motoneurons after neonatal axotomy and CNTF treatment. Neurosci Lett 218:188–92

Duncan ID, Baker GJ (1987) Experimental crush of the equine recurrent laryngeal nerve: a study of normal and aberrant reinnervation. Am J Vet Res 48:431–438

Dyck PJ, Hopkins AP (1972) Electron microscopic observations on degeneration and regeneration of unmyelinated nerve fibers. Brain 95:223–234

Ebendal T, Tomac A, Hoffer BJ, Olson L (1995) Glial cell line-derived neurotrophic factor stimulates fibre formation and survival in cultured neurons from peripheral autonomic ganglia. J Neurosci Res 40:276–284

Eccles JC, Libet B, Young RR (1958) The behaviour of chromatolyzed motoneurons studied by intracellular recording. J Physiol 143:11–40

Engel AK, Kreutzberg GW (1986) Changes in acetylcholinesterase molecular forms in regenerating motor neurons. Neuroscience 18:467–473

Engel AK, Tetzlaff W, Kreutzberg GW (1988) Axonal transport of 16S acetylcholinesterase is increased in regenerating peripheral nerve in guinea-pig, but not in the rat. Neuroscience 24:729–738

Erickson HP (1993) Tenascin-C, tenascin-R and tenascin-X: a family of talented proteins in search of functions. Curr Opin Cell Biol 5:869–876

Erzurumlu RS, Killackey HP (1979). Efferent connections of the brainstem trigeminal complex with the facial nucleus of the rat. J Comp Neurol 188:75–86

Esslen E (1960) Electromyographic findings on two types of misdirection of regenerating axons. EEG Clin Neurophysiol 12:738–741

Eustache I, Seyfritz N, Gueritaud JP (1994) Effects of insulin-like growth factors on organotypic cocultures of embryonic rat brainstem slices and skeletal muscle fibers. Brain Res Dev Brain Res 81:284–292

Evans PJ, Bain JR, Mackinnon SE, Makino AP, Hunter DA (1991) Selective reinnervation: a comparison of recovery following microsuture and conduit nerve repair. Brain Res 559:315–321

Fawcett JW, Keynes RJ (1990) Peripheral nerve regeneration. Annu Rev Neurosci 13:43–60

Fawcett JP, Bamji SX, Causing CG, Aloyz R, Ase AR, Reader TA, McLean JH, Miller FD (1998) Functional evidence that BDNF is an anterograde neuronal trophic factor in the CNS. J Neurosci 18:2808–2821

Ferguson JH (1978) Hemifacial spasm and the facial nucleus. Ann Neurol 4:97–103
Ferreira MC, Besteiro JM, Tuma Junior P (1994) Results of reconstruction of the facial nerve. Microsurgery 15:5–8
Ferri CC, Moore FA, Bisby MA (1998) Effects of facial nerve injury on mouse motoneurons lacking the p75 low-affinity neurotrophin receptor. J Neurobiol 34:1–9
Fishman HM, Tewari KP, Stein PG (1990) Injury induced vesiculation and membrane redistribution in squid giant axon. Biochim Biophys Acta 1023:421–435
Forscher P, Smith SJ (1988) Actions of cytochalasins on the organization of actin filaments and microtubules in a neuronal growth cone. J Cell Biol 107:1505–1516
Fried K, Govrin-Lippmann R, Rosenthal F, Ellisman M, Devor M (1991) Ultrastructure of afferent axon endings in a neuroma. J Neurocytol 20:682–701
Friede RL, Bischhausen R (1980) The fine structure of stumps of transected nerve fibers in subserial sections. J Neurol Sci 44:181–203
Friedman B, Scherer SS, Rudge JS, Helgren M, Morrisey D, McClain J, Wang DY, Wiegand SJ, Furth ME, Lindsay RM, Ip NY (1992) Regulation of ciliary neurotrophic factor expression in myelin-related Schwann cells in vivo. Neuron 9:295–305
Friedman B, Kleinfeld D, Ip NY, Verge VMK, Moulton R, Boland P, Zlotchenko E, Lindsay RM, Liu L (1995) BDNF and NT-4/5 exert neurotrophic influences on injured adult spinal motor neurons. J Neurosci 15:1044–1056
Fu SY, Gordon T (1995a) Contributing factors to poor functional recovery after delayed nerve repair: prolonged denervation. J Neurosci 15:3886–3895
Fu SY, Gordon T (1995b) Contributing factors to poor functional recovery after delayed nerve repair: prolonged axotomy. J Neurosci 15:3876–3885
Fu SY, Gordon T (1997) The cellular and molecular basis of peripheral nerve regeneration. Mol Neurobiol 14:67–116
Fujumoto E, Mizoguchi A, Hanada K, Yajima M, Ide C (1997) Basic fibroblast growth factor promotes extension of regenerating axons of peripheral nerve. In vivo experiments using a Schwann cell basal lamina tube model. J Neurocytol 26:511–528
Fukata Y, Itoh TJ, Kimura T, Menager C, Nishimura T, Shiromizu T, Watanabe H, Inagaki N, Iwamatsu A, Hotani H, Kaibuchi K (2002) CRMP-2 binds to tubulin heterodimers to promote microtubule assembly. Nature Cell Biol 4:583–591
Funakoshi T, Takeda S, Hirokawa N (1996) Active transport of photoactivated tubulin molecules in growing axons revealed by new electron microscopic analysis. J Cell Biol 133:1347–1354
Gallo G (1998) Involvement of microtubules in the regulation of neuronal growth cone morphologic remodeling. J Neurobiol 35:121–140
Gallo G, Letourneau PC (1998) GTPases help axons reach their targets. Curr Biol 8:R80-R82
Gallo G, Letourneau PC (1999) Different contributions of microtubule dynamics and transport to the growth of axons and collateral sprouts. J Neurosci 19:3860–3873
Gallo G, Letourneau PC (2004) Regulation of growth cone actin filaments by guidance cues. J Neurobiol. 2004 Jan;58:92–102
Ghosh A, Carnahan J, Greenberg ME (1994) Requirement for BDNF in activity dependent survival of cortical neurons. Science 263:1618–1623
Gimenez y Robota M, Revah F, Pradier L, Loquet I, Mallet J, Privat A (1997) Prevention of motoneuron death by adenovirus mediated neurotrophic factors. J Neurosci Res 48:281–285
Glazner GW, Lupien S, Miller JA, Ishii DN (1993) Insulin-like growth factor II increases the rate of sciatic nerve regeneration in rats. Neuroscience 54:791–797

Glazner GW, Morrison AE, Ishii DN (1994) Elevated insulin-like growth factor (IGF) gene expression in sciatic nerves during IGF-supported nerve regeneration. Mol Brain Res 25:265–272

Glazner GW, Mu X, Springer JE (1998) Localization of glial cell line-derived neurotrophic factor receptor alpha and c-ret mRNA in rat central nervous system. J Comp Neurol 391:42–49

Gloster A, Diamond J (1992) Sympathetic nerves in adult rats regenerate normally and restore function during an anti-NGF treatment that prevents their collateral sprouting. J Comp Neurol 326:363–374

Goldberg DJ, Burmeister DW (1986) Stages in axon formation: observation of growth cones of Aplysia axons in culture using video-enhanced contrast-differential interference contrast microscopy. J Cell Biol 104:1921–1931

Gomez N, Cuadras J, Buti M, Navarro X (1996) Histologic assessment of sciatic nerve regeneration following resection and graft or tube repair in the mouse. Restor Neurol Neurosci 10:187–196

Goodmurphy GW, Ovalle WK (1999) Morphological study of two human facial muscles: orbicularis oculi and corrugator supercilii. Clin Anat 12:1–11

Gorio A, Carmignoto G, Finesso M, Polato P Nunzi MG (1983) Muscle reinnervation—II. Sprouting, synapse formation and repression. Neuroscience 8:403–416

Gordon-Weeks PR (1991) Evidence for microtubule capture by filopodial actin filaments in growth cones. NeuroReport 2:573–576

Gordon-Weeks PR (1997) Growth cones—the mechanism of neurite advance. Bioessays 13:235–239

Graeber MB, Bise K, Mehraein P (1993) Synaptic stripping in the human facial nucleus. Acta Neuropathol (Berl) 86:179–181

Gravel C, Gotz R, Lorrain A, Sendtner M (1997) Adenoviral gene transfer of CNTF and BDNF leads to long-term survival of axotomized motor neurons. Nat Med 3:765–770

Grimby G, Einarsson G, Hedberg M, Aniansson A (1989) Muscle adaptive changes in post-polio subjects. Scand J Rehabil Med 21:19–26

Grothe C, Wewetzer K (1996) Fibroblast growth factor and its implications for developing and regenerating neurons. Int J Dev Neurosci 40:403–410

Guan KL, Rao Yi (2003) Signalling mechanisms mediating neuronal responses to guidance cues. Nat Rev Neurosci 4:941–956

Guidry C, Grinnell F (1987) Heparin modulates the organization of hydrated collagen gels and inhibits gel contraction by fibroblasts. J Cell Biol 104:1097–1103

Gundersen HJ (1986) Stereology of arbitrary particles. A review of unbiased number and size estimators and the presentation of some new ones, in memory of William R. Thompson. J Microsc 143:3–45

Guntinas-Lichius O, Neiss WF (1996) Comparison of empirical and estimated efficiency in neuron counting by the physical dissector and in volume measurement by Cavalieri's method. Acta Stereol 15:131–139

Guntinas-Lichius O, Mockenhaupt J, Stennert E, Neiss WF (1993) Simplified nerve cell counting in the rat brainstem with the physical dissector using a drawing-microscope. J Microsc 172:177–180

Guntinas-Lichius O, Effenberger K, Angelov DN, Klein J, Streppel M, Stennert E, Neiss WF (2000) Contributing factors to better functional recovery after inevitable delayed nerve repair: enhanced regeneration through the predegenerated distal nerve stump. Exp Neurol 162:98–111

Guntinas-Lichius O, Angelov DN, Tomov TL, Dramiga J, Neiss WF, Wewetzer K (2001) Transplantation of olfactory ensheathing cells stimulates the collateral sprouting from axotomized adult rat facial motoneurons. Exp Neurol 172:70–80

Guntinas-Lichius O, Wewetzer K, Tomov TL, Azzolin A, Kazemi S, Streppel M, Neiss WF, Angelov DN (2002) Transplantation of olfactory mucosa minimizes axonal branching and promotes the recovery of vibrissae motor performance after facial nerve repair in rats. J Neurosci 22:7121–7131

Gurney ME, Yamamoto H, Kwon Y (1992) Induction of motor neuron sprouting in vivo by ciliary neurotrophic factor and basic fibroblast growth factor. J Neurosci 12:3241–3247

Härkönen MHA, Kauffman FC (1974) Metabolic alterations in the axotomized superior cervical ganglion of the rat. II. The pentose phosphate pathway. Brain Res 65:141–157

Hall SM (1989) Regeneration in the peripheral nervous system. Neuropathol Appl Neurobiol 15:513–529

Halloran MC, Kalil K (1994) Dynamic behaviors of growth cones extending in the corpus callosum of living cortical brain slices observed with video microscopy. J Neurosci 14:2161–2177

Harsh C, Archibald SJ, Madison RD (1991) Double labeling of saphenous nerve neurone pools: a model for determining the accuracy of axon regeneration at the single neuron level. J Neurosci Methods 39:123–129

Harvey AR, Plant GW, Tan MML (1995) Schwann cells and the regrowth of axons in the mammalian CNS: a review of transplantation studies in the rat visual system. Clin Exp Pharmacol Physiol 22:569–579

Heidemann SR, Landers JM, Hamborg MA (1981) Polarity orientation of axonal microtubules. J Cell Biol 91:661–665

Henderson JT, Seniuk NA, Roder JC (1994) Localization of CNTF immunoreactivity to neurons and astroglia in the CNS. Brain Res Mol Brain Res 22:151–165

Hennig R, Dietrichs E (1994) Transient reinnervation of antagonistic muscles by the same motoneuron. Exp Neurol 130, 331–336

Heumann R, Linholm D, Bandtlow C, Meyer M, Radeke MJ, Misko TP, Shooter EM, Thoenen H (1987) Differential regulation of mRNA encoding nerve growth factor and its receptor in rat sciatic nerve during development, degeneration and regeneration: Role of macrophages. Proc Natl Acad Sci USA 84;8735–8739

Hinrichsen CF, Watson D (1983). Brain stem projections to the facial nucleus of the rat. Brain Behav Evol 22:153–163

Hinrichsen CF, Watson CD (1984). The facial nucleus of the rat: representation of facial muscles revealed by retrograde transport of horseradish peroxidase. Anat Rec 209:407–415

Hirata K, Kawabuchi M (2002) Myelin phagocytosis by macrophages and non-macrophages during Wallerian degeneration. Microsc Res Tech 57:541–547

Hoffman PN, Cleveland DW (1988) Neurofilament and tubulin gene expression recapitulates the developmental program during axonal regeneration. Induction of a specific β-tubulin isotype. Proc Natl Acad Sci USA 85:4530–4533

Hoffman PN, Lasek RJ (1980) Axonal transport of the cytoskeleton in regenerating motor neurons. Constancy and change. Brain Res 202:317–333

Hoffman PN, Cleveland DW, Griffin JW, Landes PW, Cowan NJ, Price DL (1987) Neurofilament gene expression: a major determinant of axonal caliber. Proc Natl Acad Sci U S A 85:4530–4533

Hoffman PN, Lopata MA, Watson DE, Luduena RF (1992) Axonal transport of Class II and III β-tubulin: evidence that the slow component wave represents the movement of only a small fraction of the tubulin in mature motor axons. J Cell Biol 119:595–604

Holm S (1979). A simple sequentially rejective multiple test procedure. Scand. J. Statist., 6, 65–70

Horch KWL, Lisney SJW (1981) On the number and nature of regenerating unmyelinated axons after lesions of the cutaneous nerves in the cat. J Physiol 313:275–286

Houle JD, Ye JH, Kane CJM (1996) Axonal regeneration by chronically injured supraspinal neurons can be enhanced by exposure to insulin-like growth factor, basic fibroblast growth factor or transforming growth factor beta. Restor Neurol Neurosci 10:205–215

Hughes RA, Sendtner M, Thoenen H (1993) Members of several gene families influence survival of rat motoneurons in vitro and in vivo. J Neurosci Res 36:663–671

Hughes RA, Sendtner M, Goldfarb M, Lindholm D, Thoenen H (1993a) Evidence that FGF-5 is a major muscle-survival factor for spinal motoneurons. Neuron 10:369–377

Huston JP, Steiner H, Weiler HT, Morgan S, Schwarting RKW (1990) The basal ganglia-orofacial system: studies on neurobehavioral plasticity and sensory-motor tuning. Neurosci Biobehav Rev 14:433–446

Inoue A, Sanes, JR (1997) Lamina specific connectivity in the brain: regulation by N-cadherin, neurotrophins, and glycoconjugates. Science 276:1428–1431

Ishii DN, Glazner GW, Pu S-F (1994) Role of insulin-like growth factors in peripheral nerve regeneration. Pharmac Ther 62:125–144

Isokawa-Akesson M, Komisaruk BR (1987). Difference in projections to the lateral and medial facial nucleus: anatomically separate pathways for rhythmical vibrissa movement in rats. Exp Brain Res 65:385–398

Ito M, Kudo M (1994) Reinnervation by axon collaterals from single facial motoneurons to multiple muscle targets following axotomy in the adult guinea pig. Acta Anat (Basel) 151:124–130

Jacquin MF, Zahm DS, Henderson TA, Golden JP, Johnson EM, Renehan WE, Klein BG (1993) Structure-function relationships in rat brainstem subnucleus interpolaris. X. Mechanisms underlying enlarged spared whisker projections after infraorbital nerve injury at birth. J Neurosci 13:2946–2964

Jeng C-B, Cogeshall RE (1984) Regeneration of axons in tributary nerves. Brain Res 310:107–121

Jenq C-B, Jenq LL, Bear HM, Coggeshall RE (1988) Conditioning lesions of peripheral nerves change regenerated axon numbers. Brain Res 457:63–69

Jin Z, Strittmatter SM (1997) Rac 1 mediates collapsin-1 induced growth cones collapse. J Neurosci 17:6256–6263

Joshi HC, Baas PW (1993) A new perspective of microtubules and axon growth. J Cell Biol 121:1191–1196

Kanje M, Skottner A, Sjoberg J, Lundborg G (1989) Insulin-like growth factor (IGF-I) stimulates regeneration of the rat sciatic nerve. Brain Res 486:396–398

Kimpinski K, Campenot RB, Mearow KM (1997) Effects of the neurotrophins NGF, NT-3 and BDNF on neurite growth from adult sensory neurons in compartmented cultures. J Neurobiol 33:395–410

Kimura J, Lyon LW (1972). Orbicularis oculi reflex in the Wallenberg syndrome: alteration of the late reflex by lesions of the spinal tract and nucleus of the trigeminal nerve. J Neurol Neurosurg Psychiatry 35:228–233

Kimura J, Rodnitzky RL, Okawara SH (1975) Electrophysiologic analysis of aberrant regeneration after facial nerve paralysis. Neurology 25:989–993

King CE, Canty AJ, Vickers JC (2001) Alterations in neurofilament associated with reactive brain changes and axonal sprouting following acute physical injury to the rat neocortex. Neuropathol Appl Neurobiol 27:115–126

Klein BG, Rhoades RW (1985). Representation of whisker follicle intrinsic musculature in the facial motor nucleus of the rat. J Comp Neurol 232:55–69

Kobayashi NR, Bedard AM, Hincke MT, Tetzlaff W (1996) Increased expression of BDNF and trkB mRNA in rat facial motoneurons after axotomy. Eur J Neurosci 8:1018–1029

Koliatsos VE, Clatterbuck RE, Winslow JW, Cayouette MH, Price DL (1993) Evidence that BDNF is a trophic factor for motor neurons in vivo. Neuron 10:359–367

Koliatsos VE, Cayouette MH, Berkemeier LR, Clatterbuck RE, Price DL, Rosenthal A (1994) Neurotrophin 4/5 is a trophic factor for mammalian facial motor neurons. Proc Natl Acad Sci USA 91:3304–3308

Komisaruk BR (1970) Synchrony between limbic system theta activity and rhythmical behaviour in rats. J Comp Physiol Psychol 70:482–492

Kopen GC, Prockop DJ, Phinney DG (1999) Marrow stromal cells migrate throughout forebrain and cerebellum, and they differentiate into astrocytes after injection into the neonatal mouse brains. Proc Natl Acad Sci USA 96:10711–10716

Krenz NR, Meakin SO, Krassioukov AV, Weaver LC (1999) Neutralizing intraspinal nerve growth factor blocks autonomic dysreflexia caused by spinal cord injury. J Neurosci 19:7405–7414

Kreutzberg GW (1963) Changes of coenzyme (TPN) diaphorase and TPN-linked dehydrogenase during axonal reaction of the nerve cell. Nature 199:393–394

Kreutzberg GW, Emmert H (1980) Glucose utilization of motor nuclei during regeneration: A ^{14}C-2-deoxyglucose study. Acta Neuropathol (Berl) 70:712–716

Kreutzberg GW, Toth L, Kaiya H (1975) Acetylcholinesterase as a marker for dendritic transport and dendritic secretion. Adv Neurol 12:269–281

Kromer LF, Cornbrooks CJ (1985) Transplants of Schwann cell cultures promote axonal regeneration in the adult mammalian brain. Proc Natl Acad Sci USA 82:6330–6334

Kujawa KA, Jones KJ (1990) Testosterone-induced acceleration of recovery from facial paralysis in male hamsters: temporal requirements of hormone exposure. Physiol Behav 48:765–768

Kuno M, Llinas R (1970) Enhancement of synaptic transmission by dendritic potentials in chromatolysed motoneurones of the cat. J Physiol (Lond) 210:807–821

Kwon YW, Gurney ME (1994) Systemic injections of ciliary neurotrophic factor induce sprouting by adult motor neurons. Neuroreport 5:789–792

Labrador RO, Buti M, Navarro X (1995) Peripheral nerve repair: role of agarose matrix density on functional recovery. Neuroreport 6:2022–2026

Labrador RO, Buti M, Navarro X (1998) Influence of collagen and laminin gels concentration on nerve regeneration after resection and tube repair. Exp Neurol 149:243–252.

Langley JN (1895) Note on regeneration of preganglionic fibres of the sympathetic. J Physiol 18:280–284

Laquerriere A, Peulve P, Jin O, Tiollier J, Tardy M, Vaudry H, Hemet J, Tadie M (1994) Effects of basic fibroblast factor and alpha melanocytic stimulating hormone on nerve regeneration through a collagen channel. Microsurgery 15:203–210

Laskowski MB, Sanes JR (1988) Topographically selective reinnervation of mammalian skeletal muscles. J Neurosci 8:3094–3099

Lee MY, Hofmann HD, Kirsch M (1997) Expression of ciliary neurotrophic factor receptor-a messenger RNA in neonatal and adult rat brain: An in situ hybridization study. Neuroscience 77:233–246

Lefcort F, Venstrom K, McDonald JA, Reichardt LF (1992) Regulation of expression of fibronectin and its receptor, alpha5beta1, during development and regeneration of peripheral nerve. Development 116:767–782

Letourneau PC (1979) Cell-substratum adhesion of neurite growth cones and its role in neurite elongation. Exp Cell Res 124:127–138
Letourneau PC (1983) Differences in the organization of actin in the growth cones compared with the neurites of cultured neurons from chick embryos. J Cell Biol 97:963–973
Letourneau PC, Ressler AH (1984) Inhibition of neurite initiation and growth by taxol. J Cell Biol 98:1355–1362
Letourneau PC, Cypher C (1991) Regulation of growth cone motility. Cell Motil Cytoskeleton 20:267–271
Letournaeu PC, Shattuck TA, Ressler AH (1987) "Pull" and "Push" in neurite elongation: observations on the effects of different concentrations of cytochalasin B and taxol. Cell Motil Cytoskel 8:193–209
Lewis ME, Neff NT, Contreras PC, Stong DB, Oppenheim RW, Grebow PE, Vaught JL (1993) Insulin-like growth factor-I: potential for treatment of motor neuronal disorders. Exp Neurol 124:73–88
Li YQ, Takada M, Kaneko T, Mizuno N (1997). Distribution of GABAergic and glycinergic premotor neurons projecting to the facial and hypoglossal nuclei in the rat. J Comp Neurol 378:283–294
Li Y, Raisman G (1994) Schwann cells induce sprouting in motor and sensory axons in the adult rat spinal cord. J Neurosci 14:4050–4063
Li Y, Field PM, Raisman G (1997) Repair of adult rat corticospinal tract by transplants of olfactory ensheathing cells. Science 277:2000–2002
Li Y, Field PM, Raisman G (1998) Regeneration of adult corticospinal axons induced by transplanted olfactory ensheathing cells. J Neurosci 18:10514–10524
Lieberman AR (1971) The axon reaction: a review of the principal features of the perikaryal response to axon injury. Int Rev Neurobiol 14:49–125
Lin CH, Forscher P (1993) Cytoskeletal remodeling during growth cone-target interactions. J Cell Biol 121:1369–1383
Lin CH, Thompson CA, Forscher P (1994) Cytoskeletal reorganization underlying growth cone motility. Curr Opin Neurobiol 4:640–647
Lindsay RM (1988) Nerve growth factors (NGF, BDNF) enhance axonal regeneration but are not required for survival of adult sensory neurons. J Neurosci 8:3337:3342
Lisney SJW (1989) Regeneration of unmyelinated axons after injury of mammalian peripheral nerve. Q J Exp Physiol 74:757–784
Liu DW, Westerfield M (1990) The formation of terminal fields in the absence of competitive interactions among primary motoneurons in the zebrafish. J Neurosci 10:3947–3959
Liuzzi FJ, Tedeschi B (1991) Peripheral nerve regeneration. Neurosurg Clin N Am 2:31–42
Lom B, Cohen-Cory S (1999) Brain-derived neurotrophic factor differentially regulates retinal ganglion cell dendritic and axonal arborization in vivo. J Neurosci 19:9928–9938
Longo FM, Skaper SD, Manthorpe M, Williams LR, Lundborg G, Varons S (1983)Temporal changes of neurotrophic activities accumulating in vivo within nerve regeneration chambers. Exp Neurol 81:756–769
Longo FM, Hayman EG, Davis GE, Ruoslahti E, Engvall E, Manthorpe M, Varon S (1984) Neurite-promoting factors and extracellular matrix components accumulating in vivo within nerve regeneration chambers. Brain Res 309:105–117
Love FM, Thompson WJ (1999) Glial cells promote muscle reinnervation by responding to activity-dependent postsynaptic signals. J Neurosci 19:10390–10396
Love FM, Son YJ, Thompson WJ (2003) Activity alters muscle reinnervation and terminal sprouting by reducing the number of Schwann cell pathways that grow to link synaptic sites. J Neurobiol 54:566–576

Lundborg G, Dahlin LB, Danielsen N, Gelberman RH, Longo FM, Powell HC, Varon S (1982) Nerve regeneration in silicone chambers: influence of gap length and of distal stump components. Exp Neurol 76:361–375

Lux HD, Schubert P (1975) Some aspects of the electroanatomy of dendrites. Adv Neurol 12:29–44

Mackinnon SE, Dellon A L, Lundborg G, Hudson AR, Hunter DA (1986) A study of neurotrophism in a primate model. J Hand Surg 11-A:888–894

Mackinnon SE, Dellon AL, Obrien JP (1991) Changes in nerve fiber diameters distal to a nerve repair in the rat sciatic nerve model. Muscle Nerve 14:1116–1122

MacLennan AJ, Devlin BK, Neitzel KL, McLaurin DL, Anderson KJ, Lee N (1999) Regulation of ciliary neurotrophic factor receptor α in sciatic motor neurons following axotomy. Neuroscience 91:1401–1413

Madison RD, Archibald SJ (1994) Point sources of Schwann cells result in growth into a nerve entubulation repair site in the absence of axons: effects of freeze-thawing. Exp Neurol 128:266–275

Madison RD, da Silva CF, Dikkes P, Chiu TH, Sidman RL (1985) Increased rate of peripheral nerve regeneration using bioresorbable nerve guides and a laminin-containing gel. Exp Neurol 88:767–772

Madison RD, da Silva CF, Dikkes P, Sidman RL, Chiu TH (1987) Peripheral nerve regeneration with entubulation repair: comparison of biodegradeable nerve guides versus polyethylene tubes and the effects of a laminin-containing gel. Exp Neurol 95:378–390

Madison RD, Da Silva CF, Dikkes P. (1988) Entubulation repair with protein additives increases the maximum nerve gap distance successfully bridged with tubular prostheses. Brain Res 447:325–334

Madison RD, Archibald SJ, Brushart TM (1996) Reinnervation accuracy of the rat femoral nerve by motor and sensory neurons. J Neurosci 16:5698–5703

Madison RD, Archibald SJ, Lacin R, Krarup C (1999) Factors contributing to preferential motor reinnervation in the primate peripheral nervous system. J Neurosci 19:11007–11016

Mamounas LA, Altar CA, Blue ME, Kaplan DR, Tessarollo L, Lyons WE (2000) BDNF promotes the regenerative sprouting, but not survival, of injured serotonergic axons in the adult brain. J Neurosci 15:771–782

Marsh L, Letourneau PC (1984) Growth of neurites without filopodial or lamellipodial activity in the presence of cytochalasin B. J Cell Biol 99:2041:2047

Martini R (1994) Expression and functional roles of neural cell surface molecules and extracellular matrix components during development and regeneration of peripheral nerves. J Neurocytol 23:1–28

Martini R, Schachner M (1988) Immunoelectron microscopic localization of neural cell adhesion molecules (L1, N-CAM, and myelin-associated glycoprotein) in regenerating adult mouse sciatic nerve. J Cell Biol 106:1735–1746

Martini R, Schachner M, Faissner A (1990) Enhanced expression of the extracellular matrix molecule J1/tenascin in the regenerating adult mouse sciatic nerve. J Neurocytol 19:601–616

Masliah E, Mallory M, Hansen L, Alford M, Albright T, DeTeresa R, Terry R, Baudier J, Saitióh T (1991) Pattern of aberrant sprouting in Alzheimer's disease. Neuron 6:729–739

Matheson CR, Wang J, Collins FD, Yan Q (1997) Long-term survival effects of GDNF on neonatal rat facial motoneurons after axotomy. Neuroreport 8:1739–1742

Mauch C, Hatamoch A, Scharffetter K, Krieg T (1988) Regulation of collagen synthesis in fibroblasts within a three-dimensional collagen gel. Exp Cell Res 178:493–503

McAllister AK, Katz LC, Lo DC (1999) Neurotrophins and synaptic plasticity. Ann Rev Neurosci 22:295–318

McHale MK, Hall GF, Cohen MJ (1995) Early cytoskeletal changes following injury of giant spinal axons in the lamprey. J Comp Neurol 353:25–37

McKinney RA, Debanne D, Gahwiler BH, Thompson SM (1997) Lesion induced axonal sprouting and hyperexcitability in the hippocampus in vitro: implications for the genesis of posttraumatic epilepsy. Nature Med 3:990–996

McMahon SB, Priestley JV (1995) Peripheral neuropathies and neurotrophic factors: animal models and clinical perspectives. Curr Opinion Neurobiol 5:616–624

McPhail LT, Stirling DP, Tetzlaff W, Kwiecien JM, Ramer MS (2004) The contribution of activated phagocytes and myelin degeneration to axonal retraction/dieback following spinal cord injury. Eur J Neurosci 20:1984–1994

Mearow KM, Kril Y (1995) Anti-NGF treatment blocks the upregulation of NGF receptor mRNA expression associated with collateral sprouting of rat dorsal root ganglion neurons. Neurosci Lett 184:55–58

Meier C, Parmantier E, Brennan A, Mirsky R, Jessen KR (1999) Developing Schwann cells acquire the ability to survive without axons by establishing an autocrine circuit involving insulin-like growth factor, neurotrophin-3, and platelet-derived growth factor-BB. J Neurosci 19:3847–3859

Meyer M, Matsuoka I, Wetmore C, Olson L, Thoenen H (1992) Enhanced synthesis of brain-derived neurotrophic factor in the lesioned peripheral nerve—different mechanisms are responsible for the regulation of BDNF and NGF messenger RNA. J Cell Biol 119:45–54

Mohiuddin L, Delcroix JD, Fernyhough P, Tomlinson DR (1999) Focally administered nerve growth factor suppresses molecular regenerative responses of axotomized peripheral afferents in rats. Neuroscience 91:265–271

Molander C, Aldskogius H (1992) Directional specificity of regenerating neurons after peripheral nerve crush or transection and epineurial suture: A sequential double-labeling study in the rat. Restor Neurol Neurosci 4:339–344

Moller AR, Jannetta PJ (1986) Blink reflex in patients with hemifacial spasm. Observations during microvascular decompression operations. J Neurol Sci 72:171–182

Montserrat L, Benito M (1988). Facial synkinesis and aberrant regeneration of facial nerve. Adv Neurol 49:211–224

Moran LB, Graeber MB (2004) The facial nerve axotomy model. Brain Res Brain Rex Rev 44:154.178

Moran CJ, Neely JG (1996). Patterns of facial nerve synkinesis. Laryngoscope 106:1491–1496

Morris J, Hudson AR, Weddell G (1972) Study of degeneration and regeneration in the divided rat sciatic nerve based on electron microscopy. II. The development of the "regenerating unit". Z Zellforsch Mikrosk Anat 124:103–130

Moskowitz PF, Smith R, Pickett J, Frankfurter A, Oblinger MM (1993) Expression of the class III β-tubulin gene during axonal regeneration of rat dorsal root ganglion neurons. J Neurosci Res 34:129–134

Munger BL, Renehan WE (1989). Degeneration and regeneration of peripheral nerve in the rat trigeminal system: III. Abnormal sensory reinnervation of rat guard hairs following nerve transection and crush. J Comp Neurol 283:169–176

Murai N, Ueba T, Takahashi JA, Yang H-Q, Kikuchi H, Hiai H, Hatanaka M, Fukumoto M (1996) Apoptosis of human glioma cells in vitro and in vivo induced by neutralizing antibody against human basic fibroblast growth factor. J Neurosurg 85:1072–1077

Murphy EH, Brown J, Iannuzzelli P, Baker R (1990) Regeneration and soma size changes following axotomy of the trochlear nerve. J Comp Neurol 292:524–536

Nacimiento W, Podoll K, Graeber MB, Topper R, Mobius E, Ostermann H, Noth J, Kreutzberg GW (1992) Contralateral early blink reflex in patients with facial nerve palsy: indication for synaptic reorganization in the facial nucleus during regeneration. J Neurol Sci 109:148–155

Naumann T, Härtig W, Frotscher M (2000) Retrograde tracing with Fluoro-Gold: different methods of tracer detection at the ultrastructural level and neurodegenerative changes of back-filled neurons in ling-term studies. J Neurosci Meths 103:11–21

Navarro X, Kennedy WR (1989) Sweat gland reinnervation by sudomotor regeneration after different types of lesions and graft repairs. Exp Neurol 104:229–234

Nawa H, Pelleymounter MA, Carnahan J (1994) Intraventricular administration of BDNF increases neuropeptide expression in newborn rat brain. J Neurosci 14:3751–3765

Near SL, Whalen LR, Miller JA, Ishii DN (1992) Insulin-like growth factor II stimulates motor nerve regeneration. Proc Natl Acad Sci USA 89:11716–11720

Neiss WF, Guntinas-Lichius O, Angelov DN, Gunkel A, Stennert E(1992) The hypoglossal-facial anastomosis as model of neuronal plasticity in the rat. Ann Anat.174:419–433

Nieto-Sampedro M, Manthorpe M, Barbin G, Varon S, Cotman CW (1983) Injury-induced neurotrophic activity in adult rat brain: correlation with survival of delayed implants in the wound cavity. J Neurosci 3:2219–2229

Newman JP, Verity AN, Hawatmeh S, Fee WE Jr., Terris DJ (1996) Ciliary neurotrophic factors enhance peripheral nerve regeneration. Arch Otolaryngol 122:399–403

Novikov L, Novikova L, Kellerth JO (1997) Brain-derived neurotrophic factor promotes axonal regeneration and long-term survival of adult rat spinal motoneurons in vivo. Neuroscience 79:765–774

Novikova L, Novikov L, Kellerth J-O (1997) Effects of neurotransplants and BDNF on the survival and regeneration of injured adult spinal motoneurons. Eur J Neurosci 9:2774–2777

Oblinger MM, Lasek RJ (1988) Axotomy-induced alterations in the synthesis and transport of neurofilaments and microtubules in the dorsal root ganglion cells. J Neurosci 8:1746–1758

Ochi M, Wakasa M, Ikuta Y, Kwong WH (1994) Nerve regeneration in predegenerated basal lamina graft: the effect of duration of predegeneration on axonal extension. Exp Neurol 128:216–225

Okabe S, Hirokawa N (1990) Turnover of fluorescently labeled tubulin and actin in the axon. Nature 343:479–482

Okabe S, Hirokawa N (1992) Differential behaviour of photoactivated microtubules in growing axons of mouse and frog neurons. J Cell Biol 117:105–120

Okabe S, Hirokawa N (1993) Do photobleached fluorescent microtubules move? Re-evaluation of fluorescence laser photobleaching both in vitro and in growing Xenopus axon. J Cell Biol 120:1177–1186

O'Leary DDM, Terashima T (1988) Cortical axons branch to multiple subcortical targets by interstitial axon budding: implications for target recognition and "waiting periods". Neuron 1:901–910

Olsson T (1980) Somatopetal transport of horseradish peroxidase following incorporation into axonal sprouts and axons in neuromas after nerve transection. Acta Path Microbiol Scand Sect A 88:195–199

Oppenheim RW, Prevette D, Qin-Wei Y, Collins F, McDonald J (1991) Control of embryonic motoneuron survival in vivo by ciliary neurotrophic factor. Science 251:1616

Owen AD, Bird MM (1997) Role of glutamate in the regulation of the outgrowth and motility of neurites from mouse spinal cord neurons in culture. J Anat 191:301–307

Oyesiku NM, Wigston DJ (1996) Ciliary neurotrophic factor stimulates neurite outgrowth from spinal cord neurons. J Comp Neurol 364:68–77

Pan YA, Misgeld T, Lichtman JW, Sanes JR (Effects of neurotoxic and neuroprotective agents on peripheral nerve regeneration assayed by time-lapse imaging in vivo. J Neurosci 23:11479–11488

Paschen W (1992) Polyamine metabolism in different pathological states of the brain. Mol Chem Neuropathol 16:241–271

Perez-Polo JR, Foreman PJ, Jackson GR, Shan DE, Tagliatela G, Thorpe LW, Werrbach-Perez K (1990) Nerve growth factor and neuronal cell death. Mol Neurobiol 4:57–91

Perry VH, Brown MC (1992) Role of macrophages in peripheral nerve degeneration and repair. Bioessays 14:401–406

Pesheva P, Spiess E, Schachner M (1989) J1–160 and J1–180 are oligodendrocyte-secreted nonpermissive substrates for cell adhesion. J Cell Biol 10:1765–1778

Pesheva P, Gennarini G, Goridis C, Schachner M (1993) The F3/11 cell adhesion molecule mediates the repulsion of neurons by the extracellular matrix glycoprotein J1–160/180. Neuron 10:69–82

Pesheva P, Probstmeier R, Skubitz APN, McCarthy JB, Furcht LT, Schachner M (1994) Tenascin-R (J1 160/180) inhibits fibronectin-mediated adhesion—functional relatedness to tenascin-C. J Cell Sci 107:2323–2333

Popratiloff AS, Neiss WF, Skouras E, Streppel M, Guntinas-Lichius O, Angelov DN (2001) Evaluation of muscle re-innervation employing pre- and post-axotomy injections of fluorescent retrograde tracers. Brain Res Bull 54:115–123

Popratiloff AS, Streppel M, Gruart A, Guntinas-Lichius O, Angelov DN, Stennert E, Delgado-Garcia JM, Neiss WF (2001 b) Hypoglossal and reticular interneurons involved in oro-facial coordination in the rat. J Comp Neurol 433:364–379

Pu S-F, Zhuang H-X, Marsh DJ, Ishii DN (1999) Time-dependent alteration of insulin-like growth factor gene expression during nerve regeneration in regions of muscle enriched with neuromuscular junctions. Mol Brain Res 63:207–216

Purves D, Thompson W, Yip JW (1981) Reinnervation of ganglia transplanted to the neck from different levels of the guinea pig sympathetic chain. J Physiol 313:49–63

Raivich G, Kreutzberg GW (1993) Peripheral nerve regeneration: Role of growth factors and their receptors. Int J Dev Neurosci 11:311–324

Ramon-Cuéto A, Plant GW, Avila J, Bunge MB (1998) Long-distance axonal regeneration in the transected adult rat spinal cord is promoted by olfactory ensheathing glia transplants. J Neurosci 18:3803–3815

Rice FL, Gomez C, Barstow C, Burnet A, Sands P (1985) A comparative analysis of the development of the primary somatosensory cortex: interspecies similarities during barrel and laminar development. J Comp Neurol 236:477–495

Rice FL, Kinnman E, Aldskogius H, Johansson O, Arvidsson J (1993). The innervation of the mystacial pad of the rat as revealed by PGP 9.5 immunofluorescence. J Comp Neurol 337:366–385

Rich MM, Lichtman JW (1989) In vivo visualization of pre- and postsynaptic change during synapse elimination in reinnervated mouse muscle. J Neurosci 9:1781–1805

Ro L-S, Chen S-T, Tang L-M, Chang H-S (1996) Local application of anti-NGF blocks the collateral sprouting in rats following chronic construction injury of the sciatic nerve. Neurosci Lett 218:87–90

Rochlin MW, Wickline KM, Bridgman PC (1996) Microtubule stability decreases axon elongation but not axoplasm production. J Neurosci 16:3236–3246

Rochlin MW, Dailey ME, Bridgman PC (1999) Polymerizing microtubules activate site-directed F-actin assembly in nerve growth cones. Mol Biol Cell 10:2309–2327

Rosenblad C, Martinez-Serrano A, Bjorklund A (1996) Glial cell line-derived neurotrophic factor increases survival growth and function of intrastriatal fetal nigral dopaminergic grafts. Neuroscience 75:979–985

Rotter A, Birdsall NJM, Burgen ASV, Field PM, Smolen A, Raisman G (1979) Muscarinic receptors in the central nervous system of the rat. IV. A comparison of the effects of axotomy and deafferentation on the binding of [^{3}H]propylbenzylcholine mustard and associated synaptic changes in the hypoglossal and pontine nuclei. Brain Res Brain Res Rev 1:207–224

Sabry JH, O'Connor TP, Kirschner MW (1995) Axonal transport of tubulin in Ti1 pioneer neurons in situ. Neuron 14:1247–1256

Sadjadpour K (1975) Postfacial palsy phenomena: faulty nerve regeneration or ephaptic transmission? Brain Res 95:403–406

Sagot Y, Tan SA, Baetge E, Schmalbruch H, Kato AC, Aebischer P (1995) Polymer encapsulated cell lines genetically engineered to release ciliary neurotrophic factor can slow down progressive motor neuropathy in the mouse. Eur J Neurosci 7:1313–1322

Sagot Y, Tan SA, Hammang JP, Aebischer P, Kato AC (1996) GDNF slows loss of motoneurons but not axonal degeneration or premature death of pmn/pmn mice. J Neurosci 16:2335–2341

Sawai H, Clarke DB, Kittlerova P, Bray GM, Aguayo AJ (1996) Brain derived neurotrophic factor and neurotrophin-4/5 stimulate growth of axonal branches from regenerating retinal ganglion cells. J Neurosci 16:3887–3894

Sahenk Z, Seharaseyon J, Mendell JR (1994) CNTF potentiates peripheral nerve regeneration. Brain Res 655:246–250

Santos Da Silva J, Dotti CG (2002) Breaking the neuronal sphere: regulation of the actin cytoskeleton in neuritogenesis. Nature Rev Neurosci 3:694–704

Schaefer AW, Kabir N, Forscher P (2002) Filopodia and actin arcs guide the assembly and transport of two populations of microtubules with unique dynamic parameters in neuronal growth cones. J Cell Biol 158:139–152

Schwarz JR, Bromm B, Spielmann P, Weytjens JL (1983) Development of Na^+ inactivation in motor and sensory myelinated nerve fibres of Rana esculenta. Pflugers Arch 398:126–129

Seckel BR (1990) Enhancement of peripheral nerve regeneration. Muscle Nerve 13:785–800

Semba K, Egger MD (1986). The facial "motor" nerve of the rat: control of vibrissal movement and examination of motor and sensory components. J Comp Neurol 247:144–158

Semba K, Szechtman H, Komisaruk BR (1980). Synchrony among rhythmical facial tremor, neocortical "alpha" waves, and thalamic non-sensory neuronal bursts in intact awake rats. Brain Res 195:281–298

Senba E, Simmons DM, Wada E, Wada K, Swanson LW (1990) RNA levels of neuronal nicotinic acetylcholine receptor subunits are differentially regulated in axotomized facial motoneurons. An in situ hybridization study. Brain Res Mol Brain Res 8:349–353

Sendtner M, Kreutzberg GW, Thoenen H (1990) Ciliary neurotrophic factor prevents the degeneration of motor neurons after axotomy. Nature 345:440–441

Sendtner M, Holtmann B, Kolbeck R, Thoenen H, Barde Y-A (1992a) BDNF prevents the death of motoneurons in newborn rats after nerve section. Nature 360:757–759

Sendtner M, Stockli KA, Thoenen H (1992b) Synthesis and localization of CNTF in the sciatic nerve of the adult rat after lesion and during regeneration. J Cell Biol 118:139–148

Sendtner M, Dittrich F, Huges RA, Thoenen H (1994) Actions of CNTF and neurotrophins on degenerating motoneurons: preclinical studies and clinical implications. J Neurol Sci 124 Suppl:77–83

Sendtner M, Götz R, Holtmann B, Thoenen H (1997) Endogenous ciliary neurotrophic factor is a lesion factor for axotomized motoneurons in adult mice. J Neurosci 17:6999–7006

Shaw G, Bray D (1977) Movement and extension of isolated growth cones. Exp Cell Res 104:55–62

Shawe GD (1954) On the number of branches formed by regenerating nerve fibers. Br J Surg 42:474–488

Sheedlo HJ, Gaur V, Seaton AD, Turner JE (1991) Transplantation to the diseased and damaged retina. Trends Neurosci 14:347–350

Siegel SG, Patton B, English AW (2000) Ciliary neurotrophic factor is required for motoneuron sprouting. Exp Neurol 166:205–212

Siironen J, Sandberg M, Vuorinen V, Roytta M (1992) Laminin-B1 and collagen type-IV gene expression in transected peripheral nerve-reinnervation compared to denervation. J Neurochem 59:2184–2192

Sinclair SR, Svendsen CN, Torres EM, Martin D, Fawcett JW, Dunnet SB (1996) GDNF enhances dopaminergic cell survival and fibre outgrowth in embryonic nigral grafts. NeuroReport 7:2547–2552

Singer P, Mehler S (1986) Glucose, leucine uptake in the hypoglossal nucleus after hypoglossal nerve transection with and without prevented regeneration in the Sprague-Dawley rat. Neurosci Lett 67:73–77

Sjoberg J, Kanje M (1989) Insulin-like growth factor-I as a stimulator of regeneration in freeze-injured rat sciatic nerve. Brain Res 485:102–108

Sjoberg J, Kanje M (1990) The initial period of peripheral nerve regeneration and the importance of the local environment for the conditioning lesion effect. Brain Res 529:79–84

Skouras E, Popratiloff AS, Guntinas-Lichius O, Streppel M, Rehm KE, Neiss WF, Angelov DN (2002) Altered sensory input improves the accuracy of muscle reinnervation. Restor Neurol Neurosci 20:1–14.

Smith DS, Skene JHP (1997) A transcription dependent switch controls competence of adult neurons for distinct modes of axon growth. J Neurosci 17:646–658

Smith GM, Rabinovsky ED, McManaman JL, Shine HD (1993) Temporal and spatial expression of ciliary neurotrophic factor after peripheral nerve injury. Exp Neurol 121:239–247

Snider WD, Johnson Jr EM (1989) Neurotrophic molecules. Ann Neurol 26:489–506

Son YJ, Trachtenberg JT, Thompson WJ (1996). Schwann cells induce and guide sprouting and reinnervation of neuromuscular junctions. Trends Neurosci 19:280–285

Sparrow JR, Kiernan JA (1979). Uptake and retrograde transport of proteins by regenerating axons. Acta Neuropathol 47:39–47

Spector JG, Lee P, Derby A, Friedrich G, Burke JJ, Vogler GP, Roufa DG (1992) Facial nerve regeneration through semipermeable chambers in the rabbit. Laryngoscope 102:784–796

Spector JG, Lee P, Derby A, Friedrich GE, Neises G, Roufa DG (1993) Rabbit facial nerve regeneration in NGF-containing silastic tubes. Laryngoscope 103:548–558

Spielmann RP, Schwarz JR, Bromm B (1983) Oscillating repolarization in action potentials of frog sensory myelinated fibres. Neurosci Lett 36:49–53

Spira ME, Benbassat D, Dormann A (1993) Resealing of the proximal and distal cut ends of transected axons: electrophysiological and ultrastructural analysis. J Neurobiol 24:300–316

Spira ME, Oren R, Dormann A, Gitler D (2003) Critical calpain-dependent ultrastructural alterations underlie the transformation of an axonal segment into a growth cone after axotomy of cultured Aplysia neurons. J Comp Neurol 457:293–312

Stöckli KA, Lillien LE, Näher-Noe M, Breitfeld G, Hughes RA, Raff MC, Thoenen H, Sendtner M (1991) Regional distribution developmental changes, and cellular localization of CNTF-mRNA and protein in the rat brain. J Cell Biol 115:447–459

Streppel M, Angelov DN, Guntinas-Lichius O, Hilgers RD, Rosenblatt JD, Stennert E, Neiss WF (1998) Slow axonal regrowth but extreme hyperinnervation of target muscle after suture of the facial nerve in aged rats. Neurobiol Aging 19:83–88

Streppel M, Azzolin N, Dohm S, Guntinas-Lichius O, Haas C, Grothe C, Neiss WF, Angelov DN (2002) Focal application of neutralizing antibodies to soluble neurotrophic factors reduces collateral axonal branching after peripheral nerve lesion. Eur J Neurosci. 15:1327–1342

Sumner AJ (1990) Aberrant reinnervation. Muscle Nerve 13:801–803

Sumner BE, Watson WE (1971). Retraction and expansion of the dendritic tree of motor neurones of adult rats induced in vivo. Nature 233:273–275

Suter DM, Forscher P (2000) Substrate-cytoskeletal coupling as a mechanism for the regulation of growth cone motility and guidance. J Neurobiol 44:97–113

Syroid DE, Zorick TS, Arbet-Engels C, Kilpatrick TJ, Eckhart E, Lemke G (1999) A role for insulin-like growth factor-I in the regulation of Schwann cell survival. J Neurosci 19:2059–2068

Szebenyi G, Gallaway JL, Dent EW, Kalil K (1998) Interstitial branches develop from active regions of the axon demarcated by the primary growth cone during pausing behaviors. J Neurosci 18:7930–7940

Takei N, Kondo J, Nagaike K, Ohsawa K, Kato K, Kohsaka S (1991) Neuronal survival factor from bovine brain is identical to neuron-specific enolase. J Neurochem 57:1178–1184

Tam SL, Gordon T (2003) Mechanisms controlling axonal sprouting at the neuromuscular junction. J Neurocytol 32:961–974

Tam SL, Archibald V, Tyreman N, Jassar B, Gordon T (2001) Increased neuromuscular activity reduces sprouting in partially denervated muscles. J Neurosci 21:655–663

Tan SA, Deglon N, Zurn AD, Baetge EE, Bamber B, Kato AC, Aebischer P (1996) Rescue of motoneurons from axotomy-induced cell death by polymer encapsulated cells genetically engineered to release CNTF. Cell Transplant 5:577–587

Tanaka E, Kirschner MW (1991) Microtubule behaviour in growth cones of living neurons during axon elongation. J Cell Biol 115:345–363

Tanaka E, Kirschner MW (1995) The role of microtubules in growth cone turning at substrate boundaries. J Cell Biol 128:139–156

Tanaka E, Ho T, Kirschner MW (1995) The role of microtubule dynamics in growth cone motility and axonal growth. J Cell Biol 128:139–155

Tanaka E, Sabry J (1995) Making the connection: cytoskeletal rearrangements during growth cone guidance. Cell 83:171–176

Taniuchi M, Clark HB, Schweitzer JB, Johnson EM (1988) Expression of nerve growth factor by Schwann cells of axotomized peripheral nerves: Ultrastructural location, suppression by axonal contact, and binding properties. J Neurosci 8:664–681

Taub E, Miller NE, Novack TA, Cook EW3rd, Fleming WC, Nepomuceno CS, Connell JS, Crago JE (1993) Technique to improve chronic motor deficit after stroke. Arch Phys Med Rehabil 74:347–354

Taylor J, Pesheva P, Schachner M (1993) Influence of janusin and tenascin on growth cone behaviour in vitro. J Neurosci Res 35:347–362

Tetzlaff W, Bisby MA (1989) Neurofilament elongation into regenerating facial nerve axons. Neuroscience 29:659–666

Tetzlaff W, Kreutzberg GW (1985a) Ornithine decarboxylase in motoneurons during regeneration. Exp Neurol 89:679–688

Tetzlaff W, Kreutzberg GW (1985b) Enzyme changes in the rat facial nucleus following a conditioning lesion. Exp Neurol 85:547–564

Tetzlaff W, Bisby MA, Kreutzberg GW (1988) Changes in cytoskeletal proteins in the rat facial nucleus following axotomy. J Neurosci 8:3181–3189

Tetzlaff W, Alexander SW, Miller FD, Bisby MA (1991) Response of facial and rubrospinal neurons to axotomy: changes in mRNA expression for cytoskeletal proteins and GAP-43. J Neurosci 11:2528–2544

Tetzlaff W, Leonard C, Krekoski CA, Parhad IM, Bisby MA (1996) Reductions in motoneuronal neurofilament synthesis by successive axotomies: a possible explanation for the conditioning lesion effect on axon regeneration. Exp Neurol 139:95–106

Thoenen H (1991) The changing scene of neurotrophic factors. Trends Neurosci 14:165–170

Thomander L (1984). Reorganization of the facial motor nucleus after peripheral nerve regeneration. An HRP study in the rat. Acta Otolaryngol (Stockh) 97:619–626

Thomas PK (1989) Focal nerve injury: guidance of axons during axonal regeneration. Muscle Nerve 12:796–802

Tilney LG, Bryan J, Bush DJ, Fujiwara K, Mooseker MS, Murphy DB (1973) Microtubules: evidence for 13 protofilaments. J Cell Biol 59:267–275

Titmus MJ, Faber DS (1990) Axotomy-induced alterations in the electrophysiological characteristics of neurons. Prog Neurobiol 35:1–51

Tohyama K, Ide C (1984) The localization of laminin and fibronectin on the Schwann cell basal lamina. Arch Histol Cytol 47:519–532

Tokiwa MA, Gaspar EM, Doering LC (1994) CNTF is superior to NGF as a survival enhancement factor for adrenal medulla cells in vitro. NeuroReport 5:549–552

Toma JG, Pareek S, Barker P, Mathew TC, Murphy RA, Acheson A, Miller FD (1992) Spatiotemporal increases in epidermal growth factor receptors following peripheral nerve injury. J Neurosci 12:2504–2515

Tomov TL, Guntinas-Lichius O, Grosheva M, Streppel M, Schraermeyer U, Neiss WF, Angelov DN (2002) An example of neural plasticity evoked by putative behavioral demand and early use of vibrissal hairs after facial nerve transection. Exp Neurol 178:207–218

Tonra JR, Curtis R, Wong V, Cliffer KD, Park JS, Timmes A, Nguyen T, Lindsay RM, Acheson A, DiStefano PS (1998) Axotomy upregulates the anterograde transport and expression of brain-derived neurotrophic factor by sensory neurons. J Neurosci 18:4374–4383

Trachtenberg JT, Thompson WJ (1996) Schwann cell apoptosis at developing neuromuscular junctions is regulated by glial growth factor. Nature 379:174–177

Travers JB, Norgren R. (1983). Afferent projections to the oral motor nuclei in the rat. J Comp Neurol 220:280–298

Trojan DA, Gendron D, Cashman NR (1991) Electrophysiology and electrodiagnosis of the post-polio motor unit. Orthopedics 14:1353–1361

Tuttle GB, Mackey T, Steers WD (1994) NGF, bFGF and CNTF increase survival of major pelvic ganglion neurons cultured from the adult rat. Neurosci Lett 173:94–98

Ulenkate HJLM, Kaal ECA, Gispen W-H, Jennekens FGI (1994) Ciliary neurotrophic factor improves muscle fibre reinnervation after facial nerve crush in young rats. Acta Neuropathol 88:558–564

Ulenkate HJ, Gispen WH, Jennekens FG (1996) Effects of ciliary neurotrophic factor on retrograde cell reaction after facial nerve crush in young adult rats. Brain Res 717–29–37

Unsicker K, Grothe C, Westermann R, Wewetzer K (1992) Cytokines in neural regeneration. Curr Opin Neurobiol 2:671–678

Unsicker K, Grothe C, Lüdecke G, Otto D, Westermann R (1993) Fibroblast growth factors: their roles in the central and peripheral nervous system. In: Loughlin SE, Fallon JH (eds.) Neurotrophic factors, Academic Press, New York, pp. 313–338

Valero-Cabre A, Tsironis K, Skouras E, Navarro X, Neiss WF (2004) Peripheral and spinal motor reorganization after nerve injury and repair. J Neurotrauma. 21:95–108

Valls-Sole J, Tolosa ES (1989). Blink reflex excitability cycle in hemifacial spasm. Neurology 39:1061–1066

Vaughan ED, Richardson D (1993) Facial nerve reconstruction following ablative parotid surgery. Br J Oral Maxillofac Surg 31:274–280

Vega QC, Worby CA, Lechner MS, Dixon JE, Dressler GR (1996) GDNF activates the receptor tyrosine kinase RET and promotes kidney morphogenesis. Proc Natl Acad Sci USA, 93:10657–10661.

Veisada R, Sagot Y, Kato AC (1994) BDNF-mediated rescue of axotomized motor neurons decreases with increasing dose. Neuroreport 5:1889–1892

Vergara J, Medina L, Maulen J, Inestrosa NC, Alvarez J (1993) Nerve regeneration is improved by insulin-like growth factor I (IGF-I) and basic fibroblast growth factor (bFGF). Restor Neurol Neurosci 5:181–189

Vignjevic D, Yarar D, Welch MD, Peloquin J, Svitkina T, Borisy GG (2003) Formation of filopodia-like bundles in vitro from a dendritic network. J Cell Biol 160:951–962

Wang Y, Tien LT, Lapchak PA, Hoffer BJ (1996) GDNF triggers fiber outgrowth of fetal ventral mesencephalic grafts from nigra to striatum in 6-OHDA-lesioned rats. Cell Tissue Res 286:225–233

Welker WI (1964). Analysis of sniffing of the albino rat. Behaviour 22:223–244

Wewetzer K, MacDonald JR, Collins F, Unsicker K (1990) CNTF rescues motoneurons from ontogenetic cell death in-vivo but not in vitro. Neuroreport 1:203–206

Wewetzer K, Heiniger C, Seilheimer B (1996) An improved cell-ELISA for the differential screening of antibodies against cell surface molecules of viable adherent Schwann cells. J Immunol Methods 191:171–178

Wewetzer K, Grothe C, Christ B, Seilheimer B (1997) Identification and characterization of differentiation-dependent Schwann cell surface antigens by novel monoclonal antibodies: introduction of a marker common to the non-myelin-forming phenotype. Glia 19:213–226

Wewetzer K, Grothe C, Claus P (2001) In vitro expression and regulation of ciliary neurotrophic factor and its α receptor unit in neonatal olfactory ensheathing cells. Neurosci Lett 306:165–158

Wewetzer K, Verdú E, Angelov DN, Navarro X (2002) Olfactory ensheathing glia and Schwann cells: two of a kind? Cell Tiss Res 309:337–345

Wilby MJ, Sinclair SR, Muir EM, Zietlow R, Adcock KH, Horelou P, Rogers JH, Dunnett SB, Fawcett JW (1999) A glial cell line-derived neurotrophic factor-secreting clone of the Schwann cell line SCTM41 enhances survival and fiber outgrowth from embryonic nigral neurons grafted to the striatum and to the lesioned substantia nigra. J Neurosci 19:2301–2312

Williams LR, Longo FM, Powell HC, Lundborg G, Varon S (1983) Spatial-temporal progress of peripheral nerve regeneration within a silicone chamber: parameters for a bioassay. J Comp Neurol 218:460–470

Williams LR, Danielsen N, Müller H, Varon S (1987) Exogenous matrix precursors promote functional nerve regeneration across a 15 mm gap within a silicone chamber in the rat. J Comp Neurol 264:284–290

Williamson T, Gordon-Weeks PR, Schachner M, Taylor J (1996) Microtubule reorganization is obligatory for growth cone turning. Proc Natl Acad Sci USA 93:15221–15226

Wilson P, Kitchener, P.D. (1996) Plasticity of cutaneous primary afferent projections to the spinal dorsal horn. Prog. Neurobiol., 48, 105–129

Wilson DL, Perry GW (1990) Some hypotheses concerning axon regeneration. Restor Neurol Neurosci 1:197–203

Wineski LE (1985) Facial morphology and vibrissal movement in the golden hamster. J Morphol 183:199–217

Woolf CJ, Shortland P, Coggeshall RR (1992). Peripheral nerve injury triggers central sprouting of myelinated afferents. Nature 355:75–78

Yamada KM, Spooner BS, Wessells NK (1970) Axon growth: roles of microfilaments and microtubules. Proc Natl Acad Sci USA 66:1206–1212

Yamada KM, Spooner BS, Wessells NK (1971) Ultrastructure and function of growth cones and axons of cultured nerve cells. J Cell Biol 49:614–635

Yan Q, Elliott JL, Snider WD (1992) Brain-derived neurotrophic factor rescues spinal motor neurons from axotomy-induced cell death. Nature 360:753–755

Yan Q, Elliott JL, Matheson C, Sun J, Zhang L, Mu X, Rex KL, Snider WD (1993) Influences of neurotrophins on mammalian motoneurons in vivo. J Neurobiol 24:1555–1577

Yan Q, Matheson C, Lopez OT (1995) In vivo neurotrophic effects of GDNF on neonatal and adult facial motor neurons. Nature 373:341–344

Yan Q, Radeke MJ, Matheson CR, Talvenheimo J, Welcher AA, Feinstein SC (1997) Immunocytochemical localization of TrkB in the central nervous system of the adult rat. J Comp Neurol 378:135–157

Yip HK, Rich KM, Lampe PA, Johnson EM (1984) The effects of nerve growth factor and its antiserum on the postnatal development and survival after injury of sensory neurons in the rat dorsal root ganglia. J Neurosci 4:2986–2992

Yu W, Baas PW (1994) Changes in microtubule number and length during axon differentiation. J Neurosci 14:2818–2829

Yu W, Baas PW (1995) The growth of the axon tip is not dependent upon net microtubule assembly and its distal tip. J Neurosci 15:6827–6833

Yu W, Ahmad DJ, Baas PW (1994) Microtubule fragmentation and partitioning in the axon during collateral branch formation. J Neurosci 14:5872–5884

Zakharenko S, Popov S (1998) Dynamics of axonal microtubules regulate the topography of new membrane insertion into the growing neurites. J Cell Biol 143:1077–1086

Zhang J-Y, Luo X-G, Xian CJ, Liu Z-H, Zhou X-F (2000) Endogenous BDNF is required for myelination and regeneration of injured sciatic nerve in rodents. Eur J Neurosci 12:4171–4180

Zhao Q, Dahlin LB, Kanje M, Lundborg G, Lu S-B (1992) Axonal projections and functional recovery following fascicular repair of the rat sciatic nerve with Y-tunneled silicone chambers. Restor Neurol Neurosci 4:13–19

Zheng JL, Helbig C, Gao W-Q (1997) Induction of cell proliferation by fibroblast and insulin-like growth factors in pure rat inner ear epithelial cell cultures. J Neurosci 17:216–226

Ziv NE, Spira ME (1997) Localized and transient elevations of intracellular Ca^{2+} induce the dedifferentiation of axonal segments into growth cones. J Neurosci 17:3568–3579

Zurn AD, Baetge EE, Hammang JP, Tan SA, Aebischer P (1994) Glial cell line-derived neurotrophic factor (GDNF), a new neurotrophic factor for motoneurons. Neuroreport 6:113–118

Subject Index